DISSOLUTION OF COLEMANITE AND CRYSTALLIZATION OF GYPSUM
DURING BORIC ACID PRODUCTION IN A BATCH REACTOR

A THESIS SUBMITTED TO
THE GRADUATE SCHOOL OF NATURAL AND APPLIED SCIENCES
OF
MIDDLE EAST TECHNICAL UNIVERSITY

BY

ANIL ERDOĞDU

IN PARTIAL FULFILLMENT OF THE REQUIREMENTS FOR THE DEGREE OF
MASTER OF SCIENCE
IN
CHEMICAL ENGINEERING

JUNE 2004

Approval of the Graduate School of Natural and Applied Sciences

_____

Prof. Dr. Canan Özgen
Director

I certify that this thesis satisfies all the requirements as a thesis for the degree of Master of Science.

_____

Prof. Dr. Timur Doğu
Head of Department

This is to certify that we have read this thesis and that in our opinion it is fully adequate, in scope and quality, as a thesis and for the degree of Master of Science.

_____

Prof. Dr. İnci Eroğlu
Supervisor

Examining Committee Members

Prof. Dr. Hayrettin Yücel   (METU,CHE) _____

Prof. Dr. İnci Eroğlu   (METU,CHE) _____

Prof. Dr. Saim Özkar   (METU,CHEM) _____

Prof. Dr. Nusret Bulutcu   (ITU,CHE) _____

Prof. Dr. Nurcan Baç   (METU,CHE) _____

I hereby declare that all information in this document has been obtained and presented in accordance with academic rules and ethical conduct. I also declare that, as required by these rules and conduct, I have fully cited and referenced all material and results that are not original to this work.

Name, Last name : Anıl, Erdoğdu

Signature   :

ABSTRACT

DISSOLUTION OF COLEMANITE AND CRYSTALLIZATION OF GYPSUM

DURING BORIC ACID PRODUCTION IN A BATCH REACTOR

Erdoğdu, Anıl

M.S., Department of Chemical Engineering

Supervisor: Prof. Dr. İnci Eroğlu

June 2004, 102 pages

One of the most commonly used boron compounds, boric acid, is produced by dissolving colemanite ($2CaO \cdot 3B_2O_3 \cdot 5H_2O$) in aqueous sulfuric acid whereby gypsum ($CaSO_4 \cdot 2H_2O$) is formed as a byproduct and must be separated from the main product. This process consists of two steps, dissolution of colemanite and formation of gypsum. The amount of boric acid formed depends on the first step, dissolution of colemanite. In the latter step, gypsum crystals are formed and stay in the reaction mixture to grow up to a size large enough to be filtered out of the solution. Filtration of gypsum crystals is a crucial process in boric acid production because it affects the purity and crystallization of boric acid. In this study it is aimed to investigate the effects of particle size of colemanite, stirring rate and reaction temperature on the dissolution of colemanite, gypsum formation and particle size distribution of gypsum formed in the reaction of boric acid production.

Colemanite, sulfuric acid and distilled water were used as reactants for the boric acid production reaction in this study.The colemanite minerals were provided from a region of Emet, Kutahya, Turkey. Three types of colemanite minerals having different chemical composition and particle size were used. The sulfuric acid was supplied by Eti Holding A.S. Hisarcık 1 and Hisarcık 2 colemanites were crushed in a jaw crusher, ground in a hammer mill and then sieved. The sieve analysis was performed to learn the size distribution of Hisarcık 1 and Hisarcık 2 colemanite. Hisarcık 3 colemanite was brought from Emet Boric Acid Plant. The maximum diameter of the colemanite minerals was 150 μm.

The experiments were performed at different particle sizes of colemanite (0-150, 0-250 and 250-1000 μm), temperatures (70- 90 °C) and stirring rates (350-500 rpm). The photographs of gypsum crystals were taken. The boric acid and calcium ion concentrations were determined for each experiment. Also, the solid content of the solution in the reactor were measured. The dissolution of colemanite can be followed by monitoring the boric acid concentration change in the slurry. The crystallization of gypsum from the solution can be found from the calcium ion concentration in the solution. The crystallization kinetics of calcium sulfate dihydrate was studied. The growth of the gypsum crystals were examined under the light microscope and the particle size distribution of gypsum crystals were analyzed by of the laser diffraction instrument.

Key words: Colemanite, Boric Acid , Gypsum.

ÖZ

KESİKLİ REAKTÖRDE BORİK ASİT ÜRETİMİ ESNASINDA KOLEMANİT ÇÖZÜNMESİ VE JİPS KRİSTALİZASYONU

Erdoğdu, Anıl

Yüksek Lisans, Kimya Mühendisliği Bölümü

Tez Yöneticisi: Prof. Dr. İnci Eroğlu

Haziran 2004, 102 sayfa

En önemli bor bileşiklerinden biri olan borik asit kolemanitin($2CaO \cdot 3B_2O_3 \cdot 5H_2O$) sülfürik asitte çözünmesinden oluşmaktadır. Bu tepkimeye sonucunda yan ürün olarak da jips ($CaSO_4 \cdot 2H_2O$) oluşur ve ana üründen ayrılmalıdır. Bu üretim iki aşamada gerçekleşmektedir; kolemanit çözünmesi ve jips oluşumu. Oluşan borik asidin miktarı ilk aşama olan kolemanit çözünmesine bağlıdır. Daha sonraki aşamada , jips kristalleri oluşmakta ve reaksiyon çamurunda filtre edilebilecek boyuta gelene kadar büyütülmektedir. Jips kristallerinin filtrasyonu borik asit üretiminde önemli bir aşamadır. Çünkü bu aşama, borik asidin kristalizasyonunu ve saflığını etkilemektedir. Bu çalışmada kolemanit parça boyutunun, karıştırma hızının ve reaksiyon sıcaklığının kolemanit çözünmesine, jips oluşumuna ve jips kristallerinin parça boyutu dağılımına etkisinin incelenmesi amaçlanmıştır.

Bu çalışmada; kolemanit, sülfürik asit ve saf su reaksiyoda girdiler olarak kullanılmıştır. Kolemanit mineralleri Kütahya'nın Emet ilçesinden sağlanmıştır. Sülfürik asit ise Eti Holding A.Ş tarafından sağlanmıştır. Farklı kimyasal ve parça boyutuna sahip üç çeşit kolemanit minerali kullanılmıştır. Hisarcık 1 ve Hisarcık 2 kolemanitleri deneylerden önce çeneli kırıcılarda kırılmış, balyozlu öğütücüde

öğütülmüş ve elenmiştir. Hisarcık 1 ve Hisarcık 2 kolemanitlerinin parça boyutu dağılımını elde etmek için parça büyüklüğü analizi yapılmıştır. Hisarcık 3 kolemaniti Emet Yeni Borik Asit Fabrikası'ndan getirtilmiştir. Hisarcık 3 kolemanit minerallerinin en büyük parça boyutu 150 µm'dir

Deneyler, farklı parça boyutunda kolemanit mineralleri(0-150,0-250 and 250-1000 µm) kullanılarak, farklı sıcaklıklarda (70- 90 °C) ve farklı karıştırma hızlarında (350-500 rpm) gerçekleştirilmiştir. Jips kristalleinin fotografları mikroskopla bakılarak elde edilmiştir. Herbir deneyde borik asit ve kalsiyum iyonunlarının zamana bağlı değişimi ölçülmüştür. Ayrıca çamurdaki katı miktar değişimi tayin edilmiştir. Kolemanitin çözünmesi, borik asit derişiminin zamana bağlı değişiminin tayin edilmesi ile izlenmiştir. Çözeltideki jips kristalizasyonu , çözeltideki kalsiyum iyon derişiminin zamana bağlı değişiminden bulunmuştur. Jipsin kristalizasyon kinetiği çalışılmıştır. Jips kristallerinin büyümesi mikroskop yardımıyla , parça boyutu dağılımı da lazer kırım aleti ile incelenmiştir.

Anahtar Sözcükler: Kolemanit, Borik Asit , Jips.

To My Mother and Father...

ACKNOWLEDGEMENTS

TABLE OF CONTENTS

LIST OF TABLES

LIST OF FIGURES

LIST OF SYMBOLS

SYMBOLS

C   :concentration of calcium ion, mol L^{-1}

C_g :concentration of gas in mol L^{-1}

C_{t1} : maximum concentration of calcium ion, mol L^{-1}

C_{H3PO4} : concentration of H_3PO_4 solution mol L^{-1}

C_{sat} : saturation concentration of calcium ion, mol L^{-1}

d   : diameter of the agitator, m

D   :particle size , mm

F_{NaOH} : factor of the NaOH used in the titration

k   :crystal growth rate constant, L mol^{-1} s^{-1}

k_s :rate constant of surface reaction, m s^{-1}

k_x :rate constant, (mol L^{-1})$^{-3/4}$ min $^{-1}$

m_{slurry} :amount of slurry, g

m_{liquid} :amount of liquid, g

M_B :molecular weight of colemanite in kg mol^{-1}

n   :stirring rate of agitator used in the experiments, rpm

N_{NaOH} : normality of NaOH, N

R   : initial particle radius of colemanite, m

SR   :stirring rate in s^{-1}

S/L   :the solid-to-liquid ratio ,g L^{-1}

V_{liquid} : volume of liquid, L

V_{NaOH} : volume of the NaOH, mL

W   :ultrasound power, W

T   :reaction temperature , °C

t   : time, s

U   : tip speed of agitator, m s^{-1}

X   :fraction of the solid reacted

Greek letters

ρ_B : density of colemanite in kg m^{-3}

CHAPTER 1

INTRODUCTION

1.1 Heterogeneous Solid-Liquid Reactions

Heterogeneous solid-liquid reactions leading to crystallization of the product are widely used in production of many industrial chemicals. Some examples for solid-liquid reaction crystallizations are listed in Table 1.1

Table 1.1 Some examples of solid-liquid reaction crystallizations (Bechtloff et al., 2001)

Reaction System
Calcium citrate + sulfuric acid $\rightarrow$ citric acid + calcium sulfate
Oxalic acid+ borax $\rightarrow$ sodium oxalate+ boric acid
Borax+ propionic acid $\rightarrow$ sodium propionate+ boric acid
Colemanite+ sulfuric acid $\rightarrow$ boric acid+ gypsum
Sodium sulfide+ benzylchloride $\rightarrow$ benzylsulfide+ sodiumchloride

Different type of behavior of reacting solid particles can be seen. Only a solid phase reaction can occur on the surface of the particles if the solid reactant is insoluble in the reaction medium. The shrinking core model developed by Yagi and Kunii (1955,1961) explains this type of behavior of reacting solid particles. According to this model, the reaction occurs first at the outer skin of the particles. Then, the zone of the reaction moves toward the center of the solid particle leaving behind a solid product layer called as ash. (Levenspiel, 1999)

If the solid has a slight or a high solubility, a liquid phase reaction may dominate the process. So, the dissolution of solid reactant and the crystallization of the product happen simultaneously. When the fluid becomes supersaturated, the solid product precipitates. However, the solid product may cover solid reactant. It may lead to a reduced reaction rate or incomplete conversion of solid reactant. (Bechtloff et al., 2001)

The reaction of colemanite with sulfuric acid is heterogeneous solid-liquid reaction leading to crystallization of the product.

1.2. Boron Minerals and Colemanite

Colemanite is used as the raw material in the boric acid production. It is one of the most important boron minerals in the world. More than 200 boron minerals have been known but relatively few of them have commercial significance (Roskill, 2002). Commercially significant boron minerals are given in Table 1.2.

Table 1.2 Commercially significant boron minerals (Özbayoğlu et al.,1992)

Boron minerals	Molecular formula	%B_2O_3	Location
Tincal	$Na_2B_4O_7.10H_2O$	36.5	Turkey, USA
Kernite	$Na_2B_4O_7.4H_2O$	51.0	Argentina, USA
Ulexite	$NaCaB_5O_9 .8H_2O$	43.0	Turkey, Argentina, Peru
Probertite	$NaCaB_5O_9 .5H_2O$	49.6	Turkey, USA
Colemanite	$Ca_2B_6O_{11}.5H_2O$	50.8	Turkey, USA
Pandermite	$Ca_4B_{10}O_{19}.7H_2O$	49.8	Turkey
Boracite	$Mg_3B_7O_{13}Cl$	62.2	Germany
Szaibelyite	$MgBO_2(OH)$	41.4	Russia
Sassolite	H_3BO_3	56.4	Italy
Hydroboracite	$CaMgB_6O_{11}.H_2O$	50.5	Germany, Russia

In the world, Turkey, USA and Russia have the important boron mines. In terms of total reserve basis, Turkey has a share of 64 %, the other important country USA has 9 %. Total world boron reserves on the basis of B_2O_3 content are 363 million tons proven. 522 million tones probable and possible, and as a total of 885 million

tons. With a share of 64 %, Turkey has a total boron reserves of 563 million tons on the basis of B_2O_3 content .The share of world boron reserves is given in Table 1.3

Table 1.3 World boron reserves thousand tons - B_2O_3 (Industrial minerals, 2001)

Country	Proven Reserve	Probable Possible Reserve	Total Reserve	Percent in Total (%)	Life Span .(Year)
Turkey	224.000	339.000	563.000	64	389
U.S.A.	40.000	40.000	80.000	9	55
Russia	40.000	60.000	100.000	11	69
China	27.000	9.000	36.000	4	25
Chile	8.000	33.000	41.000	5	28
Bolivia	4.000	15.000	19.000	2	13
Peru	4.000	18.000	22.000	2	15
Argentina	2.000	7.000	9.000	1	6
Kazakhstan	14.000	1.000	15.000	2	10
Total	**363.000**	**522.000**	**885.000**	**100,0**	**610**

Boron minerals can be used in some sectors in the industry as crude minerals. In general, their applications after refining and end-products are wider than crude ones. Boron minerals, borates and compounds have a very wide range of applications. Table 1.4 illustrates the major uses of boron minerals, borates and boron compounds

Colemanite, like other borates, is a complex mineral, that is found in desert borax deposits and Tertiary clays in old lake beds. Colemanite is a secondary mineral, meaning that it occurs after the original deposition of other minerals. The mineral borax is directly deposited in regions from the evaporation of water due to run off from nearby mountain ranges. The runoff is rich in the element boron and is highly concentrated by evaporation in the arid climate. Ground water flowing through the borax sediments is believed to react with the borax and form other minerals such as ulexite. It is believed that colemanite may have formed from ulexite. Colemanite is found in geodes within the borax sediment. It's exact means of formation are still not well understood (Amethyst Galleries, 1997). The picture of colemanite mineral is given in Figure 1.1.

The basic structure of colemanite contains endless chains of interlocking $BO_2(OH)$ triangles and $BO_3(OH)$ tetrahedrons with calcium, water molecules and extra hydroxides interspersed between the chains (Chuck Brown, 2000).

Figure 1.1 Picture of colemanite mineral

Colemanite has many important uses. It is used in the manufacture of heat resistant glass. It is also used as a cleaning agent and has other industrial, medicinal, and cosmetical uses (Hershel Friedman,1999).

Table 1.4 Major uses of boron minerals, borates and boron compounds (Industrial minerals, 2001; Roskill 2002)

Usage Area	Major Uses
Agriculture	-Essential micronutrient for all plant
Detergents and Soaps	-Act as pH buffer -Soften the washing water -Enhance the solubility of other ingredients -Act as a gentle but powerful bleaching agent
Ceramic Glazes and Enamel Frits	-Provide good fluxing properties -Provide a good base for dissolving coloring agents
Insulation Fiberglass	-Reduce the temperature at which fibers are formed -Improve the durability of the glass fibers -Reduce the viscosity of the molten glass
Timber Preservation	- Prevent and control the spread of bacteria - Inhibit corrosion - Act as flame retardant
Flame Retardants	- Enhance the performance of alumina trihydrate - Effective as flame retardants
Nuclear Power Stations	- Absorb thermal neutrons - Used to control nuclear reaction - Used in nuclear shielding.
Cosmetics and Medicine	- Neutralize fatty acid - Act as emulsifiers in certain creams - Give mild antiseptic properties
Metallurgy	- Used as cover fluxes - Dissolve and remove unwanted metal oxides as slag
Other	-Glass -Optical fibers -Magnets -Adhesives -Photography

1.3 Boric Acid

Boric acid can be viewed as a hydrate of boric oxide and exists both as a trihydrate, orthoboric acid ($B_2O_3 \cdot 3H_2O$ or H_3BO_3), and as a monohydrate, metaboric acid ($B_2O_3 \cdot H_2O$ or HBO_2). Only the more stable orthoboric acid form is of commercial importance and is usually referred to simply as boric acid. The terms "pyroboric acid" and "tetraboric acid" are sometimes encountered in the literature, but these acids do not actually exist as solid-phase compounds (Ullmann, 2002)

Boric acid is white granule or powder. Its density is 1.435 g/cm^3. It melts at 171 °C. Solubility in water at 20 °C is 4.7 g boric acid/ g solution (Patnaik, 2002). The solubility of boric acid in water at various temperatures is given in Table 1.5.

Table1.5 Solubility of boric acid in water (Seidell , 1965)

Temperature	%H$_3$BO$_3$ in Saturated Solution
25	5.43
30	6.34
35	7.19
40	8.17
45	9.32
50	10.23
55	11.54
60	12.96
65	14.42
70	15.75
80	19.06
90	23.27
100	27.52
103.3 (Boiling Point)	31.0

Boric acid is used to prepare a variety of glasses including fiber glass, heat resistant borosilicate glass and sealing glasses. It also is used to make porcelain. A major application of boric acid is to prepare a number of boron compounds including inorganic borate salts, boron halides, borate esters,

fluoroborates and many boron alloys. The compound is used as a component of welding and brazing fluxes.

Boric acid is used as an antiseptic in mouthwashes, eye washes and ointments; a preservative in natural products; to protect wood against insect damage; in washing citrus fruits; as a catalyst in hydrocarbon oxidation; as a flame retardant in cellulose insulation; in nickel electroplating baths; and as a buffer in ammonia analysis of wastewaters by acid titration (Patnaik, 2002).

1.3.1 Boric Acid Production in the World

Boric acid is manufactured industrially from borate minerals and brines. Alkali and alkaline-earth metal borates, such as borax, kernite, colemanite, ascharite, ulexite, or hydroboracite, react with strong mineral acids to form boric acid. In the United States boric acid is made primarily from sodium borate minerals, whereas in Europe it is made from colemanite imported from Turkey. In the Soviet Union magnesium borates from the Inder region are used to make boric acid. Borates found in saline lake brine in California at Searles Lake are extracted and recovered as boric acid.

The world's largest boric acid plant was constructed by U.S.Borax in 1981 at Boron, California. Crushed kernite ($Na_2O.2B_2O_3\ 4H_2O$) ore is reacted with sulfuric acid in recycled weak liquor (contains low concentration of borates) at 100 °C. Coarse gangue is separated by rake classifiers and fine particles are settled in a thickener. The boric acid strong liquor (high borate concentration) is nearly saturated with sodium sulfate. Complete solubility of sodium sulfate is maintained throughout the process by careful control of pH and temperature. The strong liquor is filtered at 98 °C and boric acid crystallized in two stages using continuous evaporative crystallizers. The temperature is dropped to 70 °C in the first stage and to 35 °C in the second. Crystals are filtered and washed with progressively weaker liquor in a countercurrent fashion. The final product is dried in rotary driers and screened for packaging. Weak liquor at 35 °C, nearly saturated in sodium sulfate, is heated to 100 °C and returned to the reactor. Sodium sulfate is removed from the process as solid in gangue and in effluent from a second-stage thickener, and is pumped to sealed solar ponds. The plant has a capacity of 113000 t/a (expressed as B_2O_3).

In Europe boric acid is produced from Turkish colemanite ($2CaO.3B_2O_3.5H_2O$) ore by reaction with sulfuric acid at 90 °C. Byproduct gypsum and gangue are filtered and the hot mother liquor cooled to crystallize boric acid. The weak liquor is recycled to the reactor.

Magnesium borate ores, primarily of ascharite (szarbelyite, $2MgO.B_2O_3.H_2O$), and hydroboracite ($CaO.MgO.3B_2O_3.6H_2O$), are finely ground and decomposed to boric acid with sulfuric acid at 95 °C. Insoluble gypsum and gangue are filtered and the mother liquor is cooled to 15 °C to crystallize boric acid. The weak liquor is nearly saturated in magnesium sulfate ($MgSO_4.7\ H_2O$), which is crystallized by concentration of the liquor at elevated temperature; the concentrated liquor is then recycled to the reactor.

Datolite ($2\ CaO.B_2O_3.2SiO_2.H_2O$) is the most common silicoborate mineral. Ore containing 5 % B_2O_3 is finely ground and reacted with sulfuric acid. Silica in the mother liquor is coagulated upon heating to 95 °C. The resulting boric acid solution is nearly free of silicic acid.

At Searles Lake, California, borax is found in brine at a concentration of about 1.5% (expressed as anhydrous borax); a number of other salts are also present. A process using liquid –liquid extraction is used to separate borax selectively from brine. Borax is extracted into a water-insoluble solvent, such as kerosene, by use of an aromatic polyol that efficiently complexes the borate ion, e.g., 3-chloro-2-hydroxy-5-isooctylbenzenemethanol. The organic phase is isolated and acidified with sulfuric acid, giving an aqueous solution of boric acid and sodium sulfate. After concentrating by evaporation, the liquor is cooled to crystallize boric acid (Ullmann, 2002)

Table 1.6 Boric acid producers and their capacities (Roskill, 2002)

Country	Company	Capacity (t/y)/10^3
Argentina	Norquimica SA	5.4
	Industrials Quimicas Baradero	9.5
	Others	15.1
Bolivia	Tierra SA	15
Chile	Quiborax	36
	SQM	16
China	Ji'an City Boron Ore	30
	Zibo Yanxiang Rolling Steel Product Company Limited	13
	Dangdong Kuandian Boron Ore	6
	Dashiqiao City Huaxin Chemical Company Limited	5
	Yingkou City Xingdong Chemical Plant	5
	Mudanjlang Number 2 Chemical Factory	4
	Others	29.3
France	Borax Francais SA	*
India	Borax Morarji	4.18
Italy	Societa Chimica di Larderello	55-60
Japan	Nippon Denko	4
Peru	JSC Inkobor	25
Russia	JSC Energomash-Bor	100
Spain	Borax Espana	*
Turkey	Eti Bor	185
USA	IMC Chemical	25
	US Borax	255-260

*Not Known

1.3.2 Boric Acid Production in Turkey

Eti Maden İşletmeleri dominates the mining and processing of boron minerals and boron compounds in Turkey. Eti Bor operates plants at Bandırma and Emet that produce boric acid. In order to meet increasing demand and enhance the position of Turkey in boron producers, it was decided to establish a boric acid plant with 100.000 tons/year production capacity in Emet district of Kütahya. Total boric acid capacity controlled by Eti Bor rose to 185.000 t/y following the construction of a New Boric Acid Plant.

In Turkey, boric acid is produced from colemanite (2 CaO .3 B_2O_3. $5H_2O$) ore by reaction with sulfuric acid. The overall reaction in the reactor is given as below;

$$2CaO.3B_2O_3.5H_2O(s) + 2\ H_2SO_4\ (l) + 4\ H_2O\ (l) \rightarrow 2Ca\ SO_4.2H_2O\ (s) + 6H_3BO_3\ (aq)$$
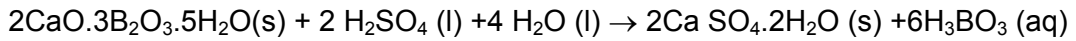
This overall reaction consists of two consecutive reactions, dissolution of colemanite and formation of gypsum. In the first reaction boric acid produced and this reaction is a very fast reaction.

Boric Acid Production Reaction:
$$2CaO.3B_2O_3.5H_2O\ (s) + 2\ H_2SO_4\ (l) + 2\ H_2O\ (l) \rightarrow 2Ca^{2+} + 2\ SO_4^{2-} + 6H_3BO_3\ (aq)$$
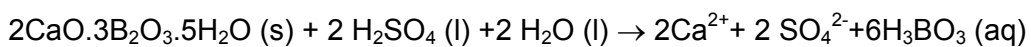
In the latter step, gypsum crystals are formed and stay in the reaction mixture to grow up to a size large enough to be filtered out of the solution.

Gypsum Crystallization Reaction:
$$Ca^{2+} + SO_4^{2-} + H_2O\ (l) \rightarrow CaSO_4.2H_2O(s)$$
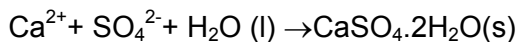
In boric acid production process at Bandırma, colemanite undergoes pimary and secondary crushing. Prior to the addition of sulphuric acid, further size reduction is employed by a ball mill. The ground material is taken to the batch reactors where returning mother liquor and sulphuric acid are mixed at 85-95 °C. The steam is used for heating purpose and it is given directly to the slurry. The slurry is stirred. The reaction time is between 45-60 minutes. The formed gypsum particles and other insolubles are filtered and the clear filtrate is sent to the crystallizer where it cooled down to 40 °C. The formed boric acid crystals are then centrifuged and dried to obtain a product of 99.5% purity (Özbayoğlu et al, 1992).

Boric acid production process at Emet is different from the boric acid production process at Bandırma. In Emet, there are six continuous flow stirred slurry reactors (CSTR) are used. In the production process, five of them are used in series. The colemanite mineral is crushed and ground. Firstly, the sulphuric acid (%93 by wt) is mixed with mother liquor (nearly %5-6 H_3BO_3). Then it is sent to the first reactor and reacted with the fed colemanite minerals (with a particle size of less than 150 μm).

The reaction temperature is between 85-88 °C. The slurry is heated by steam circulating around the reactors. A polyelectrolye is added to the slurry before the filters in order to make the filtration easier. The slurry is sent to the horizontal vacuum belt filters. The formed gypsum crystals and other insolubles are filtered and the clear filtrate is sent to the polished filters. Then obtained clear filtrate is sent to the crystallizers working in series. The formed boric acid crystals are washed with demineralized water to remove the sulfate ions. After that, it is centrifuged and dried to obtain the boric acid product.

1.4 Objective of the Study

In this work, the dissolution of colemanite in sulfuric acid was studied in a batch reactor. The effects of particle size of colemanite, stirring rate and reaction temperature on the dissolution of colemanite, gypsum formation and particle size distribution of gypsum formed in the reaction of boric acid production were investigated. Dissolution of colemanite in sulfuric acid was studied by other researchers. However, their parameters were different than the ones selected in this study. The parameters in this work were chosen by considering the batch and continuous boric acid plants in Turkey.

Different particles size ranges of colemanite were chosen in order to see the particle size effect on dissolution of colemanite. Also, the colemanites having different chemical compositions were discussed. The stirring rate was selected as a parameter to see if there was a mass transfer limitation for the reaction. Temperature range was taken as 70-90 °C in order to hinder the production of calcium sulfate hemihydrate which is not desired in the production process.

Gypsum crystal size distribution is an important parameter. The gypsum crystals should grow a suitable size to be easily removed from the boric acid solution by filtration. Therefore, the mean diameters of the crystals were evaluated by particle size analyzer to see the optimum conditions.

The second order rate of gypsum crystallization was applied to batch reactor experimental data and the rate gypsum crystallization model was found to supply the kinetics parameters for the simulation of continuous boric acid reactors.

CHAPTER 2

LITERATURE SURVEY

2.1 Dissolution of Colemanite

2.1.1 Dissolution of Colemanite in Various Mediums

Kocakerim and Alkan (1987) studied the kinetics of dissolution of colemanite in water saturated with SO_2. The effects of particle size, temperature and stirring rate were investigated. It was found that the rate of dissolution increased with decreasing particle size and with increasing temperature, but was unaffected by stirring rate. It was found that the dissolution rate was chemically controlled and the rate equation was given in Equation 2.1.

$$1 - (1 - X)^{1/3} = \frac{b\, k_s\, \lfloor C_g \rfloor M_B}{\rho_B\, R}\, t \qquad\qquad 2.1$$

where stoichiometric coefficient of colemanite with each mole of water saturated with SO_2, k_s is the rate constant of surface reaction in m s^{-1}, C_g is the concentration of gas in mol L^{-1}, M_B is the molecular weight of colemanite in kg mol^{-1}, ρ_B is the density of colemanite in kg m^{-3}, R is the initial particle radius in m and t is the time in s. The activation energy and the pre-exponential factor were calculated as 53.97 kJ mol^{-1} and 26.1 km s^{-1}, respectively.

Kum and coworkers (1993) investigated the leaching kinetics of calcined colemanite in ammonium chloride solutions. The effects of calcination temperature, solution concentration, reaction temperature and pre-hydration were evaluated. It had been declared that the rate of dissolution increased with increasing calcination

temperature, solution concentration and reaction temperature, while it was not affected by pre-hydration. It was found that the dissolution rate, based on the homogenous reaction model, was expressed as

$$(1-X)^{-1} -1= k_x[NH_4Cl]^{3/4} \, t \qquad\qquad 2.2$$

where, X is the fraction of the solid reacted, k_x is the rate constant in $(mol \, L^{-1})^{-3/4} \, min^{-1}$ and t is the time in min.

Özmetin and coworkers (1996) studied the dissolution of colemanite in aqueous acetic acid solutions in a batch reactor employing the parameters of particle size, solid-to-liquid ratio and temperature. It was determined by graphical and statistical methods that the reaction fitted a model in the form of $-ln(1-X)=kt$. The semi empirical mathematical model was established as given below

$$ln \, (1-X) = \; 56664(D)^{-1.42}(S/L)^{-0.27} \, exp \, (-6193.0/T_x).t \qquad\qquad 2.3$$

where X is the conversion fraction, D is the particle size in mm, S/L is the solid-to-liquid ratio in $g \, L^{-1}$, T_x is the reaction temperature in K and t is the time in min. It was observed that the dissolution rate increased with increasing temperature and decreasing solid-to-liquid ratio and particle size. The most effective parameter on dissolution rate was particle size of colemanite. Stirring rate had insignificant effect on dissolution. The conversion rate increased up to $3.365 \, mol \, L^{-1}$ acid concentration and then decreased with increasing acid concentration. The conversion rate increased up to $3.365 \, mol \, L^{-1}$ acid concentration and then decreased with increasing acid concentration.

Gürbüz and coworkers (1998) stated that the dissolution rate of colemanite in distilled water and boric acid solutions was very fast. The solubility of colemanite in distilled water at 90 °C was found as $1.7 \, g \, kgsolution^{-1}$. Besides this, the dissolution of colemanite in distilled water increased the pH value considerably. The solubility of colemanite in 7.5 %, 10 % and 20 % boric acid solutions at 90 °C were found as 4.3, 8.13 and 19.6 gcol./1000gsol, respectively. In the boric acid solutions, addition of colemanite did not change the pH considerably.

Temur and coworkers (2000) studied the kinetics of dissolution of colemanite in 1.43-35.69 (% by wt) H_3PO_4 solutions. It was found that dissolution rate was controlled by surface chemical reaction. The effects of particle size of colemanite, acid concentration, solid-to-liquid ratio, stirring rate and reaction temperature on the dissolution rate were determined. The overall rate equation was expressed in Eq 2.4.

$$1-(1-X)^{1/3} = (5.87 \times 10^9) (D)^{-0.744} (S/L)^{-0.453} (C_{H3PO4})^{0.328} e^{-53.91/RT} t \qquad 2.4$$

where X is the conversion fraction, D is the particle size in μm, S/L is the solid-to-liquid ratio in g mL^{-1} , C is the concentration of H_3PO_4 solution mol L^{-1} ,T is the reaction temperature in K and t is the time in min. It was stated that this boric acid production process had more advantageous than the classical sulphuric acid process because $Ca(H_2PO_4)_2$ and $CaHPO_4$ are produced as by products as a result of dissolution of colemanite in H_3PO_4 solutions. $Ca(H_2PO_4)_2$ is very soluble in water and gives Ca^{2+} and $H_2PO_4^-$ ions in the solution. If the solution is treated with strong acid-cation exchanger, Ca^{2+} is kept and H_3PO_4 is produced and reused in the process.

Küçük and coworkers (2000) investigated the dissolution of Kestelek's colemanite containing clay minerals in water saturated with sulphur dioxide as an alternative method to sulphuric acid process. Particle size of colemanite, solid-to-liquid ratio, stirring rate and reaction temperature were chosen as parameters. It was determined that the dissolution rate of colemanite increased with decreasing particle size and solid-to-liquid ratio and increasing reaction temperature, but was unaffected by the stirring rate. Semi-emprical model was found by using experimental data and package programs and it was given in Eq 2.5

$$[1-(1-X)^{1/3}]=3.423.10^4(D)^{-0.7}(S/L)^{-0.65} e^{-4754/T}.t \qquad 2.5$$

where X is the fractional conversion, D is the particle size of colemanite in mm, S/L is the solid-to-liquid ratio in g mL^{-1} and t is the time in min.

Table 2.1 Studies on dissolution of colemanite in various mediums

Researchers	Medium	Parameters	Results(Empirical formulas)
Kocakerim and Alkan (1987)	Water saturated with SO_2	Particle size (250-1700 µm) Temperature (11-40 °C) Stirring rate (200-1000 min^{-1})	$1-(1-X)^{1/3} = \dfrac{b\,k_s\,C_g\,M_B}{\rho_B\,R}\,t$
Kum and coworkers (1993)	Ammonium chloride solutions	Calcination temperature(300-460 °C) Solution concentration(1-3 mol L^{-1}) Reaction temperature (25-65 °C) Pre-hydration	$(1-X)^{-1} -1 = k[NH_4Cl]^{3/4}\,t$
Özmetin and coworkers (1996)	Aqueous CH_3COOH solutions	Particle size (0.137- 0.081 mm) Solid-to-liquid ratio (5-35 g mL^{-1}) Temperature (10.6- 50 °C)	$-\ln(1-X) =$ $56664(D)^{-1.42}(S/L)^{-0.27}\exp(-6193.0/T).t$
Gürbüz and coworkers (1998)	Boric acid solutions	Boric acid concentration (0-20 % wt)	Solubility (1.7- 19.6 g kgsolution^{-1})
Temur and coworkers (2000)	H_3PO_4 solutions	Particle size (250-1400 µm) Acid concentration (1.43-19.52 wt %) Solid-to-liquid ratio (0.02-0.08 g mL^{-1}) Stirring rate (300-600 min^{-1}) Reaction temperature (2.5 -35 °C)	$1-(1-X)^{1/3} =$ $(5.87 \times 10^9)(D)^{-0.744}(S/L)^{-0.453}(C)^{0.328}e^{-53.91/RT}\,t$
Küçük and coworkers (2000)	Water saturated with SO_2	Particle size (0.150- 1400 mm) Solid-to-liquid ratio (0.02-0.06 g mL^{-1}) Stirring rate (300-500 min^{-1}) Reaction temperature(18-40 °C)	$1-(1-X)^{1/3} =$ $3.423.10^4(D)^{-0.7}(S/L)^{-0.65}e^{-4754/T}.t$

2.1.2 Dissolution of Colemanite in Sulphuric Acid

Tunc and Kocakerim (1998) investigated the dissolution of colemanite in aqueous sulfuric acid. The parameters were temperature (10-60 °C), particle size of colemanite (0.3625-1.5 mm), solid-to-liquid ratio (0.01-0.175 g mL^{-1}), acid concentration (0.25-2 mol L^{-1}) and stirring rate (20.93-62.80 s^{-1}). It was found that temperature and stirring rate had positive effect on the rate. Conversion rate increased with the acid concentration up to 1 mol L^{-1} and decreased with the concentrations above 1 mol L^{-1}. The rate of dissolution reaction was expressed in Eq 2.6.

$$-\ln(1-X) = 82.52 \, (D)^{-0.821} \, (SR)^{0.426} \, (S/L)^{-0.383} \, e^{-3465/T} \cdot t \qquad\qquad 2.6$$

where X is the fractional conversion, D is the particle size of colemanite in mm, SR is the stirring rate in s^{-1}, S/L is the solid-to-liquid ratio g mL^{-1} and t is the time in min.

Kalafatoğlu and coworkers (2000) stated that if in the reaction of colemanite and sulfuric acid the concentration of sulfuric acid was more, besides the colemanite, some other impurities also dissolved. So, in this study, the most suitable concentration for sulfuric acid was searched and it was shown that if the acid concentration was hold around 5%, the dissolution of clay and the other impurities was less.

Dissolution kinetics of colemanite in sulfuric acid in the absence and presence of ultrasound was studied by Okur and coworkers (2002). An Avrami-type equation was used successfully to explain kinetic data. Activation energy was 30 kJ/mol in both situations. Ultrasound affected the pre-exponential factor in rate constant. The rate expression was summarized as

$$X_{B2O3} = 1 - \exp\left(-\left(\frac{C_{Ao}}{\rho_B}\right)^{-0.5} \left(\frac{0.075(1+1.5W)0.16e^{-3600/T}}{R} t^{0.7}\right) \pm 5 \times 10^{-3} \right) \qquad 2.7$$

where X is the conversion of solid reactant, C_{Ao} is the initial molar concentration in mol/dm^3, ρ_B is the molar density of solid reactant in mol dm^{-3}, W is the ultrasound

power in W, T is the temperature in K, R is the initial particle radius in m and t is the time in s.

Bilal and coworkers (2003) studied the dissolution of colemanite in sulfuric acid in a batch reactor at different temperatures (30-60 °C), initial concentration of sulfuric acid(0.1-0.5 wt %) and the amounts of boric acid (10-40 g kg solution^{-1}) initially added to the system. It was found that the reaction of colemanite with sulfuric acid was very fast and complete conversion was obtained in nearly 15 minutes. The saturation concentration of gypsum decreased with the increasing temperature. Initial boric acid concentration had insignificant effect on dissolution rate of colemanite. Increasing temperature and increasing sulfuric acid concentration up to 0.5 wt % increased the dissolution rate.

2.2 Crystallization of Gypsum

2.2.1 Crystallization of Gypsum During Various Reactions

Smith and Alexander (1970) investigated the effect of polymeric additives on the process of crystallization of calcium sulfate dihydrate from aqueous solution. Variations with polyelectroyte charge, type and molecular weight were examined. It was found that the induction period before growth began was lengthened by addition of the polyacrylic acid (PAA1) and polymethaacrylic acid (PMAA). The average size of crystals produced was much smaller than in the absence of additive. It was postulated that the absorbed polymer molecules acted as immobile impurities on the crystal surface and they inhibited crystal growth by reducing the rate of step movement across the crystal surface.

Smith and Sweett (1971) studied the crystallization of calcium sulfate dihydrate from supersaturated solutions made from calcium chloride and sodium sulfate of various compositions over a range of temperatures (30-90 °C). The kinetics of crystallization was followed by recording the conductivity of the crystallizing suspension. It was found that rate of crystallization slightly depend on the stirring conditions. As the rate of stirring increased, the growth rate approached a constant value, suggesting that the growth rate was not diffusion controlled at high stirring rates. The growth rate was found to decrease slightly with increasing pH. Crystal growth of gypsum

followed a second order kinetics. It was shown in this study that the rate-controlling step was dehydration of calcium ions.

Packter (1973) examined the precipitation of calcium sulfate dihydrate from calcium nitrate and sodium sulfate solution. It was stated that crystal growth took place mainly on the nuclei formed during the induction periods and that very few new nuclei formed during the main growth process. Final crystal lengths increased with increasing initial metal salt concentration. The reaction order for the nucleation was found as 9-10, the order of the slow growth process was 4.

Nancollas and coworkers (1973) examined the growth of calcium sulfate dihydrate seed crystals from supersaturated solutions at temperatures where the phase transformation to hemihydrate occurs. Calcium sulfate dehydrate seeded growth experiments at temperatures between 60-105 °C showed no evidence of transition to the thermodynamically stable salt, anhydrous calcium sulfate, during the experiments. The rate of reaction was proportional to the square of relative supersaturation. The data indicated that the rate determining step in $CaSO_4.2H_2O$ crystal growth involved a surface reaction. Seeded crystal growth experiments near the dihydrate-hemihydrate phase transition temperature (103°C in salt free solutions at 4 atm) showed that phase transformation accompanies the seeded growth of the less stable modification.

Lui and Nancollas (1975) investigated the effects of potential scale inhibitors such as methyl-enephosphonic acid (ENTMP), methylene phosphonic acid (TENTMP) and gelatin on the seeded crystal growth of calcium sulfate dihydrate from stable supersaturated solution at temperatures ranging from 25-55 °C. The crystal growth in the presence and absence of additives was followed microscopically and it was found that in the presence of gelatin, the crystals increased in size during growth without any appreciable change in morphology from that of seed material. The complete inhibition of growth for certain specific periods was found in supersaturated solution containing trace amounts of additives. However, after rather well defined induction periods the seed crystals again begin to grow and crystallization rate follows an equation second order in supersaturation.

Klepetsanis and coworkers (1991) studied the spontaneous precipitation of calcium sulfate in supersaturated solutions over the temperature range between 25-80 °C by monitoring the solution conductivity during the desupersaturation. From measurements of the induction times preceding the onset of precipitation the surface energy of the forming solid, identified as gypsum, was found between ca. 12 and 25 mJ/m^2 for the temperature range between 80 and 25°C, respectively. Kinetic analysis showed that over 50°C it was possible that the anhydrous calcium sulfate was forming as a transient phase converting into the more stable calcium sulfate dihydrate.

2.2.2 Crystallization of Gypsum During Boric Acid Production

The factors which affect the formation of gypsum during the dissolution of colemanite and the crystallization kinetics of gypsum were studied by Balkan and Tolun (1985). It was found that the growth rate of gypsum crystals increased as the temperature increased up to 80 °C and then decreased. The formation of easily filterable gypsum cake was obtained within 1-2 hours in a batch reactor. In the presence of impurities in the slurry caused formation of short gypsum crystals. In case of feeding colemanite on acidic solution containing sufficient gypsum seeds, the presence of 1-2% excess sulfuric acid improved the filtration characteristics of gypsum slurry. When sulfuric acid solution was fed on the colemanite suspension, the presence of sufficient seed surface area caused the formation of easily filterable gypsum slurry. When 10-30 ppm flocculant (Magnafloc 155) was added into the slurry before filtration, the filtration rate was increased.

Çetin and coworkers (2001) studied the crystallization kinetics of gypsum during the dissolution of colemanite in a batch reactor at varying the temperature (60-90°C), stirring rate (150-400 rpm), and the initial concentrations of the reactants. It was found that the crystal growth of gypsum on seed crystals follows a second order kinetics from the solution supersaturated in calcium and sulfate ions. The rate law for the crystallization was given as.

$$\text{Rate} = -\frac{d[Ca^{2+}]}{dt} = k\,([Ca^{2+}] - [Ca^{2+}]_{sat})^2 \qquad\qquad 2.8$$

where the crystal growth rate is given in mol $L^{-1}s^{-1}$, k is the rate constant in $L\ mol^{-1}\ s^{-1}$ which is assumed to be constant during the growth process and $[Ca^{2+}]_{sat}$ is the saturation concentration of calcium ion in solution. The minimum saturation concentration of the calcium ion was obtained at 80°C when the initial CaO/H_2SO_4 molar ratio was 0.85.

The effect of particle size of colemanite on gypsum crystallization in batch reactor was investigated by Erdoğdu and coworkers (2003). The growth of the gypsum crystals were analyzed under microscope. As the colemanite particle size decreased, the dissolution rate of colemanite increases. Also, formation rate of gypsum crystals were faster if particle size of colemanite was small . It was concluded that the particle size of gypsum crystals formed during the reaction increased with increasing particle size of reacted colemanite in given ranges.

Çakal and coworkers (2003) studied the simulation of gypsum crystallization in continuous boric acid reactors by microfluid and macrofluid models. In this study, the batch reactor kinetic data was used to evaluate the conversion of calcium ion in the solution to gypsum crystals in continuous reactors by either microfluid or macrofluid models. It was found that the mean conversion obtained from macrofluid model was lower than the mean conversion obtained from microfluid model.

CHAPTER 3

EXPERIMENTAL

3.1 Materials used

In this study; colemanite, sulfuric acid and distilled water were used as reactants for the boric acid production reaction.

The colemanite minerals were provided from a region of Emet, Kutahya, Turkey. Three types of colemanite minerals having different chemical composition and particle size were used. The sulfuric acid was supplied by Eti Holding A.S. Its grade was 93% by weight. The third reactant the distilled water was obtained by distilling the tap water by the use of a water distillation apparatus (Nüve NS 108) at METU Boric Acid Research Laboratory. All the other chemicals used in the analysis were purchased in reagent grade from Merck and J.T Baker.

3.2 Set-up

Experimental set-up consists of a reactor, a mechanical stirrer, a heating jacket, a pH meter, a thermocouple, a temperature control unit and a vacuum pump. The schematic representation and picture of the experimental set-up are given in Figure 3.1 and Figure 3.2, respectively.

The batch reactor is made up of borosilicate glass. Inside diameter of the reactor and height of the reactor is 12 and 30 cm, respectively. The top section of the reactor is covered by a plastic. The top section of the reactor has four entrances. At the center, stirrer is placed. One of the other entrances is for placing thermocouple which is connected to the temperature control unit. The third entrance is used for

putting reactants in the reactor and placing the electrode inside the reactor. The samples are withdrawn from the last entrance of the reactor.

A mechanical stirrer (Heidolph RZR 2041) is used to mix the slurry in the reactor and baffles are placed inside the reactor to avoid vortex formation. The stirring rate can be adjusted between 50-1200 rpm. The mixing rate of the stirrer can be seen on the monitor of the stirrer.

The reaction temperature is controlled by a temperature controller unit. This unit consists of a thermocouple, a temperature controller and heating jacket. The batch reactor is placed in a heating jacket and the thermocouple connected the temperature controller is put into the reactor. The reaction temperature is kept constant at desired temperature during each experiment by adjusting a set point on the temperature controller. The reaction temperature can be seen on the display of temperature controller.
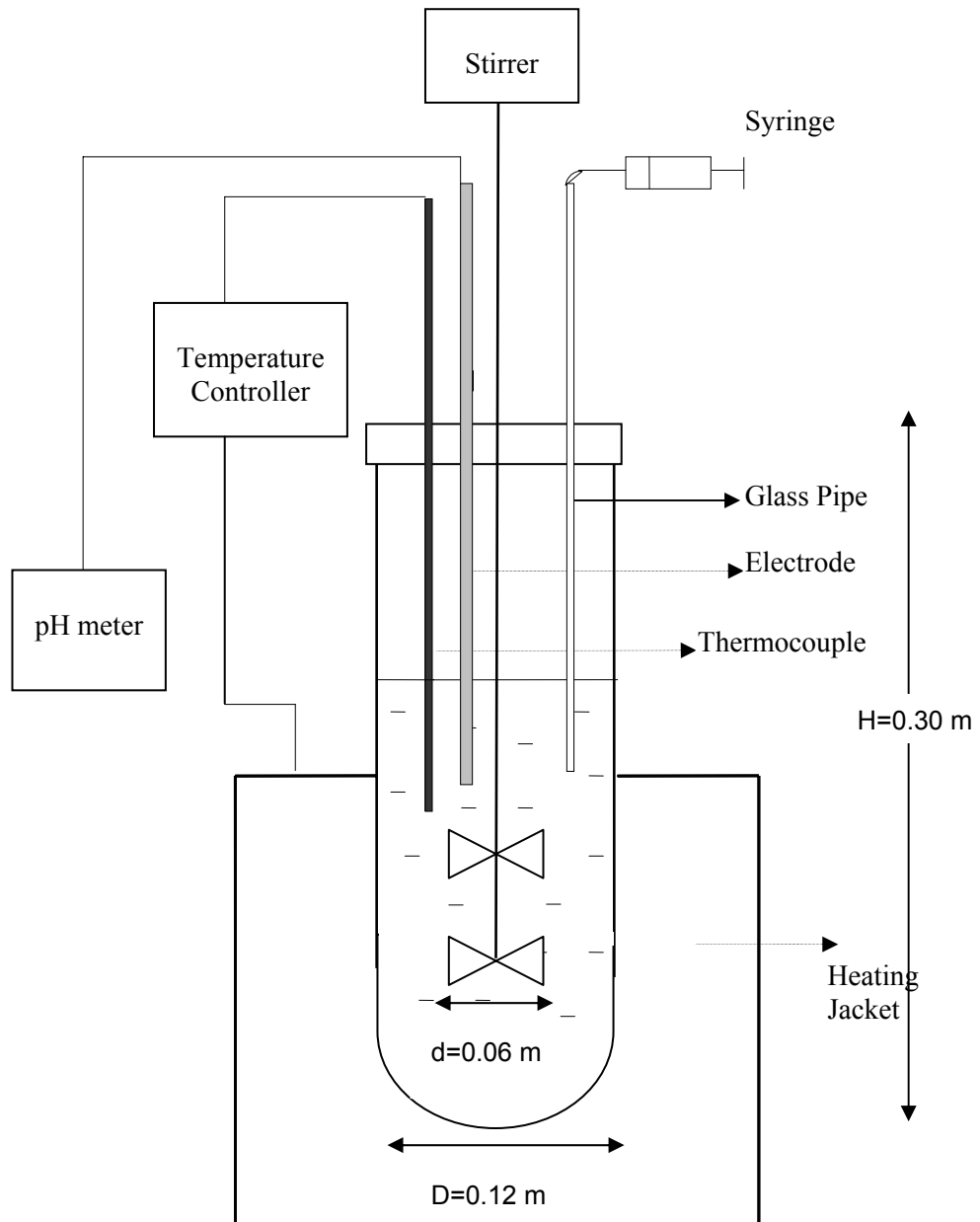
Figure 3.1. The schematic representation of the experimental set-up without filtration unit

Figure 3.2. The picture of the experimental set-up without filtration unit

The change in pH of the slurry as a function of the time is measured by a pH meter (Mettler Toledo MP 200). It is put into the reactor and pH of the slurry is recorded. Before each experiment, it is calibrated with standard buffer solutions.

A 50 ml syringe attached to a glass pipe is used to withdrawn the sample from the reactor.

The products, boric acid and gypsum are separated by use of vacuum filtration. This unit consists of a vacuum pump (KNF NO22) connected to a flask and a funnel was placed on top of flask. Filter paper is placed on the funnel and solid particles are collected on the filter paper whereas, boric acid solution is collected in the flask. The filtration unit set-up is given in Figure 3.3.
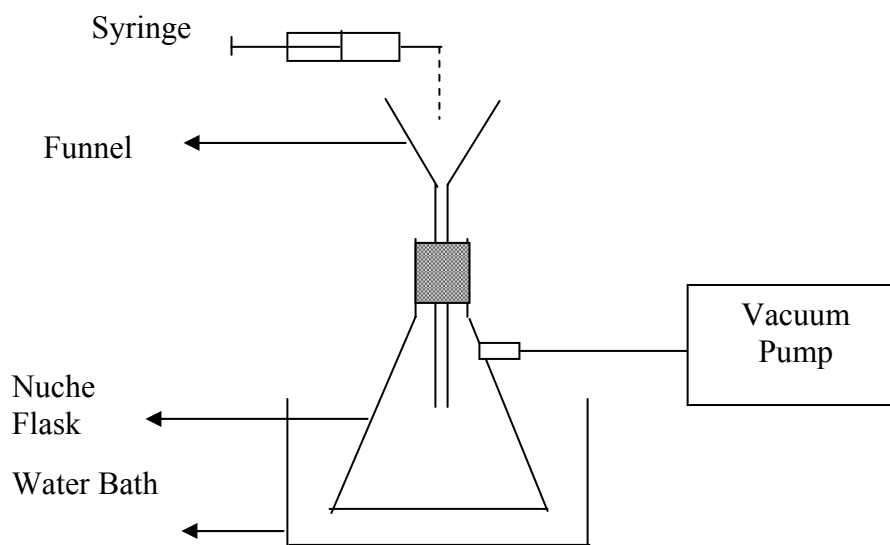
Figure 3.3 Schematic representation of filtration unit

3.3 Experimental Procedures

3.3.1 Size Reduction of Colemanite

Hisarcık 1 and Hisarcık 2 colemanite were supplied from Eti Holding A.S. The average particle sizes of these colemanite minerals were about 2.5-10 cm. Therefore, Hisarcık 1 and Hisarcık 2 colemanites were crushed in a jaw crusher, grinded in a hammer and then sieved. The sieve analysis was performed to get the size distribution of Hisarcık 1 and Hisarcık 2 colemanite.

Hisarcık 3 colemanite was brought from Emet Boric Acid Plant. The maximum diameter of the colemanite minerals was 150 μm.

3.3.2 Experimental Procedure

Firstly, a given amount of distilled water was put into the reactor. The mechanical stirrer was started to operate at desired stirring rate. Then sulfuric acid was added slowly into the reactor. An initial sulfate concentration of 0.623 M in solution was used for all experiments. The temperature control unit was adjusted to reaction temperature and kept constant. Certain amount of colemanite was fed into the reactor at once. This time was considered as the starting time of the reaction. The electrode was placed in the reactor to measure the pH of the slurry. The samples were withdrawn by 50 ml syringe attached to a glass pipe. Then, samples were filtered immediately by using vacuum pump connected to 250 ml nuche flask. A funnel was placed on top of flask. Blue band filter paper was put on the funnel. In order to prevent the boric acid solution to crystallize, the flask was placed into hot water. Solid particles and liquid were collected on filter paper and flask, respectively. The liquid portion was taken from the flask by the help of micropipettes (Finpipette, Thermo Labsystems) and analyzed for boric acid and calcium ion concentration. The filtrates were analyzed for change of crystal structure of gypsum with respect to time.

3.4. Analytical Procedures

The slurry samples taken from the reactor were filtered immediately. In the liquid phase, boric acid, calcium, sulfate and magnesium ion concentrations were determined. The crystal size distribution in the solid phase was determined. The crystal images were analyzed by using light microscope.

3.4.1. Determination of Boric Acid Concentration

The boric acid concentration was determined by using the procedure given in Appendix A. The procedure was as follows:

Two-three drops of methyl red indicator were added to 5 ml of filtrate. Then H_2SO_4, (1:3 by vol.) was added to the solution until the color of the solution was pink. The solution was titrated with 6 N NaOH until the color is changed from pink to yellow. H_2SO_4 was added until the color of the solution turns to pink. The solution was titrated with 0.5 N NaOH until a pH of 4.5 was obtained. At this step a titrator (Schott, TitroLine easy) involving a magnetic stirrer and pH-meter was used to get accurate results. Phenolphatelyn indicator and 2-3 g mannitol were added to the solution. Finally, solution was titrated with 0.5 N NaOH until the pH of the solution becomes 8.5. The volume of NaOH used in the second titration step (pH between 4.5-8.5) was recorded. Boric acid concentration in the liquid phase was calculated from the .Equation 3.1.

$$\left[C_{H_3BO_3} \right] = V_{NaOH} \ F_{NaOH} \ N_{NaOH} / V_{sample} \qquad\qquad 3.1$$

where V_{NaOH}, F_{NaOH}, N_{NaOH} and V_{sample} are the volume of the NaOH used, factor of the NaOH, normality of NaOH, which was 0.5 N for this case, and the volume of the sample, which was 5 ml for this case, respectively.

3.4.2. Determination of Calcium Ion Concentration

Calcium ion concentration of a sample was determined by using Atomic Absorption Spectrophotometer (Philips PU 9200X) in METU Chemical Engineering Department. One milliliter of liquid sample was poured to a 100 ml plastic bottles and deionized water was added on the sample. Liquid sample was directly measured at atomic absorption spectrophotometer after diluting the sample to a maximum of 15 ppm. Before each analysis the atomic absorption spectrophotometer was calibrated between 0 - 15 ppm calcium content.

3.4.3. Determination of Crystal Size Distribution

Sample taken from the reactor was filtered. The cake was washed with a large volume of water.

The particle size distributions of the solid samples were determined by a particle size analyzer (Malvern Instruments, Mastersizer 2000), in Ankara University, Chemical Engineering Department, utilizing the principle of laser ensemble light scattering. This instrument can detect the particle range of 0.02-2000 μm. The analysis was done by using wet dispersion method with a repeatability of +/- 0.5%. Tap water was used as dispersant in the analysis.

In the analysis, some amount of solid was taken from the sample bottles and put into beaker filled with water. This beaker was put on its place in the analyzer. Solid was continued to be added until the laser obscuration value on the computer reaches 14-15%. Then the analyzer was ready to give the crystal size distribution of the sample. The analysis was repeated for several times to see if the same result was obtained or not. The resulting graph could be achieved and the volume weighted mean of the curve could be obtained from the computer program.

3.4.4. Crystal Image Analysis

The cake was analyzed for crystal structure of solid particles. A small amount of solid sample was taken and put on the glass. A drop of water was added because it was not possible to analyze the dry filtrate. Then, the samples were analyzed.

Morphology of gypsum crystals was obtained by a light microscope connecting to online to a computer by a Pro Series, high performance CCD Camera. Images were seen live in monitor by Image Pro Plus 3.0 software. Views of solid samples were snapped and saved into the computer. The magnification bar was added on each picture of the crystals views.

3.5 Scope of the Experiments

Three sets of experiments were performed during the study. The effect of the particle size of colemanite, stirring rate and temperature on dissolution of colemanite, gypsum formation and particle size distribution of gypsum crystals were investigated.

In the experiments three different colemanite minerals were used. These colemanite minerals had different chemical compositions. They were named as Hisarcık 1, Hisarcık 2 and Hisarcık 3. The chemical analysis of colemanite minerals are given in result section.

In the first set of the experiments, effect of particle size of colemanite on dissolution of colemanite, gypsum formation and particle size distribution of gypsum crystals was investigated. This set of experiments was divided into three groups. In the first group, the experiments were performed at 80 °C and 500 rpm. Two different particle sizes of Hisarcık 1 colemanite minerals were used. The initial CaO/SO$_4$$^{2-}$ molar ratio was kept constant at 0.85. In the second group, the experiments were performed at 80 °C and 500 rpm. Two different particle sizes of Hisarcık 2 colemanite minerals were used. The initial CaO/SO$_4$$^{2-}$ molar ratio was 0.95. In the third group, the experiments were performed at 85 °C and 500 rpm. Hisarcık 2 colemanite particles smaller and larger than the 250 μm were used. The initial CaO/SO$_4$$^{2-}$ molar ratio was 1.0.

In the second set of the experiment, it was aimed to investigate the effect of stirring rate. In this set, the temperature was kept constant at 85 °C and Hisarcık 2 colemanite particles larger than 250 μm was used. The initial CaO/SO$_4$$^{2-}$ molar ratio was kept constant at 1.0 in these experiments. The stirring rates were 350, 400 and 500 rpm.

In the last sets of the experiments, the effect of temperature was analyzed. This set of experiments was divided into two groups. In the first group, experiments were performed at 70, 80, 85 °C and the particle size of Hisarcık 2 colemanite larger than 250 µm was used. In the second group, experiments were performed at 80, 85, 90 °C and Hisarcık 3 colemanite mineral smaller than 150 µm was used. The performed experiments are listed in Table 3.1 and 3.2.

Table 3.1. The performed experiments

Experiment Name	Type of Colemanite	Temperature, °C	Stirring Rate, rpm	Particle size of colemanite, μm	CaO/SO$_4^{2-}$ Molar Ratio	Number of Propeller on the stirrer
H1.1	1	80	500	0-250	0.85	1
H1.2	1	80	500	250-1000	0.85	1
H2.1	2	70	400	250-1000	1.00	2
H2.2	2	80	400	250-1000	1.00	2
H2.3	2	85	350	250-1000	1.00	2
H2.4	2	85	400	250-1000	1.00	2
H2.5	2	85	500	250-1000	1.00	2
H2.6	2	80	500	0-250	0.95	1
H2.7	2	80	500	0-160	0.95	1
H2.8	2	85	500	0-250	1.00	2
H3.1	3	80	400	0-150	1.00	2
H3.2	3	85	400	0-150	1.00	2
H3.3	3	85	400	0-150	1.00	2
H3.4	3	90	400	0-150	1.00	2

Table 3.2. The set of the experiments

SET 1: Effect of Particle Size of Colemanite		
Constants	**Variables**	**Experiment Name**
Hisarcık 1 Colemanite SR=500 rpm T=80 °C Ca/SO$_4^{2-}$ =0.85	0-250 µm	H1.1
	250-1000 µm	H1.2
Hisarcık 2 Colemanite SR=500 rpm T=80 °C Ca/SO$_4^{2-}$ =0.95	0-250 µm	H2.6
	0-160 µm	H2.7
Hisarcık 2 Colemanite SR=500 rpm T=85 °C Ca/SO$_4^{2-}$ =1	0-250 µm	H2.8
	250-1000 µm	H2.5
SET 2: Effect of Stirring Rate		
Hisarcık 2 Colemanite 250-1000 µm T=85 °C Ca/SO$_4^{2-}$ =1	350 rpm	H2.3
	400 rpm	H2.4
	500 rpm	H2.5
SET 3: Effect of Temperature		
Hisarcık 2 Colemanite 250-1000 µm SR=400 rpm Ca/SO$_4^{2-}$ =1	70 °C	H2.1
	80 °C	H2.2
	85 °C	H2.4
Hisarcık 3 Colemanite 0-150 µm SR=400 rpm	80 °C	H3.1
	85°C	H3.2-H3.3

CHAPTER 4

RESULTS AND DISCUSSION

4.1. Results of Colemanite Analysis

4.1.1 The Screen Analysis of Colemanite

Hisarcık 1 colemanite brought from Kutahya, Emet had average particle size between 2.5-10 cm. Therefore, firstly Hisarcık 1 colemanite was crushed in the jaw crusher, then grinded in a hammer mill. Sieve analysis was performed to get the particle size distribution.

In the experiments, particles smaller than 250 µm and greater than 250 µm were used to investigate the effect of particle size of colemanite on dissolution of colemanite, gypsum formation and particle size distribution of gypsum crystals. Firstly, sieve analysis was performed to separate the particles larger than 250 µm. The 60 mesh sieve (corresponding to 250 µm) was used for this purpose. It was seen that nearly 35 percent of the colemanite was left on this sieve. In other words, nearly 35 percent of the colemanite particles were greater than 250 µm.

The screen analyses of the Hisarcık 1 colemanite smaller and greater than 250 µm are given in Table 4.1.1 and Table 4.1.2, respectively. In these tables, the mass fractions of the colemanite on each sieve and the cumulative mass fractions of the colemanite under that sieve were represented. The particle diameter is the maximum diameter of the particles that could pass the former sieve. The average particle diameter stands for the arithmetic mean of the minimum and maximum diameter of the particles on that sieve.

Table 4.1.1. The screen analysis of Hisarcık 1 colemanite 0-250 µm

Mesh No	Dpi, µm	Mass Fraction	Avg. Dpi, µm	Cum. Mass Fraction
60	250	0.348	-	0.652
70	212	0.046	231	0.606
100	150	0.152	181	0.454
120	125	0.013	138	0.441
Pan	-	0.441	63	0

Table 4.1.2. The screen analysis of Hisarcık 1 colemanite 250-1000 µm

Mesh No	Dpi, µm	Mass Fraction	Avg. Dpi, µm	Cum. Mass Fraction
25	710	0.162	-	0.838
35	500	0.201	605	0.637
45	355	0.403	428	0.234
60	250	0.214	303	0.02
Pan	-	0.02	125	0

Figure 4.1.1 and Figure 4.1.2 present the differential particle size distribution of the Hisarcık 1 colemanite particles smaller and greater than 250 µm, respectively. The mass fractions of the colemanite particles on each sieve according to their average particle diameters were illustrated. Figure 4.1.3 and Figure 4.1.4 show the cumulative particle size distribution of the Hisarcık 1 colemanite particles smaller and greater than 250 µm, respectively. For each particle diameter, cumulative mass fraction of the colemanite smaller than that diameter was represented. When the particle size distribution of the Hisarcık 1 colemanite mineral was examined, it was seen that most of the particles had average particle sizes of 62.5 µm and 427.5 µm, for particles smaller and greater than 250 µm, respectively.
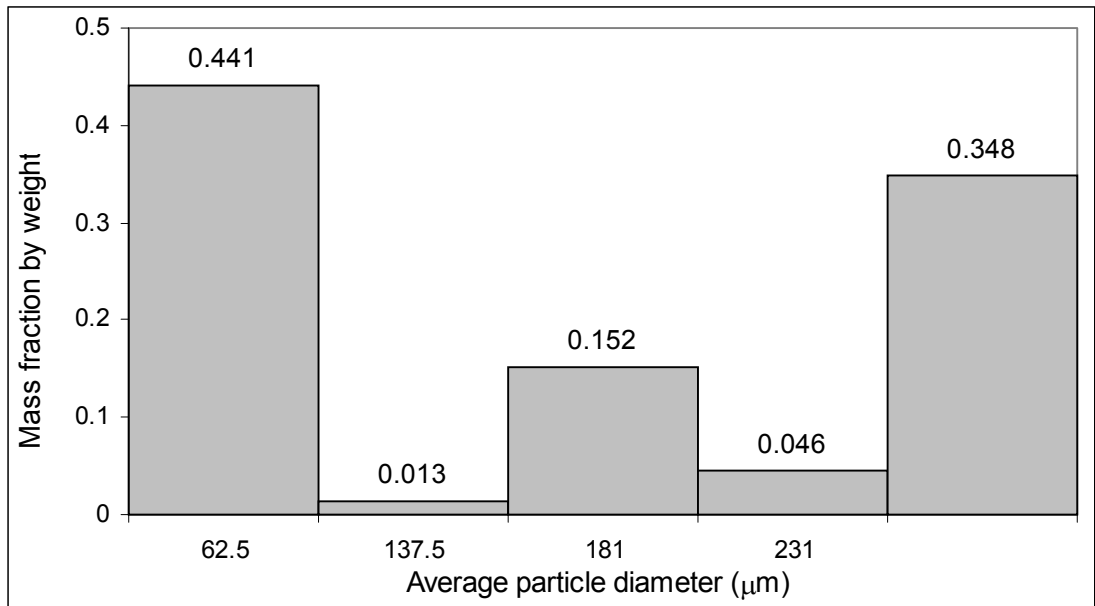
Figure 4.1.1. Differential particle size distribution of Hisarcık 1 colemanite 0-250 μm
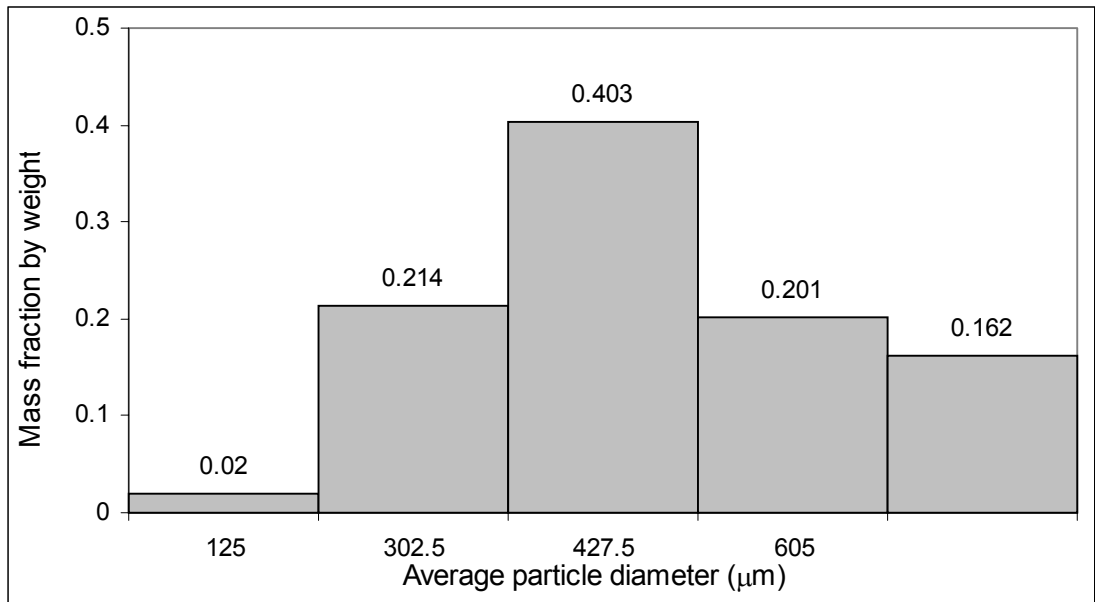
Figure 4.1.2. Differential particle size distribution of Hisarcık 1 Colemanite 250-1000 μm
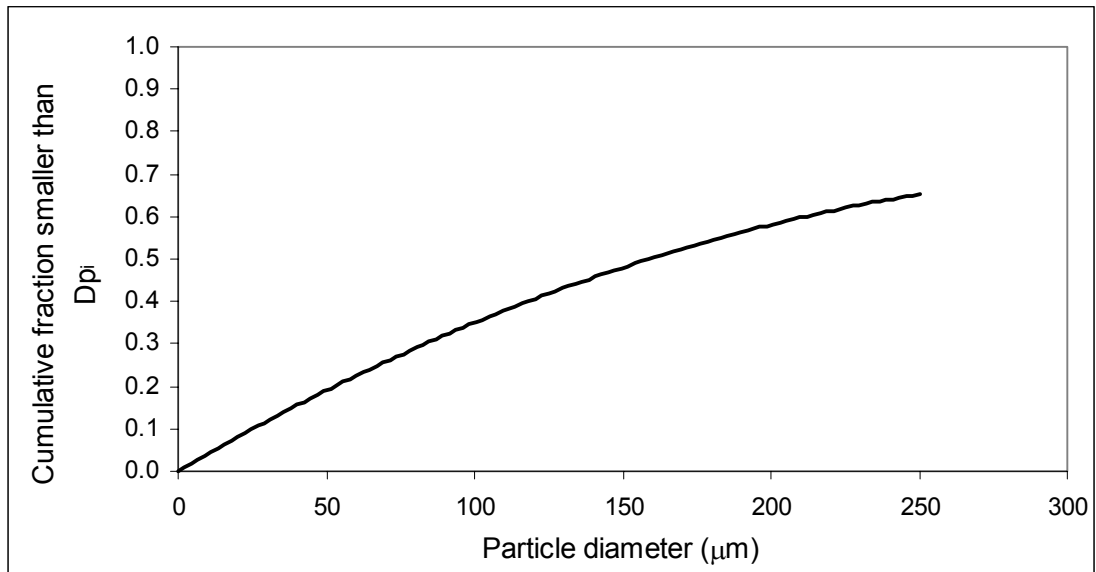
Figure 4.1.3. Cumulative particle size distribution curve for Hisarcık 1 colemanite 0-250 µm
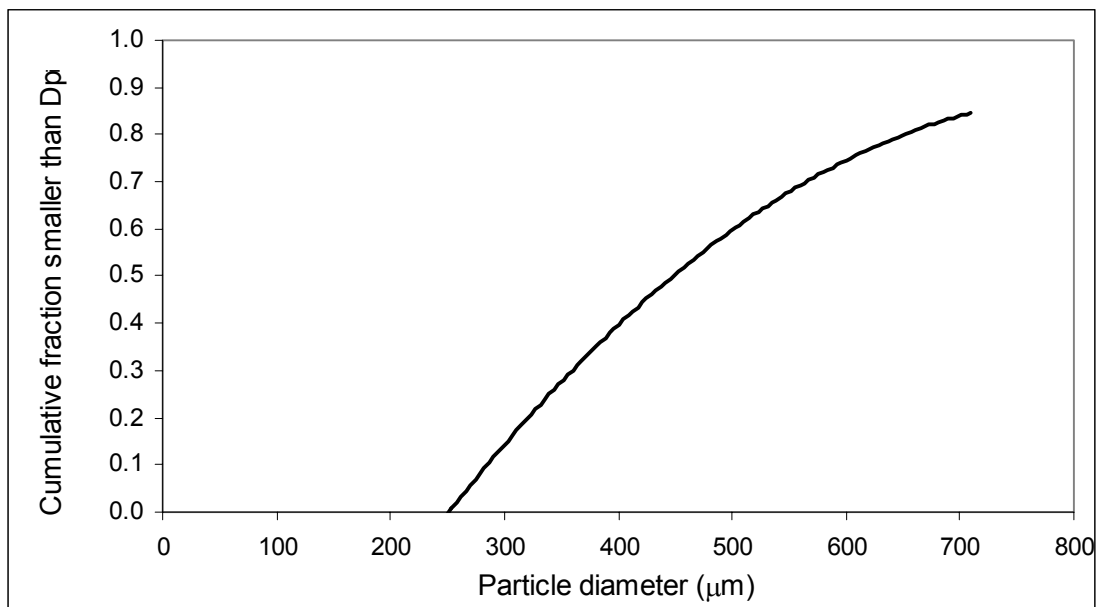
Figure 4.1.4. Cumulative particle size distribution curve for Hisarcık 1 Colemanite 250-1000 µm

Hisarcık 2 colemanite brought from Kütahya, Emet had average particle size between 2.5 and 10 cm. Therefore, Hisarcık 2 colemanite was crushed in the jaw crusher, then grinded in a hammer mill. Firstly, sieve analysis was performed to seperate the particles greater than 250 μm. The 60 mesh sieve (corresponding to 250 μm) was used for this purpose.

Table 4.1.3. The screen analysis of Hisarcık 2 colemanite 0-250 μm

Mesh No	Dpi, μm	Mass Fraction	Avg. Dpi, μm	Cum. Mass Fraction
60	250	0.280	-	0.720
100	150	0.370	200	0.350
140	106	0.170	128	0.180
170	90	0.075	98	0.105
270	53	0.063	45	0.042
Pan	-	0.042	27	0.000

Table 4.1.4. The screen analysis of Hisarcık 2 colemanite 250-1000 μm

Mesh No	Dpi, μm	Mass Fraction	Avg. Dpi, μm	Cum. Mass Fraction
25	710	0.193	-	0.807
35	500	0.305	605	0.502
45	355	0.312	428	0.19
60	250	0.176	303	0.014
Pan	-	0.014	125	0

Figure 4.1.5 and Figure 4.1.6 present the differential particle size distribution of the Hisarcık 2 colemanite particles smaller and greater than 250 μm, respectively. Figure 4.1.7 and Figure 4.1.8 show the cumulative particle size distribution of the Hisarcık 2 colemanite particles smaller and greater than 250 μm, respectively. From Figure 4.1.5 and Figure 4.1.6, it was seen that most of the particles had average particle sizes of 200 μm and 427.5 μm, for particles smaller and greater than 250 μm, respectively.
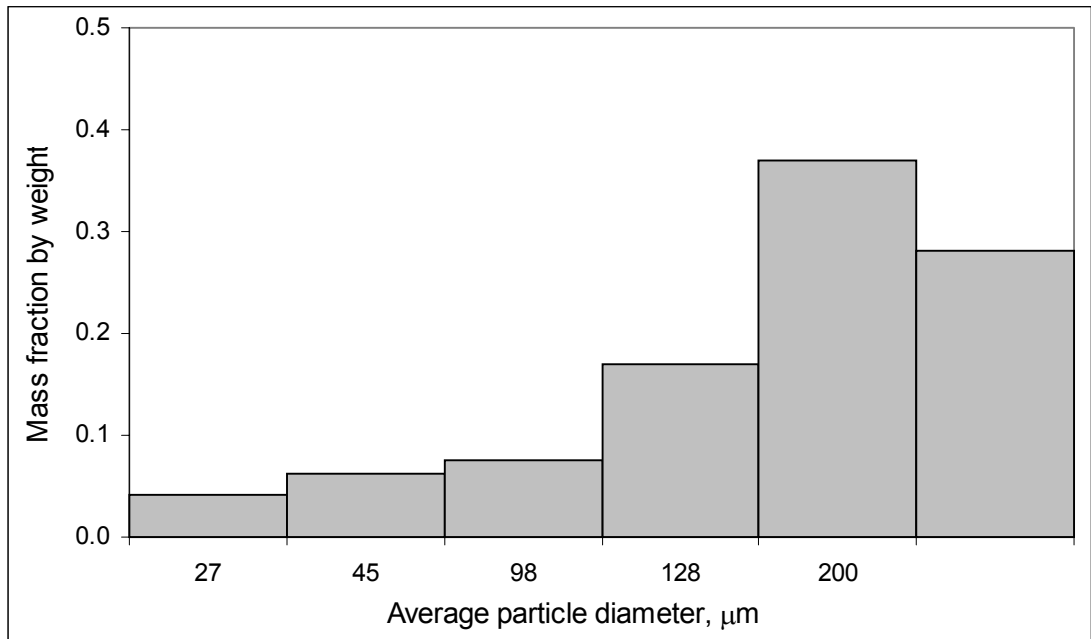
Figure 4.1.5. Differential particle size distribution of Hisarcık 2 Colemanite 0-250 µm
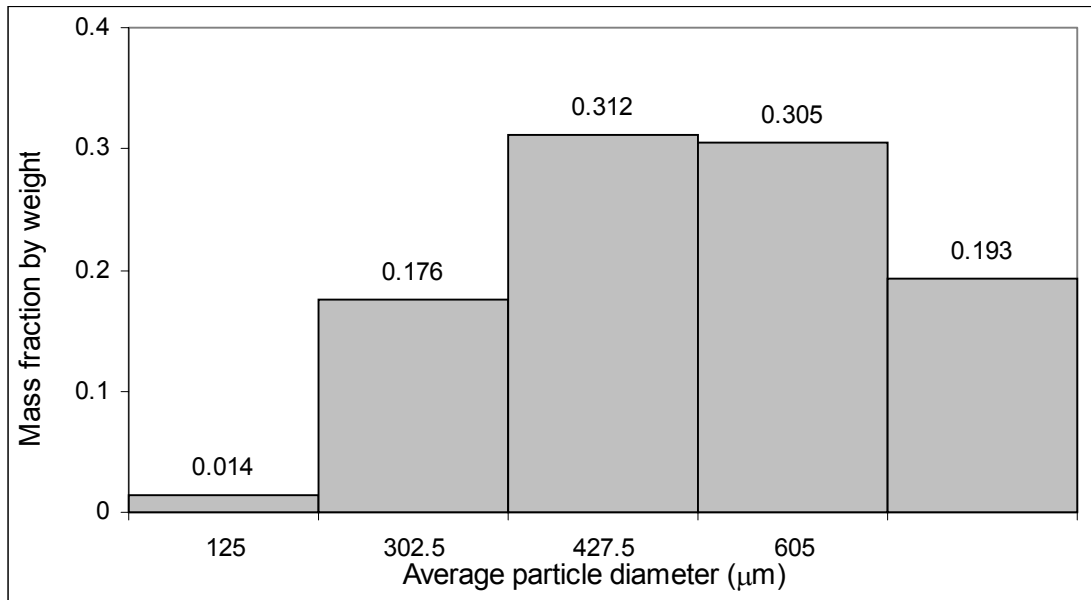
Figure 4.1.6 Differential particle size distribution of Hisarcık 2 Colemanite 250-1000 µm
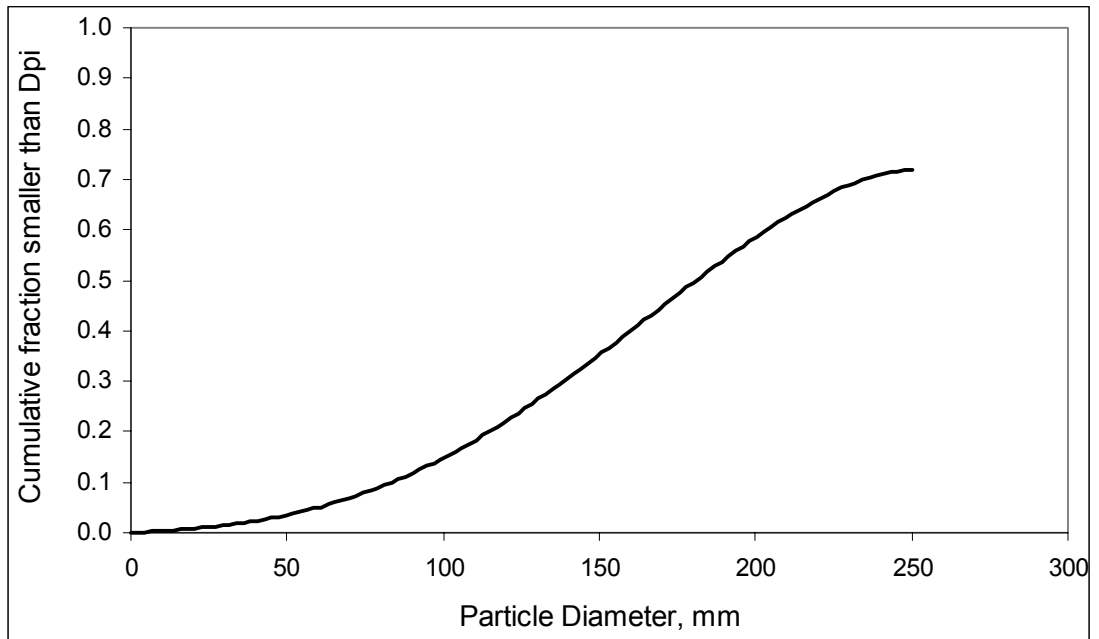
Figure 4.1.7. Cumulative particle size distribution curve for Hisarcık 2 Colemanite 0-250 µm
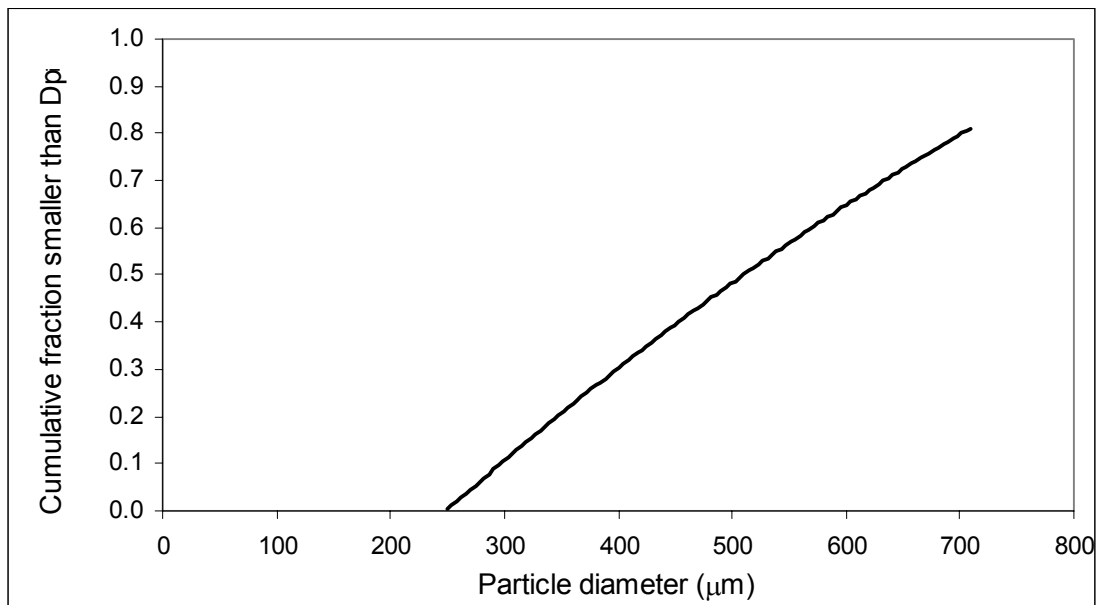
Figure 4.1.8 Cumulative particle size distribution curve for Hisarcık 2 Colemanite 250-1000 µm

Hisarcık 3 colemanite was brought from Emet Boric Acid Plant. The maximum diameter of the colemanite minerals was 150 µm. Therefore, no size reduction was necessary. The screen analysis of the Hisarcık 3 colemanite is given in Table 4.1.5. Figure 4.1.9 and Figure 4.1.10 present the differential particle size distribution and the cumulative particle size distribution of the Hisarcık 3 colemanite respectively.

Table 4.1.5. The screen analysis of Hisarcık 3 colemanite 0-150 µm

Mesh No	Dpi, µm	Mass Fraction	Avg. Dpi, µm	Cum. Mass Fraction
100	150	0.134	-	0.866
140	106	0.243	128	0.623
170	90	0.325	98	0.298
270	53	0.117	72	0.181
pan	-	0.181	26.5	0
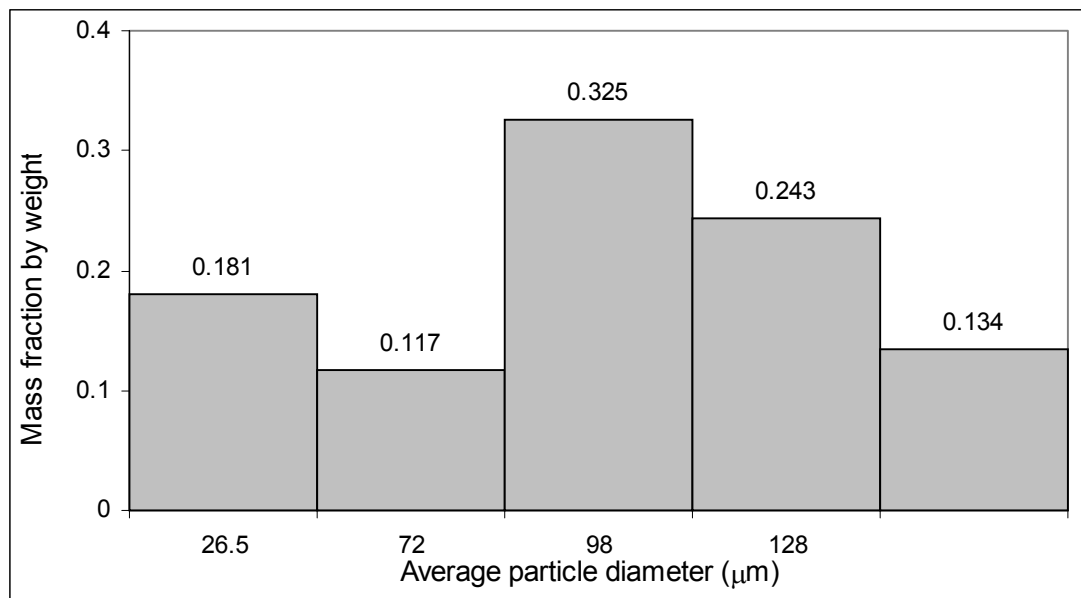
Figure 4.1.9 Differential particle size distribution of Hisarcık 3 Colemanite 0-150 µm
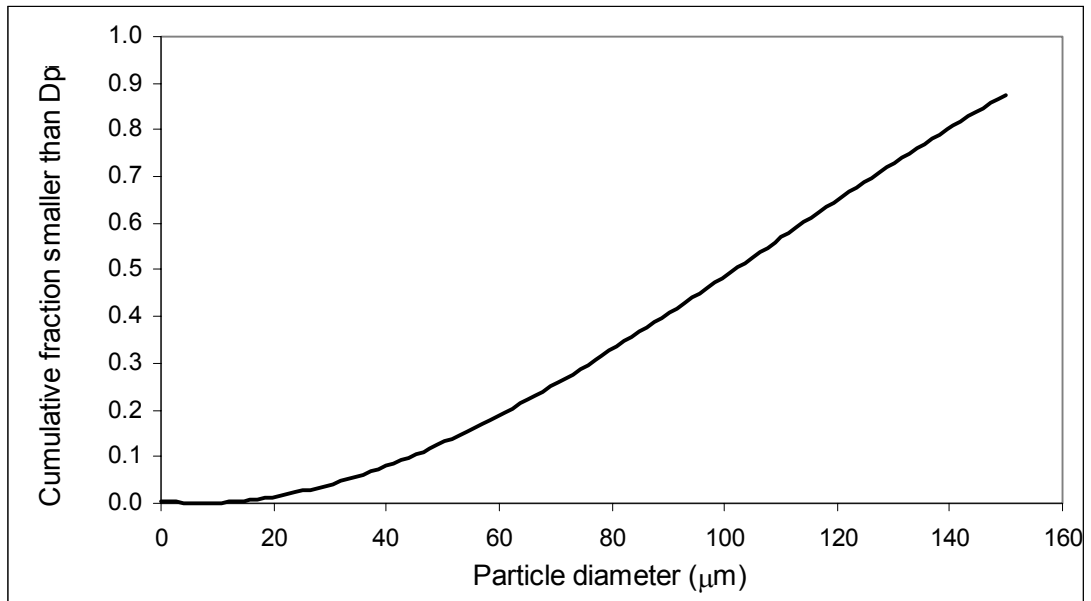
Figure 4.1.10 Cumulative particle size distribution curve for Hisarcık 3 Colemanite 0-150 µm

4.1.2. Chemical Analysis of Colemanites

The CaO and B_2O_3 contents of Hisarcık 1,2 and 3 Colemanites had to be known to calculate the amount of colemanite added to the reactor according to the CaO/SO_4^{-2} ratio chosen and the conversion of colemanite to boric acid, respectively.

Hisarcık 1,2 and 3 Colemanite were analyzed in METU, Chemical Engineering Department. The chemical analyses of colemanite used in the experiments are given in Table 4.1.5. As seen from this table, the change the result of the chemical analysis considerably; especially the calcium oxide and boron trioxide contents don't differ significantly, which are important values for the experiments.

Hisarcık 2 colemanite was the most valuable one among the three colemanites used in the study due to highest boron trioxide content. The lowest boron trioxide content was found for Hisarcık 3 colemanite.

Table 4.1.6. Chemical analysis of Hisarcık colemanites (dry basis, wt%)

Component	Hisarcık 1 Colemanite 0-250 µm	Hisarcık 1 Colemanite 250-1000 µm	Hisarcık 2 Colemanite 0-250 µm	Hisarcık 2 Colemanite 250-1000 µm	Hisarcık 3 Colemanite 0-150 µm
B_2O_3	39.17	37.72	43.57	43.87	34.61
CaO	23.63	24.23	30.90	28.61	28.40
Na_2O	0.58	0.78	0.22	0.79	1.30
MgO	1.92	1.93	0.79	0.45	2.36
Al_2O_3	1.77	1.48	0.22	0.17	1.49
SiO_2	18.51	19.71	0.60	0.21	2.23
SO_3	*	*	0.14	0.50	0.65
Fe_2O_3	1.06	0.84	0.17	0.31	0.61
As_2O_3	0.59	0.51	0.00	0.03	0.42
SrO	0.88	1.03	0.56	0.64	0.88
TiO_2	0.13	0.11	0.20	0.056	0.14
K_2O	2.27	1.55	0.08	0.059	0.74
BaO	0.02	0.02	0.005	0.015	0.017
Li	*	*	0.045	*	*
Others	9.47	10.09	22.50	17.46	26.15

* Analysis was not performed

4.2 Dissolution of Colemanite in Sulfuric Acid in a Stirred Batch Reactor

Particle size, stirring rate and temperature have been chosen as parameters to investigate their effects on the dissolution of colemanite, gypsum formation and particle size distribution of gypsum crystals.

4.2.1 The Effect of Particle Size of Colemanite

This set of experiments was divided into three groups. In the first group, the experiments were performed at 80 °C and 500 rpm by using Hisarcık 1 colemanite. The particles smaller and greater than the 250 µm were used. The initial CaO/SO$_4$$^{2-}$ molar ratio was 0.85. In the second group, the experiments were performed at 80 °C and 500 rpm stirring rate by using Hisarcık 2 colemanite. Colemanite minerals smaller than 250 µm and 160 µm were used. The initial CaO/SO$_4$$^{2-}$ molar ratio was 0.95. The third group of the experiments was performed at 85 °C and 500 rpm by

using Hisarcık 2 colemanite. The particles smaller and greater than the 250 µm were used. The initial CaO/SO_4^{2-} molar ratio was 1.0.

In the first group, two experiments were performed at the initial CaO/SO_4^{2-} molar ratio of 0.85 and at 80 °C . One propeller was used for stirring. The effect of particle size on dissolution of colemanite and formation of gypsum reactions were analyzed by using Hisarcık 1 colemanite minerals having different particle sizes. During the experiments, variations of the boric acid concentration and calcium ion concentration in the solution were determined.

The change in boric acid concentration in the liquid phase in dependency of the time at different particle size of colemanites is shown in Figure 4.2.1. As it is seen from the figure, the boric acid concentration increases with increasing time and it reaches an asymptotic value. The dissolution of colemanite can be followed by monitoring the boric acid concentration change in the slurry. As the colemanite dissolves, the boric acid concentration in the liquid phase increases. It is understood from Figure 4.2.1 that the dissolution rate of colemanite increases with decreasing particle size of colemanite because of the increasing surface area.

The crystallization of gypsum from the solution can be followed by the calcium ion concentration in the solution as it decreased by the formation of gypsum precipitate. The change in calcium ion concentration in the liquid phase as a function of time is shown in Figure 4.2.2. As it is observed in figure, calcium ion concentration in the liquid phase undergoes a rapid exponential decay and then approaches an asymptotic value of saturation concentration. The change in calcium ion with time was faster for small particle size of colemanite.
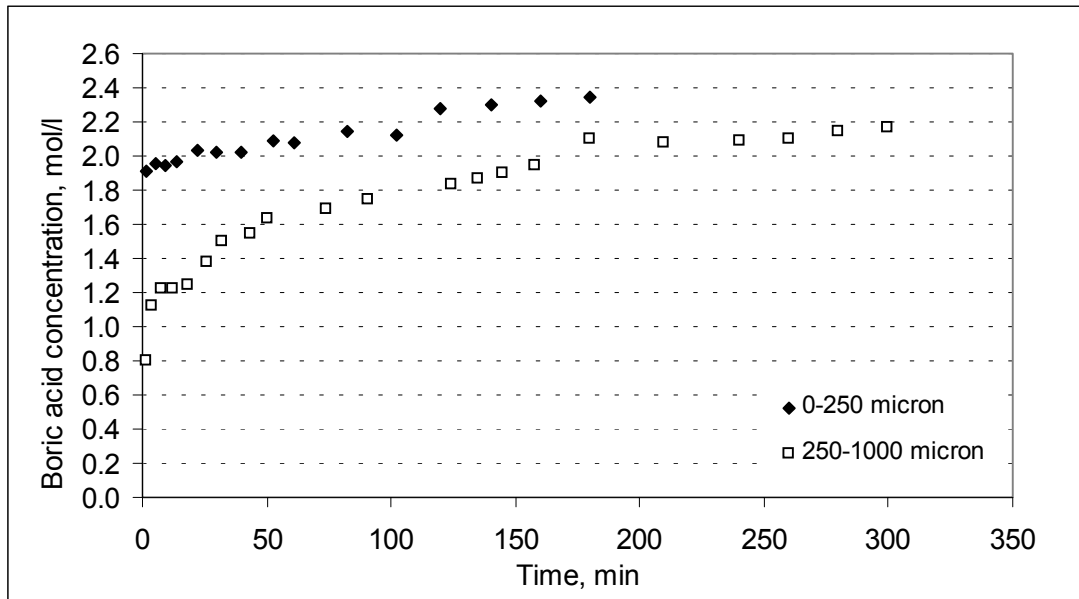
Figure 4.2.1 Variation of boric acid concentration in liquid with respect to time at different particle sizes of colemanite (Experiment H1.1 and H1.2, Hisarcık 1 Colemanite, CaO/SO_4^{2-} = 0.85, Stirring Rate = 500 rpm, T= 80°C)
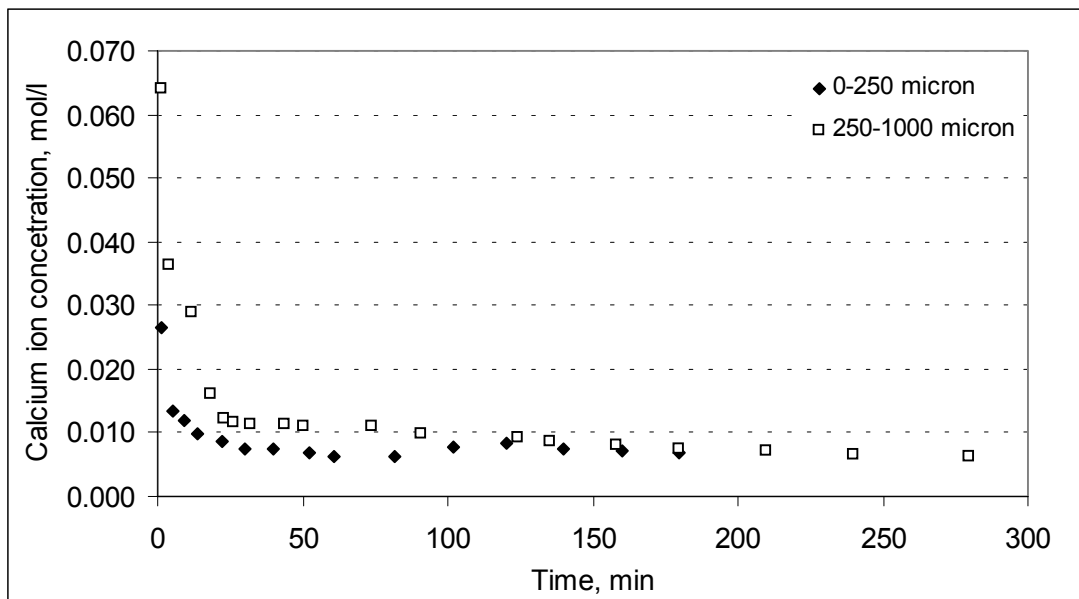
Figure 4.2.2. Variation of calcium ion concentration in liquid with respect to time at different particle sizes of colemanite (Experiment H1.1 and H1.2, Hisarcık 1 Colemanite, CaO/SO_4^{2-} = 0.85, Stirring Rate = 500 rpm, T= 80°C)

In the second group, there experiments were performed at the initial CaO/SO_4^{2-} molar ratio of 0.95 and at 80 °C. The effect of particle size on dissolution of colemanite and formation of gypsum reactions were analyzed by using Hisarcık 2 colemanite minerals having different particle sizes. During the experiments, variations of the boric acid concentration and calcium ion concentration in the liquid phase were determined.

Figure 4.2.3 shows that, the change of the boric acid concentration in the liquid phase with respect to time is slower for colemanite particles smaller than 250 μm. Also, a slightly inclined plateau is observed between 15 and 50 minutes only for these particles. Obviously, the colemanite particle size affects the dissolution reaction rate.

The change in calcium ion concentration in the liquid phase in dependency of the time is shown in Figure 4.2.4. In this figure it can be seen that the calcium ion in solution decreases faster for small particle size of colemanite. It means that the rate of gypsum crystallization reaction depends on the colemanite particle size.
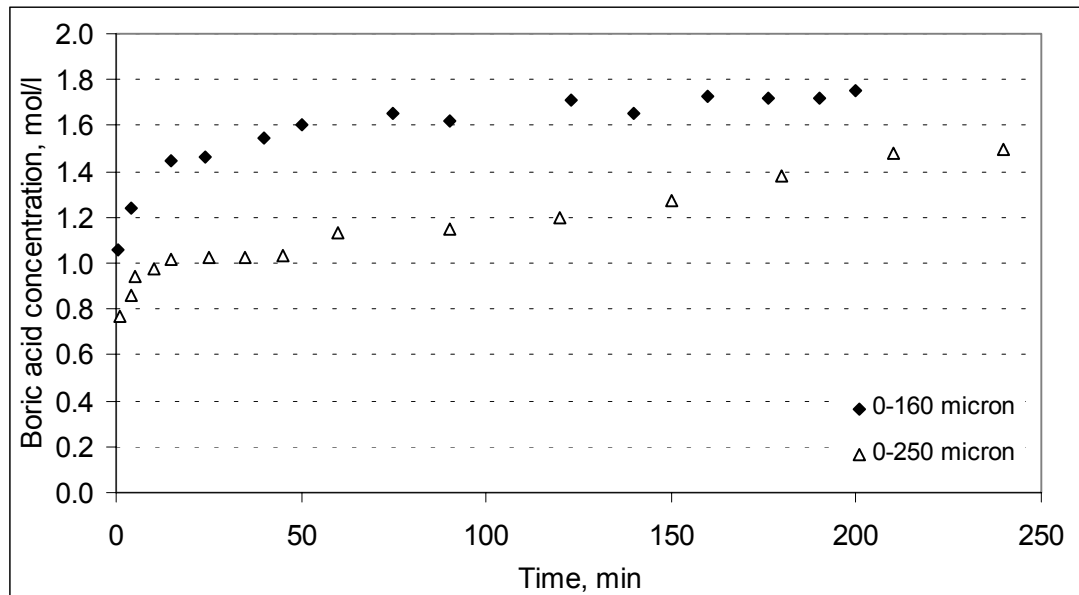
Figure 4.2.3 Variation of boric acid concentration in liquid with respect to time at different particle sizes of colemanite (Experiment H2.6 and H2.7, Hisarcık 2 Colemanite, CaO/SO_4^{2-} = 0.95, Stirring Rate = 500 rpm, T= 85 °C)
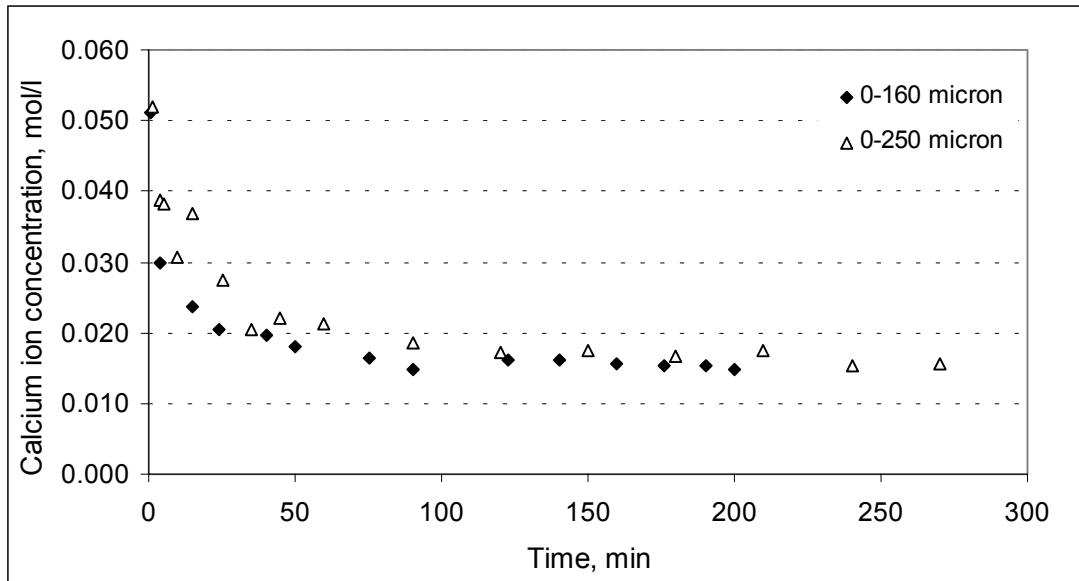
Figure 4.2.4. Variation of calcium ion concentration in liquid with respect to time at different particle sizes of colemanite (Experiment H2.6 and H2.7, Hisarcık 2 Colemanite, CaO/SO_4^{2-} = 0.95, Stirring Rate = 500 rpm, T= 85 °C)

In the third group, two experiments were performed at the initial CaO/SO_4^{2-} molar ratio of 1.00. In these experiments, temperature and stirring rate were kept constant at 85 °C and 500 rpm, respectively. The Hisarcık 2 colemanite minerals having two different particle sizes, greater and smaller than 250 μm were used. During the experiments, variation of the boric acid concentration, calcium ion concentration in the liquid phase and pH of the slurry with respect to time were determined.

Figure 4.2.5 illustrates the change in boric acid concentration in the liquid phase versus time at 85 °C, 500 rpm and initial CaO/SO_4^{2-} molar ratio of 1.00 for different particle sizes of colemanite. The reaction mixture was stirred by using two propellers As seen from the figure, the variation of boric acid concentration shows same trends for both particle sizes. In other words, insignificant effect of particle size of colemanite is observed if the experiments are performed with stirrer having two propeller. It means that stirrer type affects the dissolution.

The change in calcium ion concentration in the liquid phase in dependency of the time is shown in Figure 4.2.6. In this figure it can be seen that the same trend was

46

observed for two different particle sizes of colemanites. The saturation concentration of calcium ion is the same for both experiments. Because, the saturation concentration is depend on temperature. In these experiments, the temperature was kept constant at 85° C.

Effect of particle size of colemanite on dissolution and gypsum formation reactions becomes negligible if the stirrer used has two propellers. This showed that the stirrer type used is a critical parameter for boric acid production.

Figure 4.2.7 shows the change in the pH of the slurry with respect to time at 85 °C , 500 rpm and initial CaO/SO_4^{2-} molar ratio of 1.00 for different particle sizes. As te colemanite reacts with sulfuric acid, boric acid is produced and sulfuric acid is consumed. As the boric acid is a weak acid with respect to sulfuric acid, the pH of the slurry increases with increasing time.

For small particle size of colemanite, the pH of the slurry increases and then it decreases up to 0.72. For larger particles, the pH of the slurry increases with time. Then, it reaches a steady state value of 0.69.
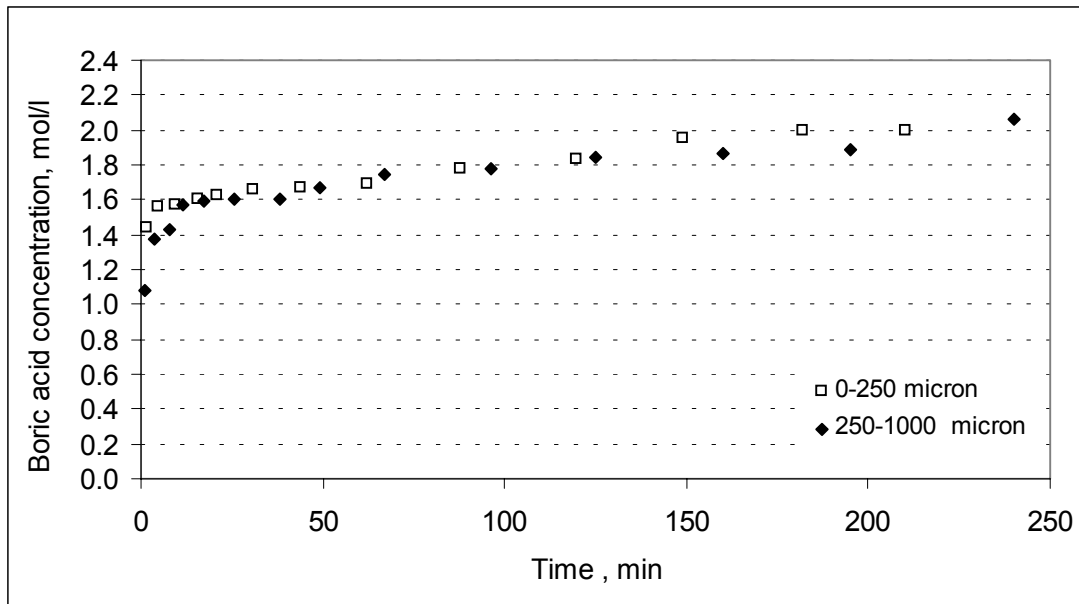
Figure 4.2.5 Variation of boric acid concentration in liquid with respect to time at different particle sizes of colemanite (Experiment H2.5 and H2.9, Hisarcık 2 Colemanite, CaO/SO_4^{2-} = 1, Stirring Rate = 500 rpm, T= 85 °C)
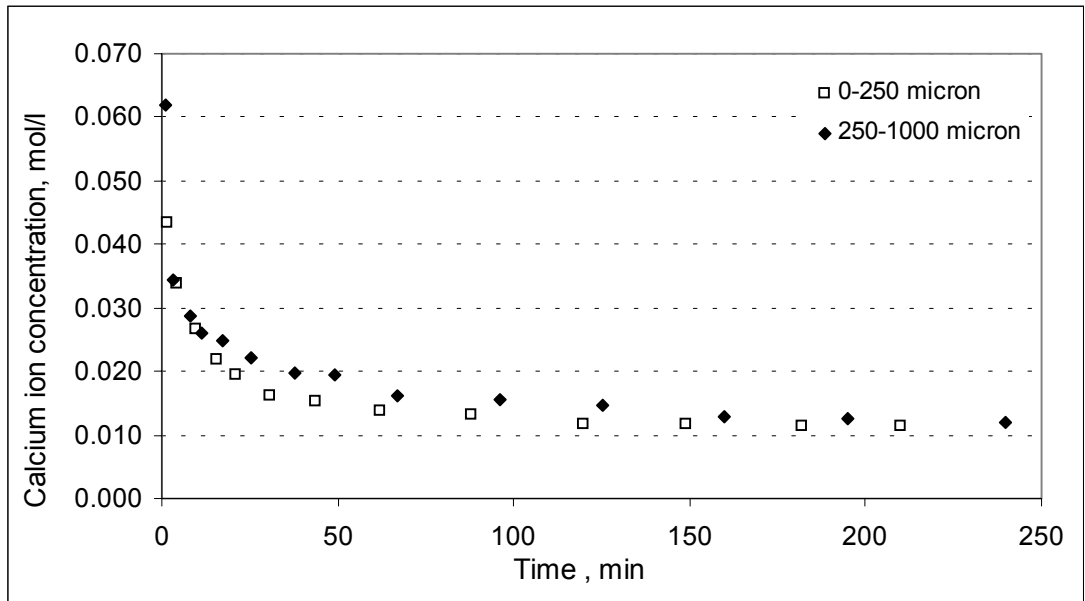
Figure 4.2.6. Variation of calcium ion concentration in liquid with respect to time at different particle sizes of colemanite (Experiment H2.5 and H2.9, Hisarcık 2 Colemanite, CaO/SO_4^{2-} = 1, Stirring Rate = 500 rpm, T= 85 °C)
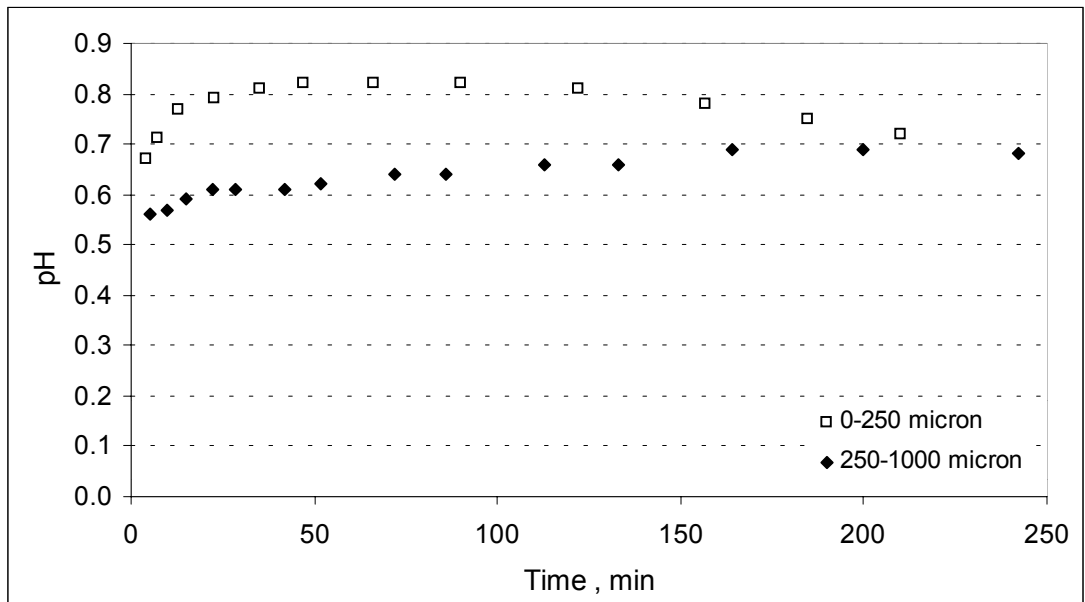
Figure 4.2.7 Variation of pH of the slurry with respect to time at different particle sizes of colemanite(Experiment H2.5 and H2.9,Hisarcık 2 Colemanite,CaO/SO_4^{2-}= 1, Stirring Rate = 500 rpm, T= 85 °C)

4.2.2 The Effect of Stirring Rate

Three experiments were performed at the initial CaO/SO_4^{2-} molar ratio of 1.00 and at 85 °C. The effect of stirring rate on dissolution of colemanite and formation of gypsum reactions were analyzed at 350, 400 and 500 stirring rates. During the experiments, variation of the boric acid concentration, calcium ion concentration in the liquid phase and pH of the slurry with respect to time were determined.

The tip speed of agitator was calculated from the Equation 4.1.

$$U = \pi \, d \, \frac{n}{60} \qquad\qquad 4.1$$

where U is the tip speed in m s^{-1}, d is the diameter of the agitator in m and n is the stirring rate in rpm.

The diameter of the agitator was 0.06 m. The agitator tip speeds were calculated for 350, 400 and 500 rpm stirring rates and found as 1.1, 1.26 and 1.57 m s^{-1}, respectively.

The change in boric acid concentration in the liquid phase in dependency of the time at different stirring rate is shown in Figure 4.2.8. As seen from the figure, the boric acid concentration at certain time increases with increasing stirring rate. This means that the dissolution of colemanite reaction is limited by the rate of diffusion of sulfate ions through the surface of the solid colemanite particles. The increasing stirring rate increases the mass transfer of H$^+$ ions in solution through colemanite particles so the boric acid concentration increases with increasing stirring rate. The maximum boric acid concentration is obtained as 2.06 mol L^{-1} at 500 rpm stirring rate.

Figure 4.2.9 illustrates the effect of stirring rate on calcium ion concentration in the liquid phase. As seen from the figure, the calcium ion concentration at 500 rpm decreases faster. It means that increasing stirring rate increases the mass transfer of H+ ions through colemanite and it dissolves faster and gives Ca ion but these calcium ions spontaneously react with sulfate ions and so this increases rate of the formation of gypsum crystals so the calcium ion in the solution decreases faster with increasing stirring rate.

49

The change in pH of slurry in dependency of the time at different stirring rate is shown in Figure 4.2.10. The stirring rate affects the dissolution reaction and formation of gypsum reaction so the pH changes with different stirring rates. The highest boric acid concentration was obtained at 500 rpm, therefore the lowest pH was determined at this stirring rate.
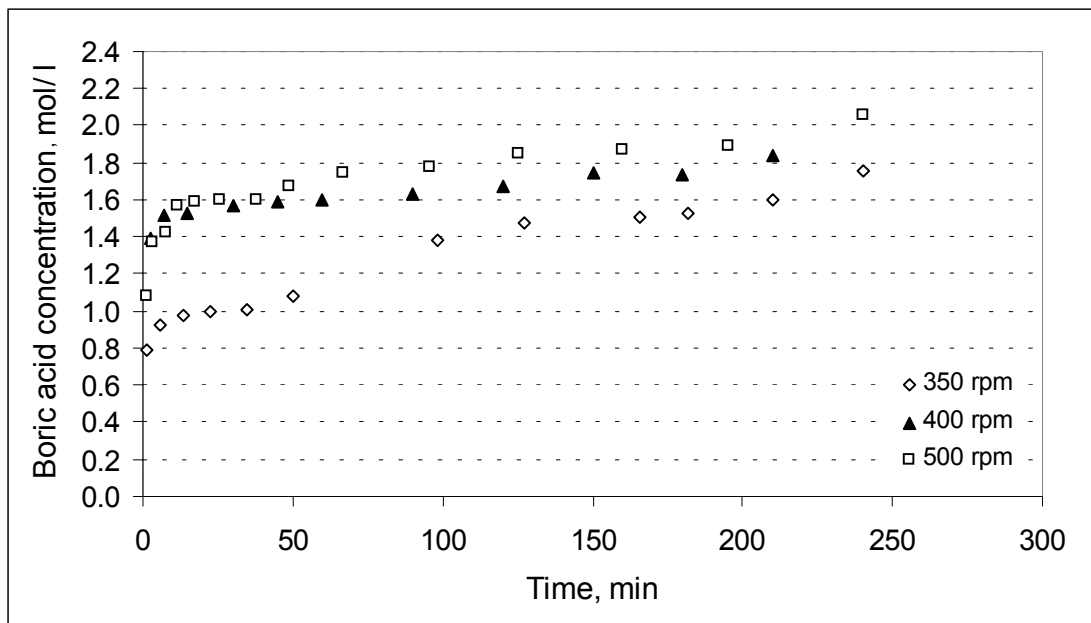
Figure 4.2.8.Variation of boric acid concentration in liquid with respect to time at different stirring rates (Experiment H2.3, H2.4 and H2.5, Hisarcık 2 Colemanite, CaO/SO_4^{2-} = 1, Stirring Rate = 500 rpm, T= 85 °C)
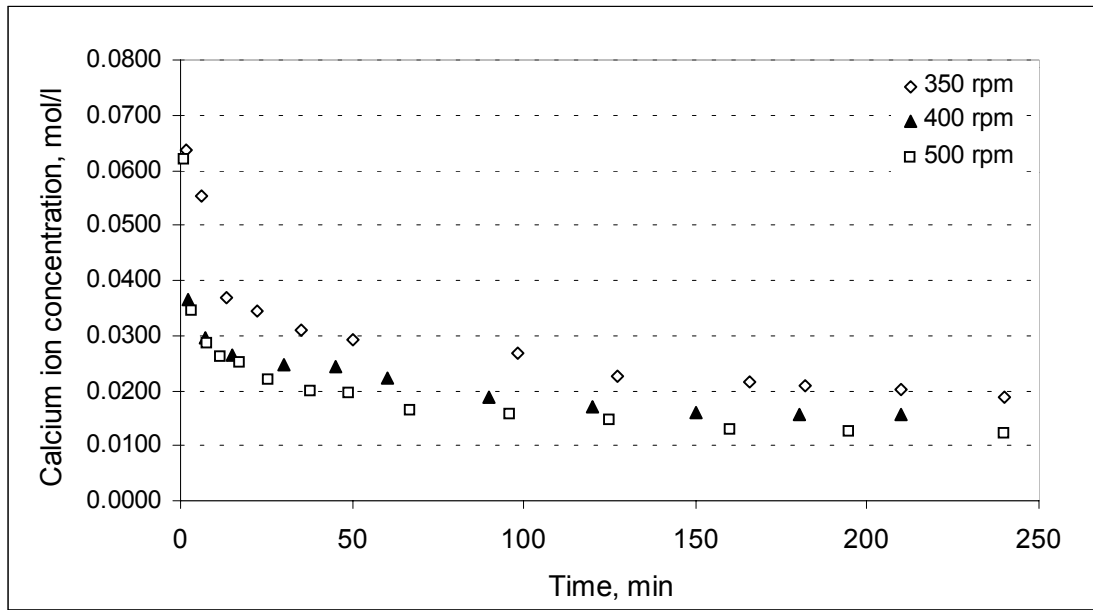
Figure 4.2.9. Variation of calcium ion concentration in liquid with respect to time at different stirring rates (Experiment H2.3, H2.4 and H2.5, Hisarcık 2 Colemanite, CaO/SO$_4^{2-}$ = 1, Stirring Rate = 500 rpm, T= 85 °C)
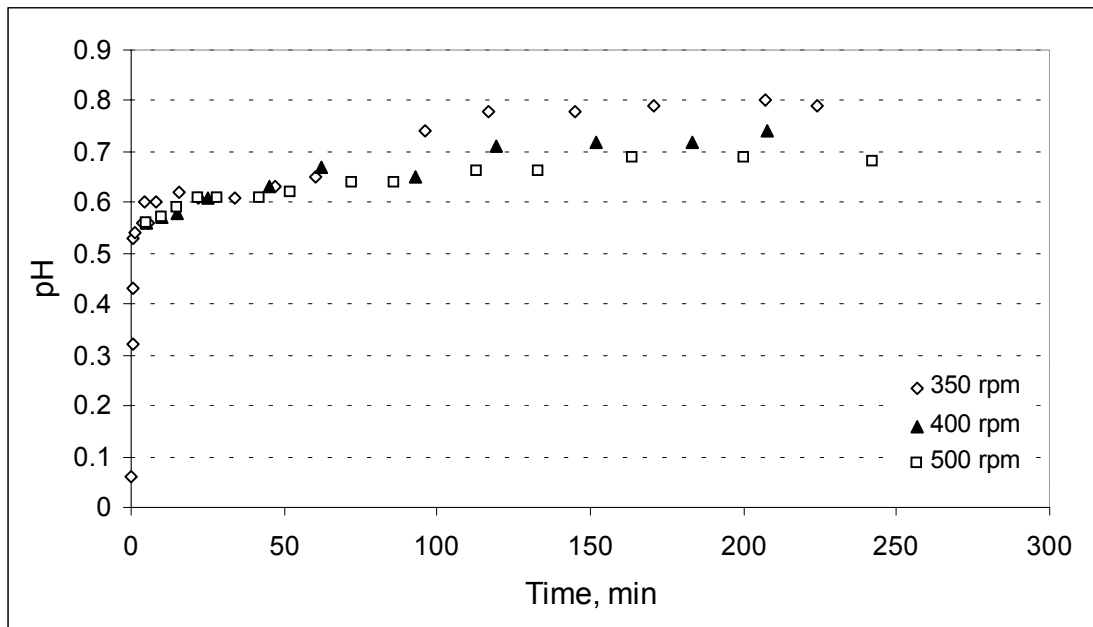
Figure 4.2.10. Variation of pH of the slurry with respect to time at different stirring rates (Experiment H2.3, H2.4 and H2.5, Hisarcık 2 Colemanite, CaO/SO$_4^{2-}$ = 1, Stirring Rate = 500 rpm, T= 85 °C)

4.2.3 The Effect of Temperature

Two different types of colemanite were used. Experiments were performed at 70, 80, 85 °C for the particle size of Hisarcık 2 colemanite greater than 250 μm and 80, 85, 90 °C for Hisarcık 3 colemanite particles smaller than 150 μm.

In the first group, three experiments were performed at the initial CaO/SO_4^{2-} molar ratio of 1.00,. In these experiments, stirring rate was kept constant at 400 rpm. The Hisarcık 2 colemanite minerals particle sizes greater than 250 μm were used. During the experiments, variation of the boric acid concentration, calcium ion concentration in the liquid phase and pH of the slurry with respect to time were determined.

The change in boric acid concentration in the liquid phase in dependency of the time at different temperatures is shown in Figure 4.2.11. As seen from the figure, the boric acid concentration at certain time increases with increasing temperature. Temperature affects the dissolution rate of colemanite. In this range of temperature, the dissolution rate increases with increasing temperature. This means that the rate of boric acid production depends on the reaction temperature.

Figure 4.2.12 shows the change in calcium ion concentration with respect to time at different temperatures. As seen from the figure, saturation concentration of calcium ion increases with decreasing temperature. At 85 °C, the calcium ion concentration reaches the minimum point at the end of the experiment.

The change in pH of slurry in dependency of the time at different temperatures is shown in Figure 4.2.13. The temperature change affects the dissolution reaction and formation of gypsum reaction so it affects the pH of the slurry also. In all experiments, the pH of the slurry increases with time and then it approaches a steady state value.
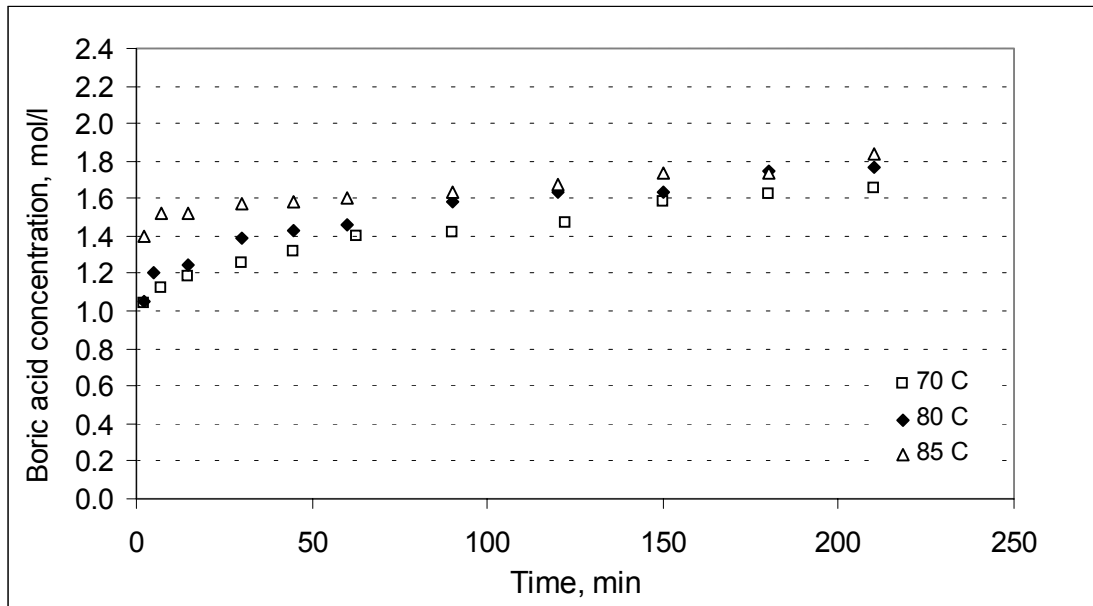
Figure 4.2.11.Variation of boric acid concentration in liquid with respect to time at different temperatures (Experiment H2.1, H2.2, and H2.4, Hisarcık 2 Colemanite, CaO/SO_4^{2-} = 1, Stirring Rate = 400 rpm)
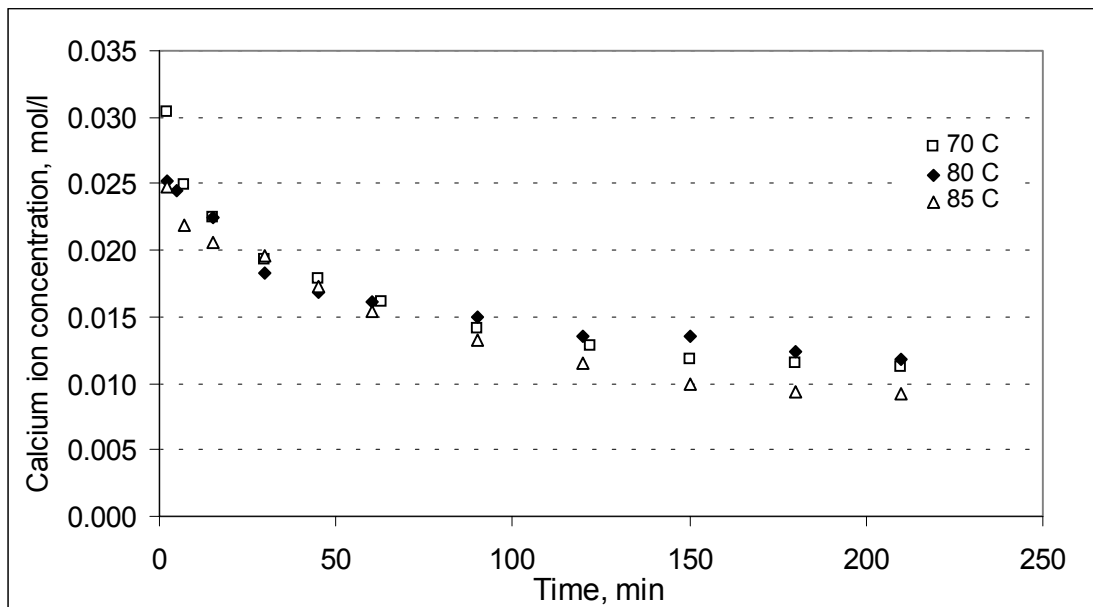
Figure 4.2.12. Variation of calcium ion concentration in liquid with respect to time at different temperatures (Experiment H2.1, H2.2, and H2.4, Hisarcık 2 Colemanite, CaO/SO_4^{2-} = 1, Stirring Rate = 400 rpm)
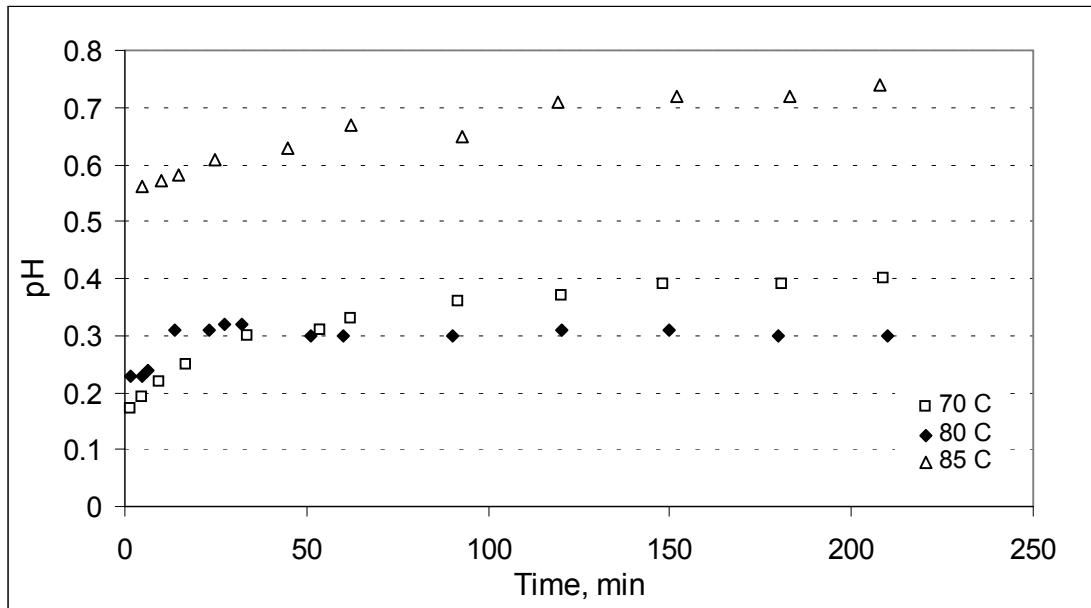
Figure 4.2.13. Variation of pH of the slurry with respect to time at different temperatures (Experiment H2.1, H2.2, and H2.4, Hisarcık 2 Colemanite,CaO/SO_4^{2-} =1, Stirring Rate = 400 rpm)

In the second group, four experiments were performed at the initial CaO/SO_4^{2-} molar ratio of 1.00. The Hisarcık 3 colemanite particles smaller than 150 μm were used. The stirring rate was kept constant at 400 rpm. The effect of temperature on dissolution of colemanite and formation of gypsum reactions was studied at 80, 85, 90 °C. During the experiments, variation of the boric acid concentration, calcium ion concentration in the liquid phase and pH of the slurry with respect to time were determined.

The variation of boric acid concentration in the liquid phase with respect to time at different temperatures is given in Figure 4.2.14. As seen from the figure, the change in boric acid concentration in dependency of time is slower at 80 °C than 85 and 90 °C. Also, fastest dissolution is observed at 85 °C. However, further increase in the reaction temperature decreases the dissolution rate of colemanite as it is seen in Figure 4.2.14. The dissolution rate at 90 °C is slower than the dissolution rate at 85 °C.

Figure 4.2.15 illustrates the effect of temperature on calcium ion concentration in the liquid phase. It shows that the lowest saturation concentration of calcium ion is obtained at 90 °C. As seen from the figure, saturation concentration of calcium ion increases with decreasing temperature.

The change in pH of slurry in dependency of the time at temperatures is shown in Figure 4.2.16. In all experiments, the pH of the slurry increases with time and finally it reaches an asymptotic value. The highest pH of the slurry was obtained at 90 °C.
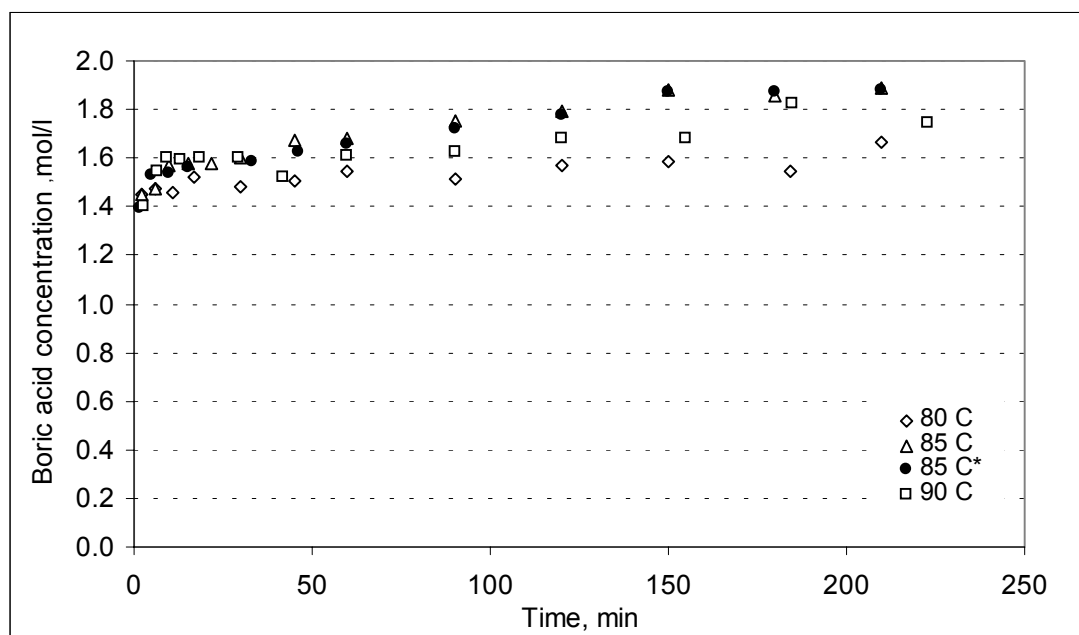
Figure 4.2.14. Variation of boric acid concentration in liquid with respect to time at different temperatures (Experiment H3.1, H3.2, H3.3 and H3.4, Hisarcık 3 Colemanite, CaO/SO_4^{2-} = 1, Stirring Rate = 400 rpm)
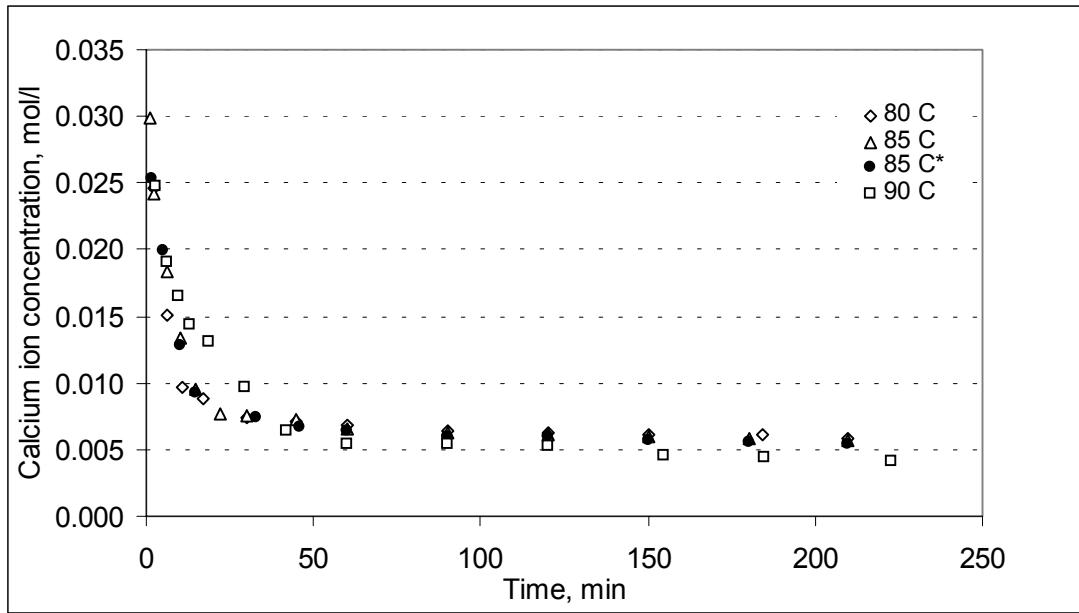
Figure 4.2.15. Variation of calcium ion concentration in liquid with respect to time at different temperatures (Experiment H3.1, H3.2, H3.3 and H3.4, Hisarcık 3 Colemanite, CaO/SO$_4^{2-}$ = 1, Stirring Rate = 400 rpm)
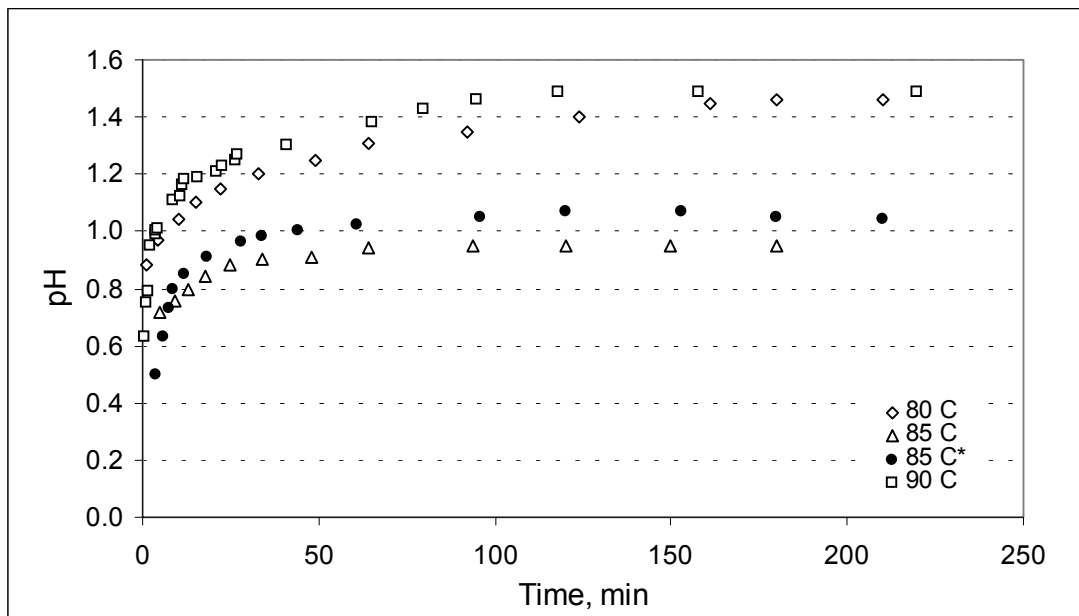
Figure 4.2.16. Variation of pH of the slurry with respect to time at different stirring rates (Experiment H3.1, H3.2, H3.3 and H3.4, Hisarcık 3 Colemanite, CaO/SO$_4^{2-}$ = 1, Stirring Rate = 400 rpm)

4.3 Kinetics of Dissolution Reaction

Boric acid production reaction is a very fast reaction. Nearly %90 of the colemanite dissolves in first 10-15 minutes. So, the dissolution of colemanite is a fast reaction and the rate equation can not be found from the obtained data. Researchers who studied the dissolution of colemanite (Tunc et.al,1998 ; Okur et.al,2002) had used different range of parameters, such as low temperatures, larger particle size and low stirring rates. They correlate the empirical formulas for the dissolution of colemanite in sulfuric acid. However, in these working ranges it was not possible to find the rate expression of dissolution reaction.

4.4 Kinetics of Gypsum Crystallization

Crystallization kinetics of gypsum during the dissolution of colemanite has been studied before.[Çetin et.al, 2001; Balkan and Tolun 1985,]. The crystallization kinetics of calcium sulfate dihydrate was studied during the dissolution of colemanite in aqueous sulfuric acid in a previous study with the same experimental set-up [Çetin, 2000] and the rate law for the crystallization found is given in Eq. 4.4.1.

$$\text{Rate} = -\frac{d[Ca^{2+}]}{dt} = k \, ([Ca^{2+}] - [Ca^{2+}]_{sat})^2 \qquad\qquad 4.4.1$$

where the crystal growth rate is given in mol $L^{-1} s^{-1}$, k is the rate constant in L $mol^{-1} s^{-1}$ which is assumed to be constant during the growth process and $[Ca^{2+}]_{sat}$ is the saturation concentration of calcium ion at known temperature. A further investigation on the effect of particle size of colemanite, stirring rate and temperature on gypsum crystallization kinetics were examined in this study.

If $[Ca^{2+}]_1$ is the concentration of calcium ion at time t_1 which is earliest time to start (usually 2-3 min) samples from the reactor. Eq. 4.4.1 can be integrated between t_1 and t as follows:

$$\frac{1}{[Ca^{2+}] - [Ca^{2+}]_{sat}} - \frac{1}{[Ca^{2+}]_1 - [Ca^{2+}]_{sat}} = k \, (t-t_1) \qquad\qquad 4.4.2$$

The reciprocal concentration of calcium ion versus time plot gives a straight line for the crystallization of gypsum from the solution obtained by the dissolution of colemanite in aqueous sulfuric acid. The rate constant of the gypsum crystallization reaction for each experiment was found from the slopes of the straight lines.

The model parameters of the batch reactor experiments are given in Table 4.4.1.

Figure 4.4.1 shows reciprocal concentration of calcium ion versus time plot for the crystallization of gypsum from the supersaturated solution obtained by dissolution of colemanite in sulfuric acid at different particle sizes. As it is seen from the figure, the second order rate constants of the crystallization reaction were found as 0.049 and 0.087 L mol^{-1} s^{-1} for the experiments performed with particles larger and smaller than 250 μm, respectively. It was concluded that as the particle size of colemanite decreases the crystallization rate of gypsum increases.

Figure 4.4.2 illustrates the reciprocal concentration of calcium ion versus time plot for the crystallization of gypsum from the supersaturated solution obtained by dissolution of colemanite sulfuric acid at different stirring rates. As it is seen from the figure, the second order rate constants of the crystallization reaction were found as 0.049, 0.044 and 0.036 L mol^{-1} s^{-1} for the experiments performed at 500, 400 and 350 rpm, respectively. It was concluded that as stirring rate decreases the crystallization rate of gypsum decreases.

Figure 4.4.3 shows the reciprocal concentration of calcium ion versus time plot for the crystallization of gypsum from the supersaturated solution obtained by dissolution of colemanite sulfuric acid at different temperature. The nearly same trend was observed for 80 and 85 °C. Therefore, the rate constants of the crystallization reaction at 80 and 85 °C were found same. As it is seen from the figure, the second order rate constants of the crystallization reaction were found as 0.479 at 80 and 85 °C and 0.138 L mol^{-1} s^{-1} for the experiments performed at 90 °C. According to the Arhenius equation, the rate constant of the reaction increases with increasing temperature. Therefore, it was concluded that at temperatures higher than the 85 °C, the side reactions occur and the second order rate equation is not applicable.
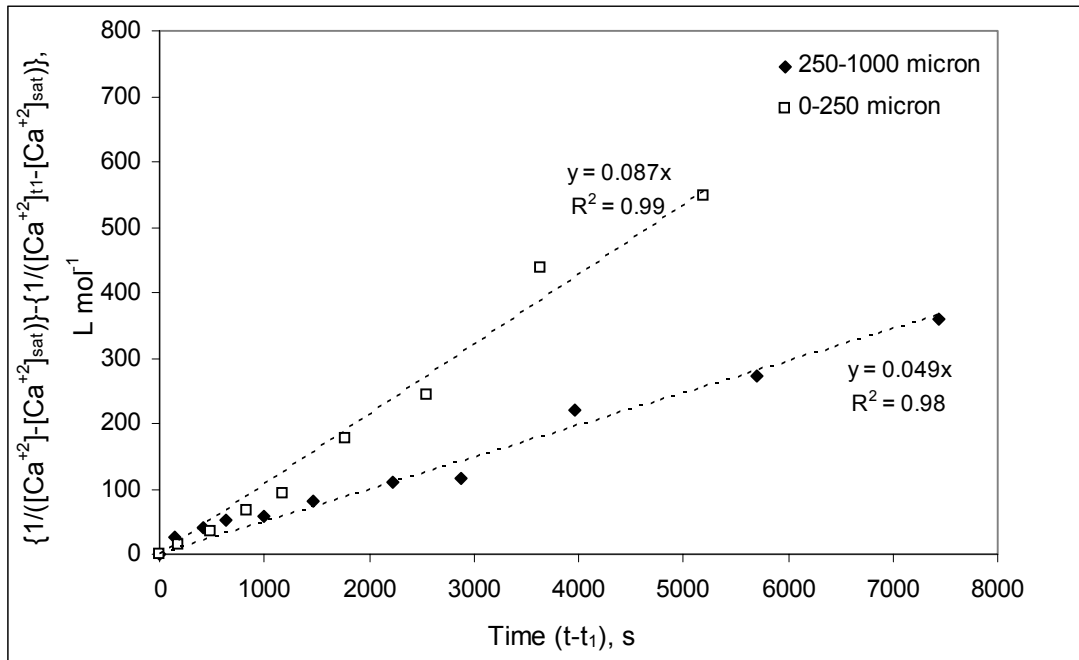
Figure 4.4.1. Reciprocal concentration of calcium ion versus time plot for the crystallization of gypsum from the supersaturated solution obtained by dissolution of colemanite in aqueous sulfuric acid at different particle sizes (Experiment H2.5 and H2.9, Hisarcık 2 Colemanite, CaO/SO_4^{2-} = 1, Stirring Rate = 500 rpm, T= 85 °C)
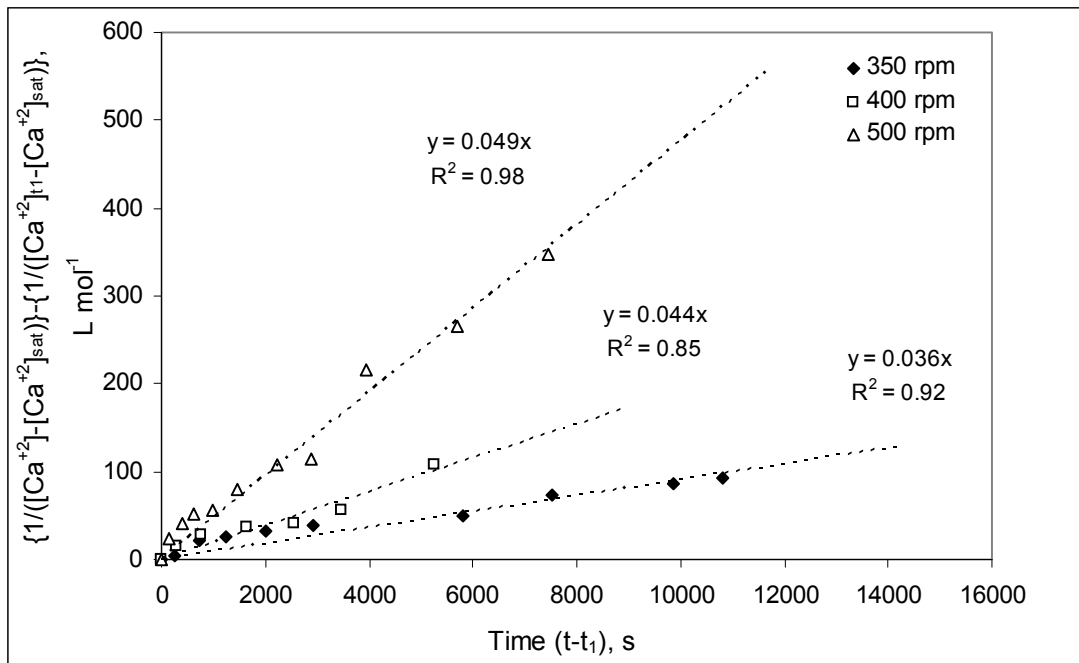
Figure 4.4.2. Reciprocal concentration of calcium ion versus time plot for the crystallization of gypsum from the supersaturated solution obtained by dissolution of colemanite in aqueous sulfuric acid at different stirring rates (Experiment H2.3, H2.4 and H2.5, Hisarcık 2 Colemanite, CaO/SO_4^{2-} = 1,Stirring Rate = 500 rpm,T= 85 °C)
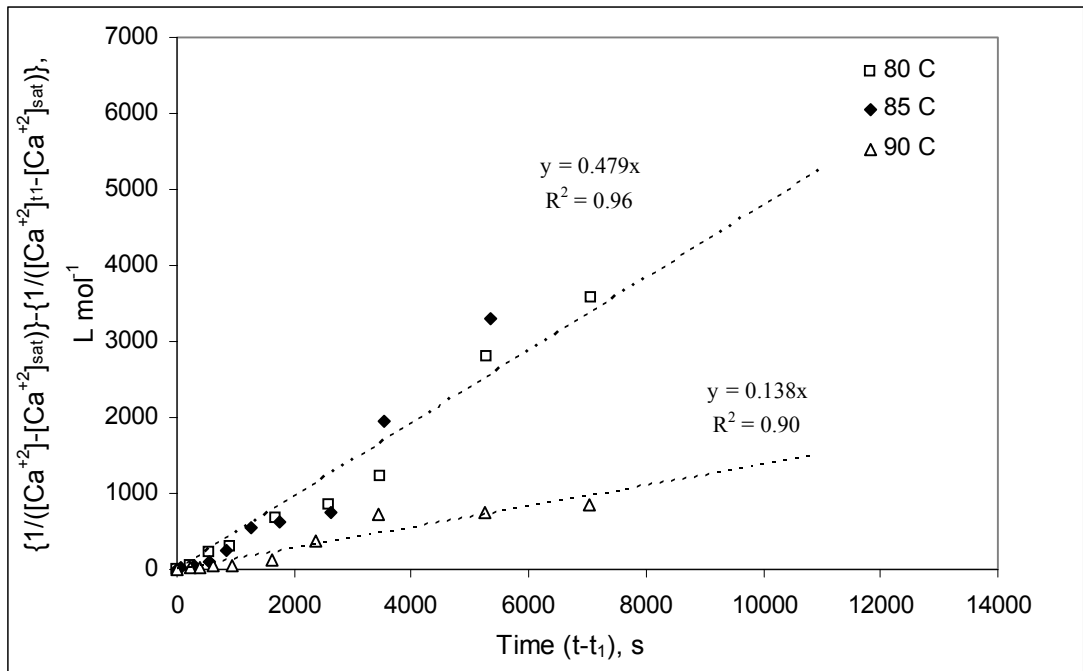
Figure 4.4.3. Reciprocal concentration of calcium ion versus time plot for the crystallization of gypsum from the supersaturated solution obtained by dissolution of colemanite in aqueous sulfuric acid at different temperatures (Experiment H3.1, H3.2 and H3.4, Hisarcık 3 Colemanite, CaO/SO_4^{2-} = 1, Stirring Rate = 400 rpm)

Table 4.4.1. The model parameters of the batch reactor experiments

Experiment Name	Colemanite	Particle Size	CaO/SO$_4^{2-}$ Molar Ratio	Temperature, °C	Stirring Rate, rpm	k, L.mol^{-1}.s^{-1}	C$_{t1}$, mol L^{-1}	C$_{sat}$, mol L^{-1}
H2.3	Hisarcık 2	250-1000 µm	1.0	85	350	0.036	0.064	0.012
H2.4	Hisarcık 2	250-1000 µm	1.0	85	400	0.044	0.036	0.012
H2.5	Hisarcık 2	250-1000 µm	1.0	85	500	0.049	0.062	0.012
H2.9	Hisarcık 2	0-250 µm	1.0	85	500	0.087	0.043	0.012
H3.1	Hisarcık 3	0-150 µm	1.0	80	400	0.479	0.025	0.006
H3.2	Hisarcık 3	0-150 µm	1.0	85	400	0.479	0.030	0.006
H3.4	Hisarcık 3	0-150 µm	1.0	90	400	0.138	0.025	0.004

4.5 Particle Size Distribution of the Gypsum Crystals

After taking the samples in the reactor for chemical analysis, the remaining slurry in the reactor was filtered. The solid collected on the filtration paper was washed out with hot water to get rid of the boric acid solution on it. Then samples for particle size distribution of gypsum were prepared. The sample preparation and the analysis of the samples were explained in detail in the experimental part. The all graphs obtained from the particle size distribution analysis are given in Appendix D.

The software of the laser diffraction instrument calculated the volume weighted mean diameter of the gypsum crystals obtained at the end of the each experiment. The mean diameters of gypsum crystals obtained at the end of the experiments are given in Table 4.5.1

Table 4.5.1.Volume weighted mean diameter of gypsum crystals

Experiment Name	Parameters	Reaction Time, min	Volume weighted mean diameter, μm
H2.2	250-1000 μm , 80 °C, 400 rpm, CaO/SO_4^{2-}=1.0	210	361.6
H2.3	250-1000 μm , 85 °C, 350 rpm, CaO/SO_4^{2-}=1.0	240	563.0
H2.4	250-1000 μm , 85 °C, 400 rpm, CaO/SO_4^{2-}=1.0	210	427.3
H2.5	250-1000 μm , 85 °C, 500 rpm, CaO/SO_4^{2-}=1.0	240	377.2
H2.8	0-250 μm , 80 °C, 500 rpm, CaO/SO_4^{2-}=1.0	210	72.1
H3.1	0-150 μm , 80 °C, 400 rpm, CaO/SO_4^{2-}=1.0	210	37.4
H3.2	0-150 μm , 85 °C, 400 rpm, CaO/SO_4^{2-}=1.0	210	36.9
H3.3	0-150 μm , 85 °C, 400 rpm, CaO/SO_4^{2-}=1.0	210	37.9
H3.4	0-150 μm , 90 °C, 400 rpm, CaO/SO_4^{2-}=1.0	223	32.1

The effects of temperature, stirring rate and particle size of colemanite on the particle size distribution and volume weighted mean diameter of the solid products were investigated in the next part.

4.5.1 Effect of Particle Size of Colemanite on Particle Size Distribution of Gypsum Crystals

Three experiments were performed at the initial CaO/SO_4^{2-} molar ratio of 1.00. In these experiments, temperature and stirring rate were kept constant at 85 °C .The colemanite minerals having three different particle sizes were used. These were smaller than 150 µm, smaller and greater than 250 µm .

Figure 4.5.1 illustrates the effect of particle size of colemanite on particle size distribution of gypsum crystals obtained at the end of the experiments.
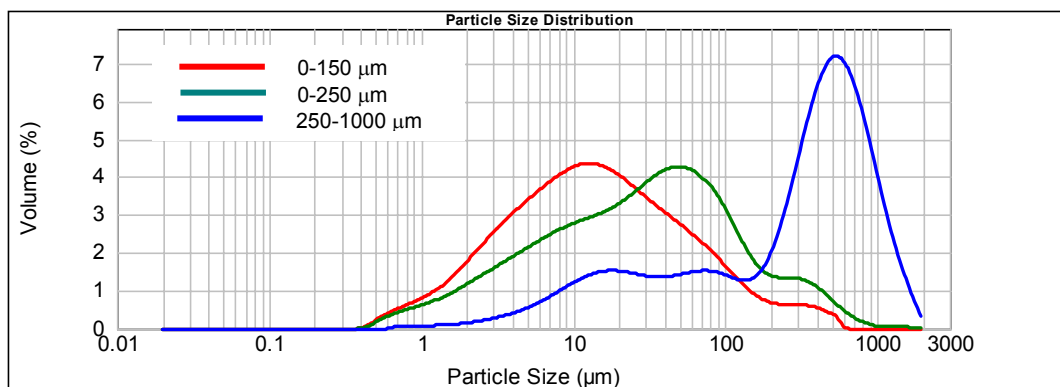
Figure 4.5.1. Particle size distribution of the gypsum crystals at different particle sizes of colemanite (Experiment H2.5, H2.9 and H3.2, CaO/SO_4^{2-} = 1.0, Stirring Rate = 500 rpm, T= 85 °C)

The variation of the mean diameters of the crystals at different particle sizes of colemanite is drawn in Figure 4.5.2. It was observed that, the mean diameter of the crystals increases with increasing particle size of colemanite. Volume weighted mean diameter of the solid products are 37.9, 72.1 and 427.3 µm for colemanite particles smaller than 150 µm, smaller and greater than 250 µm, respectively. As the colemanite particle size decreases, the faster dissolution is observed. Therefore, the nucleation is also expected to be very fast compared to the crystal growth. So many

nuclei are formed. Therefore, volume weighted mean diameter of gypsum crystals is smaller for smaller particle size of colemanite. However for greater colemanite particles dissolution rate is slower. Less number of nuclei is formed. As colemanite further dissolves with respect to time the Ca^{2+} ion and SO_4^{2-} ions combine on the crystal surface. Therefore, the crystal particle size increases.
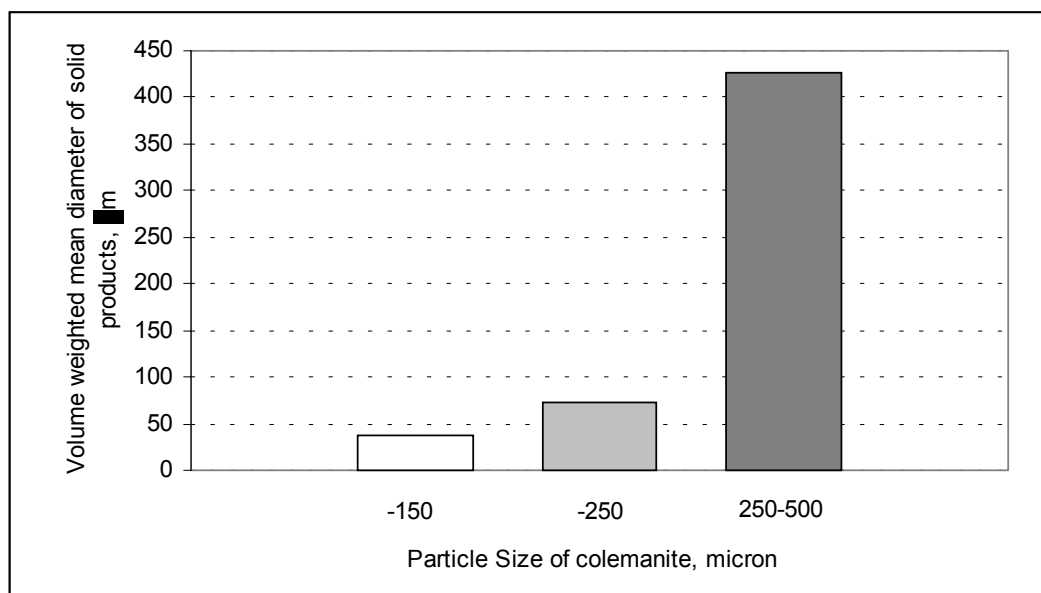
Figure 4.5.2.Variation of the volume weighted mean diameters of the solid products at different colemanite particle sizes (Experiment H2.5, H2.9 and H3.2, CaO/SO$_4^{2-}$ = 1.0, Stirring Rate = 500 rpm, T= 85 °C)

4.5.2 Effect of Stirring Rate on Particle Size Distribution of Gypsum Crystals

Three experiments were performed at the initial CaO/SO$_4^{2-}$ molar ratio of 1.00 and at 85 °C. Colemanite minerals with particle size greater than 250 µm were used. The effect of stirring rate on particle size distribution and volume weighted mean diameter of the gypsum crystals obtained during the reaction time of 210 minutes were analyzed. Stirring rates were 350, 400 and 500 rpm.

The change in particle size distribution of gypsum crystals in dependency of the stirring rate is shown in Figure 4.5.3.
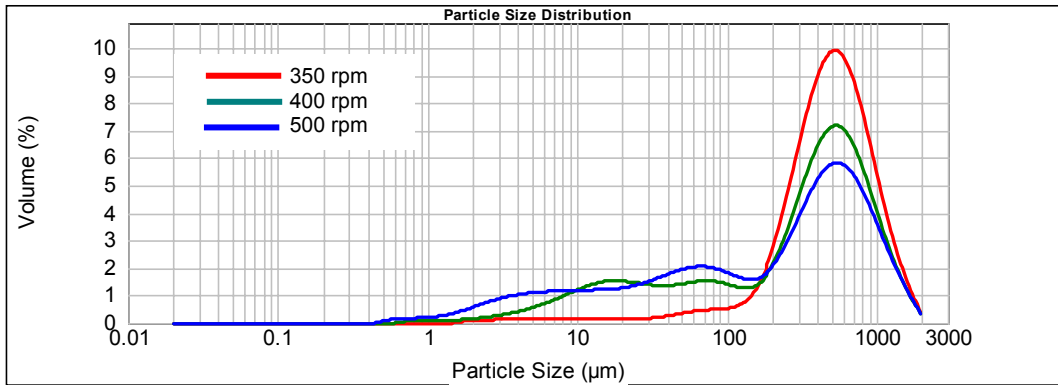
Figure 4.5.3. Particle size distribution of the gypsum crystals at different stirring rates (Experiment H2.3, H2.4 and H2.5, Hisarcık 2 Colemanite, CaO/SO_4^{2-} = 1.0, Stirring Rate = 500 rpm, T= 85 °C)

The variation of the mean diameters of the crystals at different stirring rates is drawn in Figure 4.5.4. As seen in this figure, the mean diameter of the crystals decreases with increasing the stirring rate. Volume mean diameter of the gypsum crystals at 350, 400 and 500 rpm are 563.0, 427.3 and 377.2 µm, respectively. Gypsum crystals can be broken at higher stirring rates.
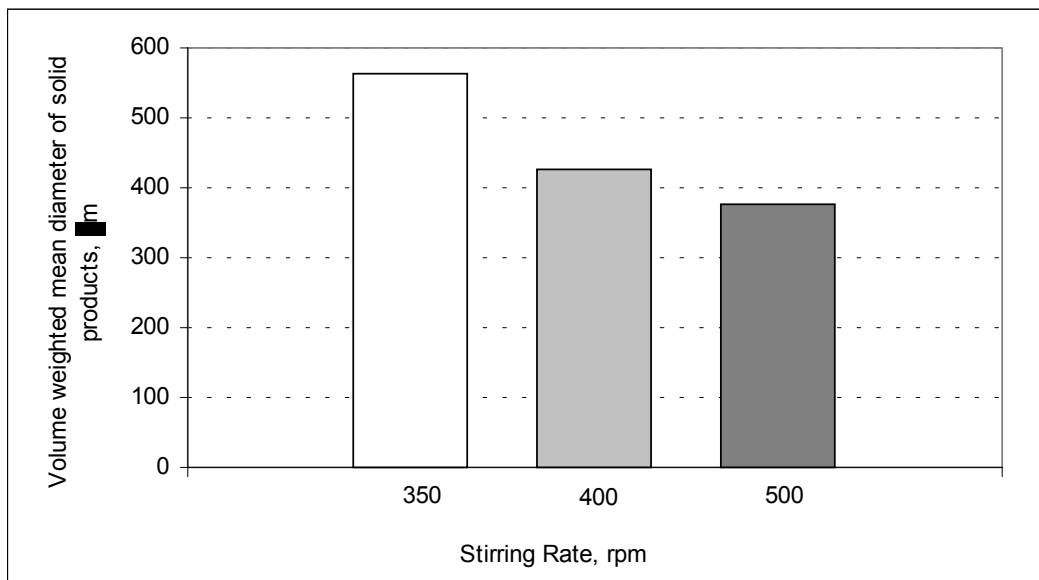
Figure 4.5.4. Variation of the volume weighted mean diameters of the solid products at different stirring rates (Experiment H2.3, H2.4 and H2.5, Hisarcık 2 Colemanite, CaO/SO_4^{2-} = 1.0, Stirring Rate = 500 rpm, T= 85 °C)

4.5.3 Effect of Temperature on Particle Size Distribution of Gypsum Crystals

At the initial CaO/SO_4^{2-} molar ratio of 1.00, three experiments were performed. In these experiments, stirring rate were kept constant 500 rpm and colemanite minerals having particle size smaller than 150 micron was used. The experiments were performed at 80 °C, 85 °C and 90 °C. The solid portion of obtained the product as a result of the reaction was analyzed.

Figure 4.5.5 illustrates the effect of temperature on particle size distribution of gypsum crystals obtained at the end of the experiments performed with Hisarcık 3 colemanite particle size of 0-150 µm .
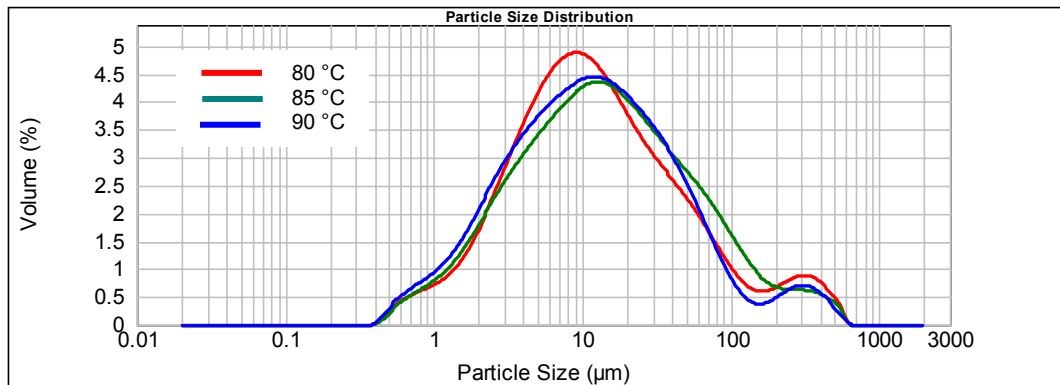
Figure 4.5.5. Particle size distribution of the gypsum crystals at different temperatures (Experiment H3.1, H3.2 and H3.4, Hisarcık 3 Colemanite, CaO/SO_4^{2-} = 1.0, Stirring Rate = 400 rpm)

The change in volume weighted mean diameter of the solid products in dependency of the temperature is shown in Figure 4.5.6. In this figure it can be seen that there is no significant differences in mean diameters of solid products obtained at 80 and 85 °C. Volume mean diameter of the solid products at 80 and 85 °C are 37.4, 37.9 µm respectively. However, the mean diameter of solid obtained at 90 °C was smaller than those obtained at 80 and 85 C. It was 32.1 µm.
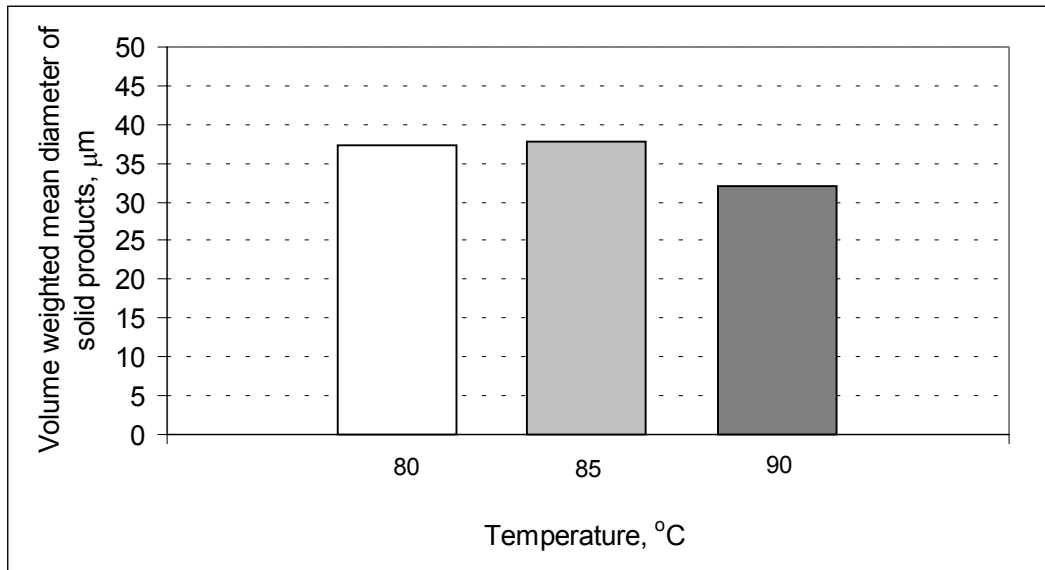
Figure 4.5.6. Variation of the volume weighted mean diameters of the solid products at different temperatures (Experiment H3.1, H3.2 and H3.4, Hisarcık 3 Colemanite, CaO/SO_4^{2-} = 1.0, Stirring Rate = 400 rpm)

4.6 Gypsum Crystal Images

The growth of the gypsum crystals were examined under the light microscope, Prior Laboratory Microscope B 3000 that was connected online to a computer by a Pro Series, high performance CCD Camera.

The light images of gypsum are given in Figures. 4.6.1, 4.6.2 and 4.6.3 for experiments performed with colemanite particle sizes of smaller than 150 µm , and smaller and greater than 250 µm, respectively.

The time dependent growth of gypsum crystals can be seen from the Figures. 4.6.1, 4.6.2 and 4.6.3. In the first minutes, the crystals are small and thin. On the prolong crystallization, the gypsum crystals become longer and wider.
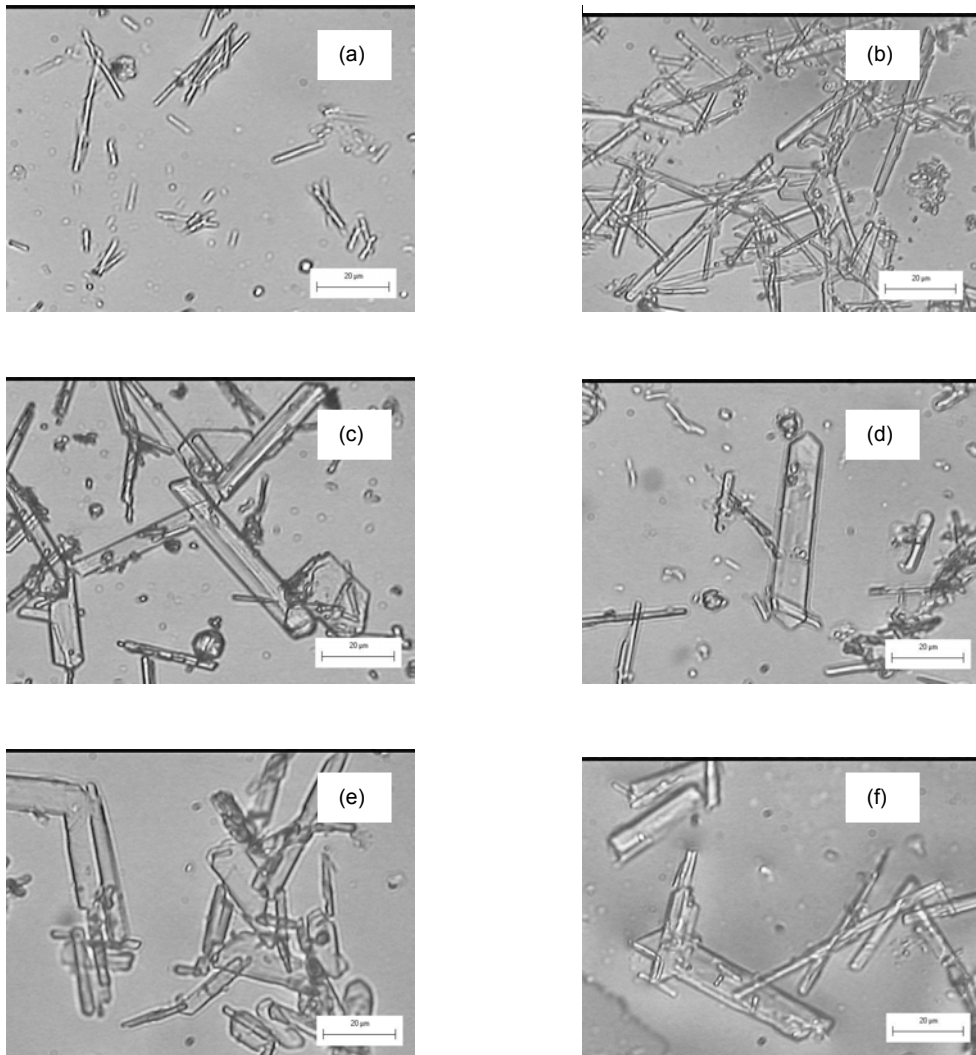
Figure 4.6.1. Light microscope images of gypsum (ExperimentH3.1,Hisarcik 3 colemanite,0-150μm, CaO/SO$_4^{2-}$ = 1.0, Stirring Rate = 400 rpm, T= 80 °C) (a) 6.5 min, (b)13 min, (c)30 min, (d)60 min, (e) 90 min, (f)120 min

As it is seen in Figure 4.6.1, the first samples taken in 6.5 min after the dissolution of colemanite in aqueous sulfuric acid showed needle-like crystals having average dimensions of 1-15 μm length and 1 μm width. The crystals became wider and taller on prolong crystallization as it can be seen from the images of the samples taken at 30th, 60th, 90th and 120th minutes of reaction time.
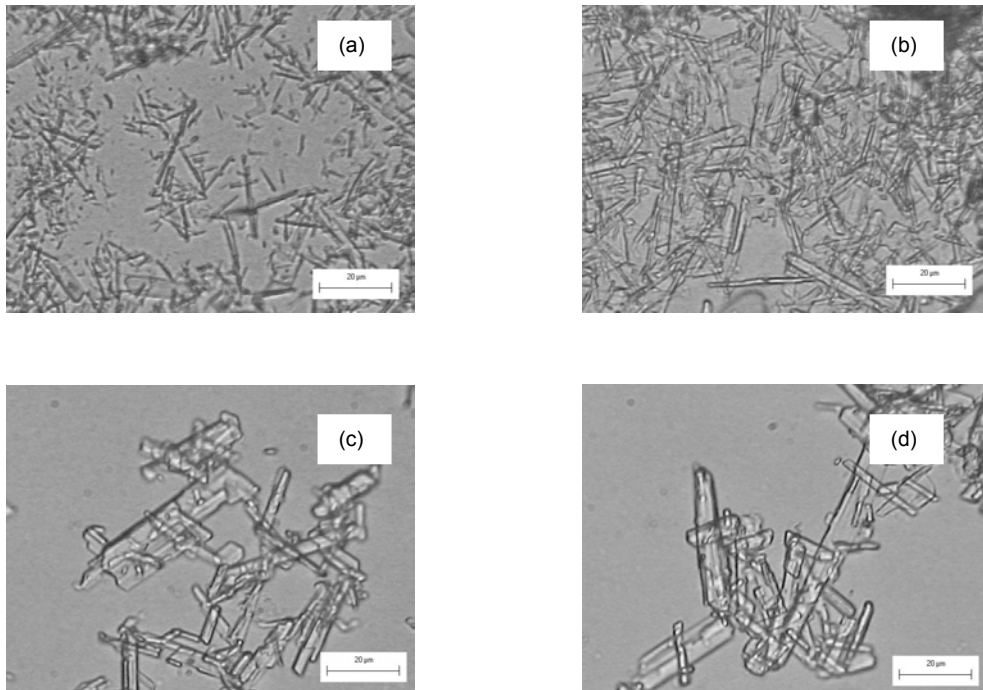
Figure 4.6.2. Light microscope images of gypsum (Experiment H2.8,Hisarcik 2 colemanite,0-250μm, CaO/SO$_4^{2-}$ = 1.0, Stirring Rate = 500 rpm, T= 85 °C) (a) 4.5 min, (b)30 min, (c)120 min, (d)210 min

As it is seen in Figure 4.6.2, the first samples taken in 4.5 min after the dissolution of colemanite in aqueous sulfuric acid showed needle-like crystals having average dimensions of 1-15 μm length. The crystals obtained at 210 min have average dimensions of 5-35 μm length and 2 μm width.

Figure 4.6.3 illustrates gypsum crystals images obtained during the experiment performed with colemanite particle sizes larger than 250 micron. As it seen, larger gypsum crystals are obtained in first few minutes. Average dimensions of crystals are 1-70 μm length and 1-10 width. The clamp formation of gypsum crystals is observed during the prolong crystallization. Since, they hinder valuable boric acid solution inside of them. The clamp formation decreases the yield of the process. Therefore, It is undesired in production process of boric acid.
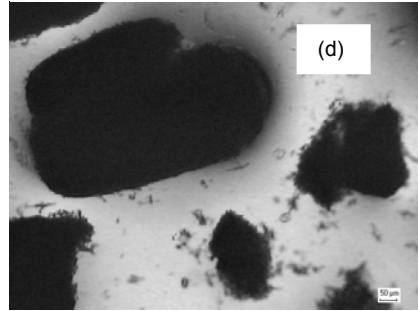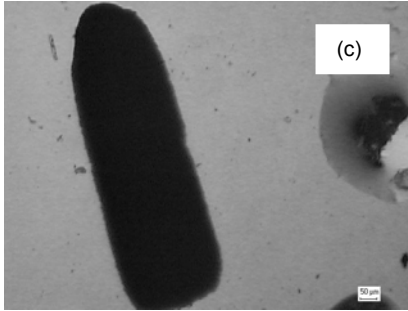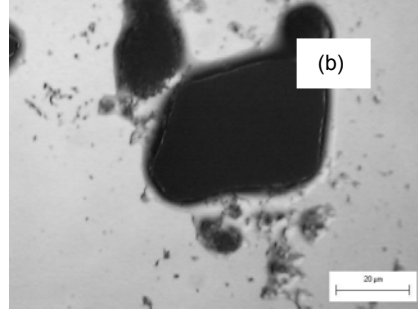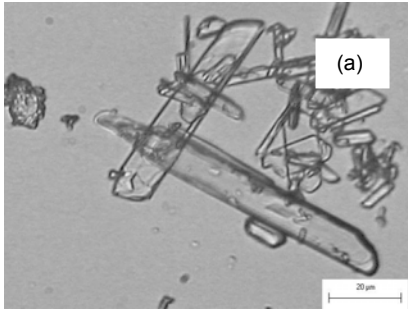
Figure 4.6.3. Light microscope images of gypsum (ExperimentH2.3,Hisarcik 2 colemanite, 250-1000 μm, CaO/SO$_4^{2-}$ = 1.0, Stirring Rate = 350 rpm, T= 85 °C) (a) 6.5 min, (b)60 min, (c)98 min, (d)180 min

CHAPTER 5

CONCLUSION AND RECOMMENDATIONS

One of the most commonly used boron compounds, boric acid, can be produced by dissolving colemanite ($2CaO \cdot 3B_2O_3 \cdot 5H_2O$) in aqueous sulfuric acid whereby gypsum ($CaSO_4 \cdot 2H_2O$) is formed as a by-product and must be separated from the main product. This process consists of two steps, dissolution of colemanite and formation of gypsum. The amount of boric acid formed depends on the first step, dissolution of colemanite. In the latter step, gypsum crystals are formed and stay in the reaction mixture to grow up to a size large enough to be filtered out of the solution.

In this study it is aimed to investigate the effects of particle size of colemanite, stirring rate and reaction temperature on the dissolution of colemanite, gypsum formation and particle size distribution of gypsum formed in the reaction of boric acid production.

The dissolution of colemanite can be followed by monitoring the boric acid concentration change in the slurry. As the colemanite dissolves, the boric acid concentration in the liquid phase increases and it reaches an asymptotic value. The crystallization of gypsum from the solution can be found from the calcium ion concentration in the solution as it decreased by the formation of gypsum precipitate. Therefore, the change in calcium ion concentration in the liquid phase in dependency of the time is determined during the experiments.

From the material balance calculation, it is observed that nearly %90 of the colemanite dissolves during first few minutes in the experiments performed with

colemanite particle size of greater than 250 μm.. So, the dissolution of colemanite is a fast reaction and the rate equation can not be found from the obtained data. Also, it was seen that, the colemanite dissolution rate increases with decreasing particle size of colemanite (0-150 μm,0-250 μm, 250-1000 μm) because of increasing surface area, increasing stirring rate (350-500 rpm) due to increasing the mass transfer of H^+ ions in solution through colemanite particles and increasing temperature up to 85 °C. The dissolution rate of colemanite was faster at 85 C. Therefore, the optimum temperature for the production of boric acid should be between 80 and 85 °C.

The crystallization kinetics of calcium sulfate dihydrate was studied during the dissolution of colemanite in aqueous sulfuric acid in a previous study with the same experimental set-up [Çetin, 2000] and the crystallization rate of gypsum was found to follow a second order kinetics with respect to saturation level. A further investigation on the effect of particle size of colemanite, stirring rate and temperature on gypsum crystallization kinetics were examined in this study. It was observed that gypsum crystallization rate increases with decreasing particle size of colemanite (0-150 μm,0-250 μm, 250-1000 μm) and increasing stirring rate (350-500 rpm) . It was found that, side reactions occur at temperatures higher than the 85 °C. Therefore, second order kinetic analysis is not applicable at temperatures higher than 85 °C. The optimum temperature for the crystallization of gypsum was found as 85 °C.

The software of the laser diffraction instrument calculated the volume weighted mean diameter of the solid gypsum obtained at the end of the each experiment. Volume weighted mean diameter of gypsum crystals decreases with decreasing particle size of colemanite As the colemanite particle size decreases, the faster the dissolution is observed. Therefore, the nucleation of gypsum crystals is also expected to be very fast compared to the crystal growth. So many small crystals are obtained. Gypsum crystals can be broken at higher stirring rates. Temperature has insignificant effect on particle size distribution of gypsum crystals.

The growth of the gypsum crystals were examined under the light microscope and it was seen that the length and width of crystals increased for prolonged

crystallization. The clamp formation of gypsum crystals is observed during the prolong crystallization of gypsum when the colemanite particles larger than 250 μm were used in the experiments. Since, clamps hinder valuable boric acid solution inside of them. Therefore, the clamp formation decreases the yield of the process. It is undesired in production process of boric acid. So, colemanite particles smaller than 250 μm should be used during the boric acid production.

REFERENCES

Amethyst Galleries, 1997
URL: http://mineral.galleries.com/minerals/carbonat/colemani/colemani.htm

Balkan A. and Tolun R., "Factors Affecting the Formation of Gypsum in the Production of Boric Acid from Colemanite", Bull. Tech. Univ. İstanbul, Vol. 38, pp. 207-231, 1985

Bechtloff B., Jüsten P., Ulrich J., "The Kinetics of Hetergenous Solid-liquid Reaction Crystallizations-An Overview and Examples", Chemie Ingenieur Technik, Vol.73, pp.453-460, 2001

Bilal C., Taylan N., Gürbüz H., Bulutcu A.N., "Effect of H_2SO_4, H_3BO_3 and Gypsum on the Dissolution of Colemanite in Sulfuric Acid Solution" ,Workshop on Advance In Sensoring In Industrial Crystallization, 18-20 June, pp.65-72, 2003

Chuck Brown, "Minerals-n-More", 2000
URL:http://www.minerals-n-more.com/Colemanite_Info.html

Çakal G.Ö., Erdoğdu A., Özkar N., Özkar S., Eroğlu İ., "Simulation of Gypsum Crystallization In Continuous Boric Acid Reactors By Microfluid and Macrofluid Models",Workshop on Advance In Sensoring In Industrial Crystallization, 18-20 June, pp.57-64, 2003

Çetin E., "Investigation on the Kinetics of Gypsum Formation in the Reaction of Boric Acid Production from the Colemanite and Sulphuric Acid", M.Sc. Thesis, METU, Ankara, Turkey, 2000

Çetin E., Eroğlu İ. and Özkar S., "Kinetics of Gypsum Formation and Growth during the Dissolution of Colemanite in Sulfuric Acid", Journal of Crystal Growth, Vol. 231, pp. 559-567, 2001

Gürbüz H., Öçgüder S., Yavaşoğlu-Taylan N., Sayan P. and Bulutcu A.N., "Kolemanitin Borik Asit Çözeltilerinde Çözünürlüğü", UKMK 3, Erzurum, 2-4 Eylül, pp. 1259-1264, 1998

Easton A.J., "Chemical Analysis of Silicate Rocks", Elsevier Publishing Company, London, 1972

Erdoğdu A., Çakal G.Ö., Özkar N., Özkar S., Eroğlu İ., "Effect of Particle Size of Colemanite on Gypsum Formation During Boric Acid Production" ,Workshop on Advance In Sensoring In Industrial Crystallization, 18-20 June, pp.41-48, 2003

Hershel Friedman," The Mineral and Gemstone Kingdom",1999
URL: http:www.minerals.net/mineral/borates/colemani/colemani.htm

Industrial Minerals, 2001
URL:www.etiholding.gov.tr

Levenspiel O., "Chemical Reaction Engineering", 3rd Ed., pp.566-585, 1999

Liu S.T., Nancollas G.H., "A Kinetic and Morphological Study of the Seeded Growth of Calcium Sulfate Dihydrate in the Presence of Additives", Journal of Colloid and Interface Science, Vol. 52, pp. 593-601, 1975b

Kalafatoğlu İ.E., Örs N. and Özdemir S.S, "Hisarcık Kolemanitinin Sülfürik Asitle Çözünme Davranışı", UKMK 4, İstanbul, 4-7 Eylül, 2000

Kirk Othmer, "Encyclopedia of Chemical Technology", 4th Ed., John Wiley and Sons Inc., N.Y., 1992

Klepetsanis P.G., Koutsoukos P.G., "Spontaneous Precipitation of Calcium Sulfate at Conditions of Sustained Supersaturation", Journal of Colloid and Interface Science, Vol. 143, pp. 299-308, 1991

Kocakerim M.M., Alkan M., "Dissolution Kinetics of Colemanite in SO_2-Saturated Water", Hydrometallurgy, Vol. 19, pp. 385-392, 1987

Kum C., Alkan M., Kocakerim M.M., "Dissolution Kinetics of Calcined Colemanite in Ammonium Chloride Solution", Hydrometallurgy, Vol. 36, pp. 259-268, 1993

Küçük Ö., Kocakerim M.M., Yartaşı A., Çopur M., "Dissolution of Kestelek's Colemanite Containing Clay Minerals In Water Saturated With Sulphur Dioxide", 14th International Congress of Chemical and Process Engineering, 2000

Nancollas G. H., Reddy M.M. and Tsai F., "Calcium Sulfate Dihydrate Crystal Growth in Aqueous Solution at Elevated Temperatures", Journal of Crystal Growth, Vol. 20, pp. 125-134, 1973

Okur H., Tekin T., Ozer A.K., Bayramoğlu M., "Effect of Ultrasound on Dissolution of Colemanite in H_2SO_4", Hydrometallurgy, Vol. 67 pp. 79-86, 2002

Özbayoğlu G. and Poslu K., "Mining and Processing of Borates in Turkey", Mineral Processing and Extractive Metallurgy Review, Vol. 9, pp. 245-254, 1992

Özmetin C., Kocakerim M.M., Yapıcı S. and Yartaşı A., "A Semiempirical Kinetic Model for Dissolution of Colemanite in Aqueous CH_3COOH Solutions", Ind. Eng. Chem. Res., Vol. 35, No. 7, pp. 2355-2359, 1996

Packter A., "The Precipitation of Calcium Sulphate Dihydrate from Aqueous Solution: Induction Periods, Crystal Numbers and Final Size", Journal of Crystal Growth, Vol. 21, pp. 191-194, 1973

Patnaik P., " Handbook of Inorganic Chemicals", Mc. Graw-hill Handbooks, New York, pp. 119-120, 2002

Roskill., "The Economics of Boron", 10th Ed., pp.11-20, 2002

Smith B.R., Alexander A.E., "The Effect of Additives on the Process of Crystallization II. Further Studies on Calcium Sulphate (1)", Journal of Colloid and Interface Science, Vol. 34, No.1, pp. 81-90, 1970

Smith B.R. and Sweett F., "The Crystallization of Calcium Sulphate Dihydrate", Journal of Colloid and Interface Science, Vol. 37, No.3, pp. 612-618, 1971

Seidell A., Linke W.F., "Solubilities of Inorganic and Metaorganic compounds", American Chem. Soc., Vol. 2, 1965

Temur H., Yartaşı A., Çopur M., Kocakerim M., "The Kinetics of Colemanite in H_3PO_3 Solutions", Ind. Eng. Chem. Res., Vol. 39, pp. 4114-4119, 2000

Tunç M. and Kocakerim M.M., "Kolemanitin H_2SO_4 Çözeltisinde Çözünme Kinetiği", UKMK 3, Erzurum, 2-4 Eylül, pp. 1235-1240, 1998

Ullmann ., "Ullmann's Encyclopedia of Industrial Chemistry", 6th Ed., USA, 2002

APPENDIX A

Chemical Analysis of Colemanite

A.1. Determination of B_2O_3 Content

1 g of ground colemanite is weighed and put into a 250 ml flask. Then, 10 ml of H_2SO_4 (1/3 by volume) and 75 ml of distilled water are added. Condenser is attached to the flask. The obtaining slurry is heated until the boiling point of the slurry. After that, 10 drops of methyl-red indicator are added and the slurry is neutralized with dehydrated Na_2CO_3 by adding it slowly. Condenser is again attached to the flask and the slurry is heated until it boils. After that step, the slurry is filtered by using blue band filter paper. The cake and flask are washed with hot distilled water until the volume of the filtrate reaches a final volume of about 150 ml. 1:3 (by vol.) H_2SO_4 is added to the solution until the color of the solution changes from yellow to pink. After obtaining the pink color, 1ml of H_2SO_4 is added as excess. The solution in the flask is heated until it boils. Condenser is attached to the flask at the heating procedure. If the color of the solution turns back to yellow, a small amount of sulfuric acid is added. The solution in the flask is cooled to the room temperature. Water bath can be used for cooling. Then, 6 N NaOH is put into the flask until the color changes from pink to yellow. After this step, H_2SO_4 is again added to the solution until the color turns back to pink. This solution is titrated with 0.1 N NaOH until a pH of 4.5 is obtained. At this step a titrator involving a magnetic stirrer and pH-meter may be used to get accurate results. Then, phenolphatelyn indicator and 10-15 g mannitol are added to the solution. The solution is again titrated with 0.1 N NaOH until the pH of the solution becomes 8.5. The volume of the NaOH used in the second step of titration is recorded and used to calculate the percentage of boron trioxide, B_2O_3, from the following formula:

% B_2O_3 = (V $_{NaOH}$ * F $_{NaOH}$ * 0.1) / n * (69.6202/2) * (100/1000)

78

$$= 0.348101 * (V_{NaOH} * F_{NaOH}) / n$$

where

V_{NaOH} = Volume of NaOH required for titration after adding the mannitol to the solution, ml

F_{NaOH} = Factor of the 0.1 N NaOH solution

n = Amount of sample, g

A.2. Determination of SiO_2 Content

One gram sample is put into a platinum crucible and mixed with 4-6 grams of Na_2CO_3. The mixture is covered with 2 g Na_2CO_3. Temperature of the oven is increased to 1000 °C. The mixture is put into oven and it is waited for an hour. The mixture melts and the crucible is taken out the oven. The mixture is cooled and put inside 50 ml HCl (1+1) into a beaker. The solution is vaporized in an hot-plate until it becomes dry. This process is repeated twice. Then, 10 ml HCl and 100 ml hot water is added to the dry and cold solid mixture.

The solution is filtered through Whatman 42 filter paper. The inside of the beaker is washed with hot HCl (1+99). The filtrate is washed 10 times with hot HCl (1+99) and 5 times with hot water. After this process, the liquid portion of the last washing process is analyzed if chlorine ions remain in the cake. Therefore, three drops of liquid are mixed with 2 ml 0.1 N $AgNO_3$ and 1 drop 4N HNO_3. If white precipitation occurs, it means the filtrate contains chlorine ions. The filtrate is washed until the removal of chlorine ions.

The filter cake is burned in an 1000 °C oven and weighed. Then, into the crucible, a few drops of H_2SO_4 (1+1) and 10 ml HF are added. The mixture is vaporized in hote-plate gradually until white fume comes. The crucible is kept at 1000 °C for 2 minutes. Then weighed again. The difference of two values is the weight of SO_2 (Easton, 1972).

A.3 Determination of Na$_2$O and K$_2$O Content

Into a platinum crucible, 0.5-1 g of sample is put. 5 ml of H$_2$SO$_4$ is added and the solution is mixed. Then, 5 ml of hydrofluoric acid is added and the solution is heated until sulfuric acid evaporates. When the solution is cooled, the procedure is repeated until the solid particles disappear. The solution is cooled; the wet sample is solved in water. The solution is heated until it becomes clear. After the solution is cooled, it is put inside a 200-ml flask and water is added. Then Na$_2$O and K$_2$O content of the solution are determined by Flame Photometer (Jenway PFP7 Flame Photometer) (Easton, 1972).

A.4. Determination of CaO, MgO, Al$_2$O$_3$, Fe$_2$O$_3$, SrO and TiO$_2$ Content

One gram of sample is put into a platinum crucible and mixed with 4-6 grams of Na$_2$CO$_3$. The mixture is covered with 2 g Na$_2$CO$_3$. Temperature of the oven is increased to 1000 °C. The mixture is put into oven and it is waited for an hour. The mixture melts and the crucible is taken out the oven. The mixture is cooled and put inside 50 ml HCl (1+1) into an beaker. The solution is vaporized in an hote-plate until it becomes dry. This process is repeated twice. Then, 10 ml HCl and 100 ml hot water is added to the dry and cold solid mixture. The solution is filtered through Whatman 42 filter paper. The liquid is analyzed in Atomic Absorbtion Spectrophotometer for CaO, MgO, Al$_2$O$_3$, Fe$_2$O$_3$, SrO and TiO$_2$ content(Easton, 1972).

APPENDIX B

RAW DATA OF EXPERIMENTS

Table B.1. Boric acid and calcium ion concentrations during the Experiment H1.1, Hisarcık 1 Colemanite, 0-250 μm, CaO/SO_4^{2-} = 0.85, Stirring Rate = 500 rpm, T= 80°C

t, min	m_{Ca}, ppm	$[Ca^{2+}]$, mol/l	V_{NaOH}, ml F_{NaOH}=1	$[H_3BO_3]$, mol/l
1.17	1064	0.0266	19.11	1.91
5	536	0.0134	19.57	1.96
9.17	476	0.0119	19.50	1.95
13.5	399	0.0100	19.70	1.97
22	344	0.0086	20.36	2.04
30	298	0.0075	20.21	2.02
40	296	0.0074	20.24	2.02
52.5	276	0.0069	20.94	2.09
61	249	0.0062	20.82	2.08
82	249	0.0062	21.41	2.14
102	307	0.0077	21.28	2.13
120	334	0.0084	22.76	2.28
140	297	0.0074	23.00	2.30
160	282	0.0070	23.20	2.32
180	274	0.0068	23.47	2.35

Table B.2. Boric acid and calcium ion concentrations during the Experiment H1.2, Hisarcık 1 Colemanite, 250-1000 μm, CaO/SO$_4^{2-}$ = 0.85, Stirring Rate = 500 rpm, T= 80°C

t, min	m$_{Ca}$, ppm	[Ca^{2+}], mol/l	V$_{NaOH}$, ml F$_{NaOH}$=1	[H$_3$BO$_3$], mol/l
1.17	2566	0.0641	7.96	0.80
4	1458	0.0364	11.25	1.12
8	-	-	12.21	1.22
12	1159	0.0290	12.18	1.22
18	646	0.0162	12.40	1.24
23	484	0.0121	-	-
26	468	0.0117	13.80	1.38
32	456	0.0114	15.00	1.50
43.5	448	0.0112	15.50	1.55
50	440	0.0110	16.30	1.63
74	439	0.0110	16.90	1.69
91	396	0.0099	17.40	1.74
124	364	0.0091	18.38	1.84
135	348	0.0087	18.70	1.87
158	327	0.0082	19.00	1.90
180	301	0.0075	19.50	1.95
210	291	0.0073	20.99	2.10
240	259	0.0065	20.80	2.08
280	256	0.0064	20.90	2.09

Table B.3. Boric acid and calcium ion concentrations during the Experiment H2.1, Hisarcık 2 Colemanite, 250-1000 μm, CaO/SO$_4^{2-}$ = 1, Stirring Rate = 400 rpm, T= 70°C

t, min	m$_{Ca}$, ppm	[Ca^{2+}], mol/l	V$_{NaOH}$, ml F$_{NaOH}$=1	[H$_3$BO$_3$], mol/l
2	1215	0.0304	10.42	1.04
7	995	0.0249	11.28	1.13
15	897	0.0224	11.88	1.19
30	771	0.0193	12.56	1.26
45	715	0.0179	13.17	1.32
63	644	0.0161	14.03	1.40
90	562	0.0141	14.24	1.42
122	511	0.0128	14.70	1.47
150	475	0.0119	15.80	1.58
180	462	0.0116	16.24	1.62
210	451	0.0113	16.58	1.66

Table B.4. Variation in pH of slurry during the Experiment H2.1, Hisarcık 2 Colemanite, 250-1000 μm, CaO/SO$_4^{2-}$ = 1, Stirring Rate = 400 rpm, T= 70°C

t, min	pH	t, min	pH
1.5	0.17	62	0.33
4.5	0.19	92	0.36
9.5	0.22	120	0.37
17	0.25	148	0.39
34	0.30	181	0.39
54	0.31	209	0.40

Table B5. Boric acid and calcium ion concentrations during the Experiment H2.2, Hisarcık 2 Colemanite, 250-1000 µm, CaO/SO$_4^{2-}$ = 1, Stirring Rate = 400 rpm, T= 80°C

t, min	m$_{Ca}$, ppm	[Ca^{2+}], mol/l	V$_{NaOH}$, ml F$_{NaOH,}$=1	[H$_3$BO$_3$], mol/l
2	1011	0.0253	10.50	1.05
5	981	0.0245	12.08	1.21
15	896	0.0224	12.50	1.25
30	733	0.0183	13.86	1.39
45	676	0.0169	14.28	1.43
60	647	0.0162	14.60	1.46
90	599	0.0150	15.88	1.59
120	544	0.0136	16.35	1.64
150	540	0.0135	16.36	1.64
180	493	0.0123	17.43	1.74
210	470	0.0118	17.62	1.76

Table B.6. Variation in pH of slurry during the Experiment H2.2, Hisarcık 2 Colemanite, 250-1000 µm, CaO/SO$_4^{2-}$ = 1, Stirring Rate = 400 rpm, T= 80°C

t, min	pH	t, min	pH
1.75	0.23	51	0.30
4.5	0.23	60	0.30
6.5	0.24	90	0.30
13.5	0.31	120	0.31
23	0.31	150	0.31
27.5	0.32	180	0.30
32	0.32	210	0.30

Table B.7. Boric acid and calcium ion concentrations during the Experiment H2.3, Hisarcık 2 Colemanite, 250-1000 µm, CaO/SO$_4^{2-}$ = 1, Stirring Rate = 350 rpm, T= 85°C

t, min	m$_{Ca}$, ppm	[Ca^{2+}], mol/l	V$_{NaOH}$, ml F$_{NaOH}$=1	[H$_3$BO$_3$], mol/l
1.5	2546	0.0637	7.94	0.794
6	2206	0.0552	9.28	0.928
13.5	1473	0.0368	9.74	0.974
22.5	1377	0.0344	9.98	0.998
35	1240	0.0310	10.09	1.009
50	1175	0.0294	10.81	1.081
98	1069	0.0267	13.81	1.381
127	907	0.0227	14.80	1.480
166	862	0.0216	15.10	1.510
182	837	0.0209	15.23	1.523
210	801	0.0200	16.03	1.603
240	757	0.0189	17.54	1.754

Table B.8. Variation in pH of slurry during the Experiment H2.3, Hisarcık 2 Colemanite, 250-1000 µm, CaO/SO$_4^{2-}$ = 1, Stirring Rate = 350 rpm, T= 85°C

t, min	pH	t, min	pH
0	0.06	22	0.61
0.45	0.32	34	0.61
0.58	0.43	47	0.63
0.75	0.53	60	0.65
1	0.54	96	0.74
4	0.56	117	0.78
4.67	0.6	145	0.78
5.42	0.56	171	0.79
8	0.6	207	0.8
16	0.62	224	0.79

Table B.9. Boric acid and calcium ion concentrations during the Experiment H2.4, Hisarcık 2 Colemanite, 250-1000 µm, CaO/SO$_4^{2-}$ = 1, Stirring Rate = 400 rpm, T= 85°C

t, min	m$_{Ca}$, ppm	[Ca^{2+}], mol/l	V$_{NaOH}$, ml F$_{NaOH}$,=1	[H$_3$BO$_3$], mol/l
2.3	1455	0.0364	13.97	1.40
7	1184	0.0296	15.20	1.52
15	1056	0.0264	15.25	1.53
30	992	0.0248	15.72	1.57
45	971	0.0243	15.85	1.59
60	896	0.0224	16.03	1.60
90	748	0.0187	16.34	1.63
120	688	0.0172	16.71	1.67
150	638	0.0160	17.41	1.74
180	628	0.0157	17.32	1.73
210	628	0.0157	18.42	1.84

Table B.10. Variation in pH of slurry during the Experiment H2.4, Hisarcık 2 Colemanite, 250-1000 µm, CaO/SO$_4^{2-}$ = 1, Stirring Rate = 400 rpm, T= 85°C

t, min	pH	t, min	pH
5	0.56	93	0.65
10	0.57	119	0.71
15	0.58	152	0.72
25	0.61	183	0.72
45	0.63	208	0.74
62	0.67	-	-

Table B.11. Boric acid and calcium ion concentrations during the Experiment H2.5, Hisarcık 2 Colemanite, 250-1000 µm, CaO/SO$_4^{2-}$ = 1, Stirring Rate = 500 rpm, T= 85°C

t, min	m$_{Ca}$, ppm	[Ca^{2+}], mol/l	V$_{NaOH}$, ml F$_{NaOH,}$=1.03	[H$_3$BO$_3$], mol/l
1	2478	0.0619	10.53	1.08
3.5	1377	0.0344	13.35	1.38
8	1146	0.0286	13.86	1.43
11.5	1040	0.0260	15.23	1.57
17.5	998	0.0249	15.46	1.59
25.5	880	0.0220	15.54	1.60
38	790	0.0198	15.56	1.60
49	778	0.0195	16.22	1.67
67	650	0.0163	16.94	1.74
96	620	0.0155	17.25	1.78
125	589	0.0147	17.95	1.85
160	511	0.0128	18.12	1.87
195	497	0.0124	18.37	1.89
240	483	0.0121	20.02	2.06

Table B.12. Variation in pH of slurry during the Experiment H2.5, Hisarcık 2 Colemanite, 250-1000 µm, CaO/SO$_4^{2-}$ = 1, Stirring Rate = 500 rpm, T= 85°C

t, min	pH	t, min	pH
5	0.56	72	0.64
10	0.57	86	0.64
15	0.59	113	0.66
22	0.61	133	0.66
28.5	0.61	164	0.69
42	0.61	200	0.69
52	0.62	242	0.68

Table B.13. Boric acid and calcium ion concentrations during the Experiment H2.6, Hisarcık 2 Colemanite, 0-250 μm, CaO/SO$_4^{2-}$ = 0.95, Stirring Rate = 500 rpm, T= 80°C

t, min	m$_{Ca}$, ppm	[Ca^{2+}], mol/l	V$_{NaOH}$, ml F$_{NaOH}$=1.15	[H$_3$BO$_3$], mol/l
1	2072	0.0518	6.72	0.77
4	1544	0.0386	7.49	0.86
5	1527	0.0382	8.18	0.94
10	1224	0.0306	8.50	0.98
15	1470	0.0368	8.83	1.02
25	1101	0.0275	8.89	1.02
35	822	0.0205	8.92	1.03
45	884	0.0221	8.97	1.03
60	855	0.0214	9.87	1.13
90	738	0.0185	9.99	1.15
120	685	0.0171	10.41	1.20
150	702	0.0176	11.05	1.27
180	663	0.0166	11.97	1.38
210	704	0.0176	12.90	1.48
240	611	0.0153	12.99	1.49
270	620	0.0155	13.00	1.49

Table B.14. Boric acid and calcium ion concentrations during the Experiment H2.7, Hisarcık 2 Colemanite, -160 μm, CaO/SO$_4^{2-}$ = 0.95, Stirring Rate = 500 rpm, T= 80°C

t, min	m$_{Ca}$, ppm	[Ca^{2+}], mol/l	V$_{NaOH}$, ml F$_{NaOH}$=1.15	[H$_3$BO$_3$], mol/l
0.75	2045	0.0511	9.19	1.06
4	1198	0.0299	10.77	1.24
15	948	0.0237	12.60	1.45
24	823	0.0206	12.72	1.46
40	785	0.0196	13.46	1.55
50	720	0.0180	13.96	1.61
75	658	0.0164	14.40	1.66
90	596	0.0149	14.12	1.62
123	645	0.0161	14.91	1.71
140	649	0.0162	14.39	1.65
160	623	0.0156	15.03	1.73
176	614	0.0153	14.92	1.72
190	619	0.0155	14.95	1.72
200	595	0.0149	15.24	1.75

Table B.15. Boric acid and calcium ion concentrations during the Experiment H2.8, Hisarcık 2 Colemanite, 0-250 µm, CaO/SO$_4^{2-}$ = 1, Stirring Rate = 500 rpm, T= 85°C

t, min	m$_{Ca}$, ppm	[Ca^{2+}], mol/l	V$_{NaOH}$, ml F$_{NaOH,}$=1.03	[H$_3$BO$_3$], mol/l
1.5	1736	0.0434	13.98	1.44
4.5	1349	0.0337	15.16	1.56
9.5	1059	0.0265	15.21	1.57
15.5	874	0.0218	15.53	1.60
21	783	0.0196	15.78	1.63
31	651	0.0163	16.05	1.65
44	605	0.0151	16.25	1.67
62	545	0.0136	16.45	1.69
88	529	0.0132	17.25	1.78
120	464	0.0116	17.75	1.83
149	462	0.0116	18.97	1.95
182	460	0.0115	19.39	2.00
210	459	0.0115	19.37	2.00

Table B.16. Variation in pH of slurry during the Experiment H2.8, Hisarcık 2 Colemanite, 0-250 µm, CaO/SO$_4^{2-}$ = 1, Stirring Rate = 500 rpm, T= 85°C

t, min	pH	t, min	pH
4	0.67	66	0.82
7	0.71	90	0.82
13	0.77	122	0.81
23	0.79	157	0.78
35	0.81	185	0.75
47	0.82	210	0.72

Table B.17. Boric acid and calcium ion concentrations during the Experiment H3.1, Hisarcık 3 Colemanite, 0-150 µm, CaO/SO_4^{2-} = 1, Stirring Rate = 400 rpm, T= 80°C

t, min	m_{Ca}, ppm	$[Ca^{2+}]$, mol/l	V_{NaOH}, ml F_{NaOH}=1	$[H_3BO_3]$, mol/l
2	984	0.0246	14.50	1.45
6	605	0.0151	14.75	1.48
11	389	0.0097	14.56	1.46
17	351	0.0088	15.19	1.52
30	294	0.0074	14.84	1.48
45	284	0.0071	15.02	1.50
60	271	0.0068	15.43	1.54
90	254	0.0064	15.15	1.52
120	251	0.0063	15.70	1.57
150	244	0.0061	15.82	1.58
184	242	0.0061	15.42	1.54
210	231	0.0058	16.63	1.66

Table B.18. Variation in pH of slurry during the Experiment H3.1, Hisarcık 3 Colemanite, 0-150 µm, CaO/SO_4^{2-} = 1, Stirring Rate = 400 rpm, T= 80°C

t, min	pH	t, min	pH
1	0.88	64	1.31
4.5	0.97	92	1.35
10	1.04	124	1.40
15	1.10	161	1.45
22	1.15	180	1.46
33	1.20	210	1.46
49	1.25	-	-

Table B.19. Boric acid and calcium ion concentrations during the Experiment H3.2, Hisarcık 3 Colemanite, 0-150 μm, CaO/SO$_4^{2-}$ = 1, Stirring Rate = 400 rpm, T= 85°C

t, min	m$_{Ca}$, ppm	[Ca^{2+}], mol/l	V$_{NaOH}$, ml F$_{NaOH}$,=1	[H$_3$BO$_3$], mol/l
1	1196	0.0299	-	-
2.3	968	0.0242	14.50	1.45
6	735	0.0184	14.76	1.48
10	536	0.0134	15.69	1.57
15	380	0.0095	15.78	1.58
22	308	0.0077	15.80	1.58
30	300	0.0075	16.03	1.60
45	290	0.0073	16.74	1.67
60	260	0.0065	16.80	1.68
90	252	0.0063	17.50	1.75
120	245	0.0061	17.90	1.79
150	240	0.0060	18.80	1.88
180	235	0.0059	18.60	1.86
210	225	0.0056	18.90	1.89

Table B.20. Variation in pH of slurry during Experiment H3.2, Hisarcık 3 Colemanite, 0-150 μm, CaO/SO$_4^{2-}$ = 1, Stirring Rate = 400 rpm, T= 85°C

t, min	pH	t, min	pH
5	0.72	48	0.91
9	0.76	64	0.94
13	0.80	94	0.95
18	0.84	120	0.95
25	0.88	150	0.95
34	0.90	180	0.95

Table B.21. Boric acid and calcium ion concentrations during the Experiment H3.3, Hisarcık 3 Colemanite, 0-150 μm, CaO/SO_4^{2-} = 1, Stirring Rate = 400 rpm, T= 85°C

t, min	m_{Ca}, ppm	$[Ca^{2+}]$, mol/l	V_{NaOH}, ml F_{NaOH}=1	$[H_3BO_3]$, mol/l
1.5	1015	0.0254	13.97	1.40
5	798	0.0200	15.26	1.53
10	514	0.0129	15.38	1.54
15	370	0.0093	15.65	1.57
33	295	0.0074	15.82	1.58
46	267	0.0067	16.24	1.62
60	256	0.0064	16.57	1.66
90	240	0.0060	17.18	1.72
120	237	0.0059	17.78	1.78
150	229	0.0057	18.69	1.87
180	220	0.0055	18.75	1.88
210	217	0.0054	18.82	1.88

Table B.22. Variation in pH of slurry during the Experiment H3.3, Hisarcık 3 Colemanite, 0-150 μm, CaO/SO_4^{2-} = 1, Stirring Rate = 400 rpm, T= 85°C

t, min	pH	t, min	pH
4	0.5	44	1.00
6	0.63	61	1.02
7.5	0.73	96	1.05
8.5	0.8	120	1.07
12	0.85	153	1.07
18.5	0.91	180	1.05
28	0.96	210	1.04
34	0.98	-	-

Table B.23. Boric acid and calcium ion concentrations during the Experiment H3.4, Hisarcık 3 Colemanite, 0-150 µm, $CaO/SO_4^{2-} = 1$, Stirring Rate = 400 rpm, T= 90°C

t, min	m_{Ca}, ppm	$[Ca^{2+}]$, mol/l	V_{NaOH}, m F_{NaOH}=1	$[H_3BO_3]$, mol/l
2.75	990	0.0248	14.06	1.41
6.5	765	0.0191	15.44	1.54
9.5	660	0.0165	16.05	1.61
13	575	0.0144	15.93	1.59
18.5	526	0.0132	16.01	1.60
29.5	385	0.0096	16.05	1.61
42	256	0.0064	15.21	1.52
60	216	0.0054	16.08	1.61
90	214	0.0054	16.26	1.63
120	209	0.0052	16.81	1.68
155	182	0.0046	16.81	1.68
185	176	0.0044	18.23	1.82

Table B.24. Variation in pH of slurry during the Experiment H3.4, Hisarcık 3 Colemanite, 0-150 µm, $CaO/SO_4^{2-} = 1$, Stirring Rate = 400 rpm, T= 90°C

t, min	pH	t, min	pH
0.8	0.63	21	1.21
1	0.75	22.5	1.23
1.5	0.79	26.5	1.25
2	0.95	27	1.27
3.6	0.99	41	1.30
4	1.00	65	1.38
4.3	1.01	80	1.43
8.8	1.11	95	1.46
11	1.12	118	1.49
11.5	1.16	158	1.49
12	1.18	220	1.49
15.5	1.19	21	1.21

SAMPLE CALCULATIONS

In this part the sample calculations are given on a representative Experiment H2.2. The following sample calculations are given:

C.1 Unit Conversion

- Calcium Ion Concentration

The calcium ion results have the units of ppm. It should be converted to mol Ca^{2+}/min. In order to do the conversion, the following expression is used.

Ca^{2+} concentration at time 210= 628 ppm

$$Ca^{2+}(ppm) = (628\,ppm) \cdot \left(\frac{1\,mg/l}{1\,ppm}\right) \cdot \left(\frac{1\,mol\,Ca^{2+}}{40\,g.}\right) \cdot \left(\frac{1g}{1000\,mg}\right)$$

Ca^{2+} = 0.0157 mol/min

C.2 CaO / SO_4^{2-} Molar Ratio Calculation

Amount of Colemanite added to the reactor: 182 g

Volume of Sulphuric Acid (%93 by weight) added to the reactor: 53.57 ml

CaO and SO_4^{2-} come to the reactor from colemanite and sulfuric acid, respectively.

$$CaO = (182\ g\,.colemanite) \cdot \left(\frac{0.2861\,g.\,CaO}{g.\,colemanite}\right) \cdot \left(\frac{1\,mol\,CaO}{56\,g.}\right) = 0.93\,mol$$

$$SO_4^{2-} = (53.57\text{ml.acid})\left(\frac{1.84 \text{ g.} \textit{acid}}{1\text{ml} \textit{acid}}\right)\left(\frac{93 \textit{ g } H_2SO_4}{100 \textit{ g.acid}}\right)\cdot\left(\frac{1\text{mol} H_2SO_4}{98 \text{ g.} H_2SO_4}\right)\cdot\left(\frac{1\text{mol} SO_4^{2-}}{1\text{mol} H_2SO_4}\right) = 0.93 \text{ mol}$$

$$\frac{CaO}{SO_4^{2-}} = \frac{0.93 \text{ mol}}{0.93 \text{ mol}} = 1$$

APPENDIX D

PARTICLE SIZE DISTRUBUTION GRAPHS OF GYPSUM CRYSTALS
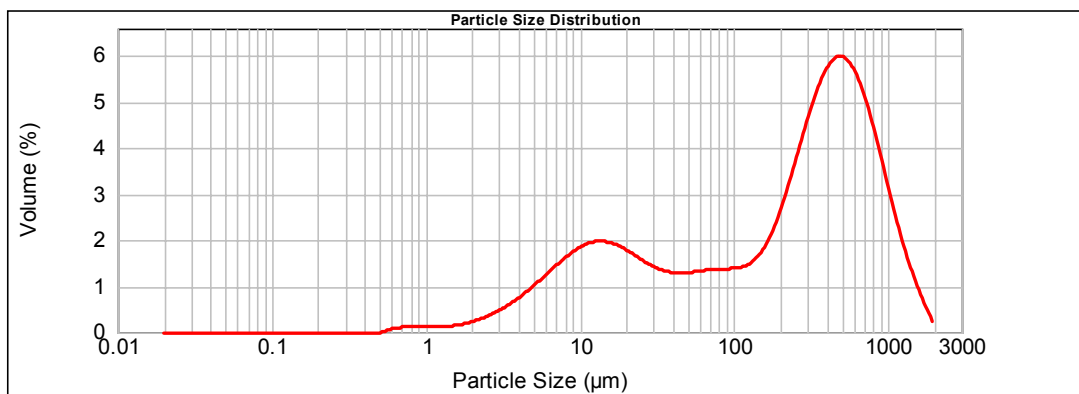
Figure D.1 . Particle size distribution of the gypsum crystals taken from the reactor at 210 minutes (Experiment H2.2, Hisarcık 2 Colemanite, +250 μm, CaO/SO_4^{2-} = 1.0, Stirring Rate = 400 rpm, T= 80°C)
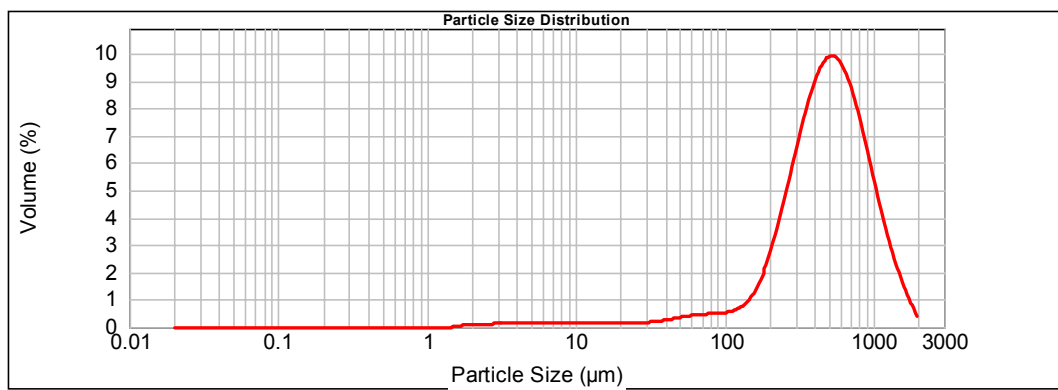
Figure D.2. Crystal size distribution of the solid taken from the reactor at 240 minutes Experiment H2.3, Hisarcık 2 Colemanite, +250 μm, CaO/SO_4^{2-} = 1.0, Stirring Rate = 350 rpm, T= 85°C
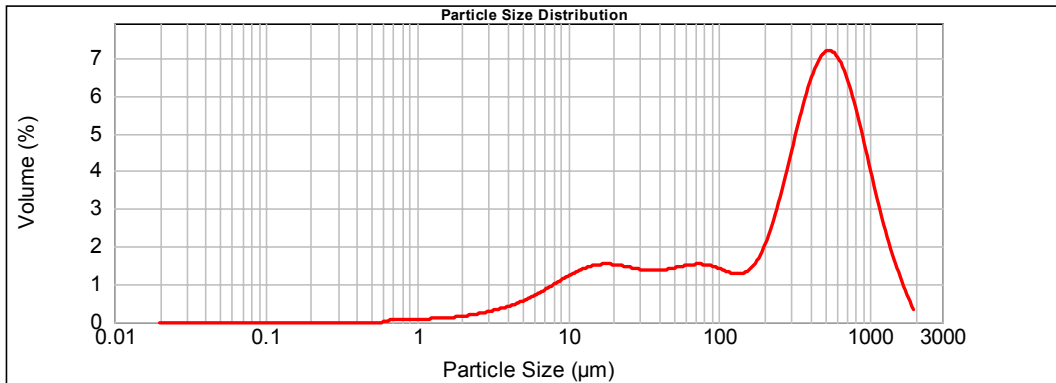
Figure D.3. Crystal size distribution of the solid taken from the reactor at 210 minutes (Experiment H2.4, Hisarcık 2 Colemanite, +250 µm, CaO/SO$_4^{2-}$ = 1.0, Stirring Rate = 400 rpm, T= 85°C)
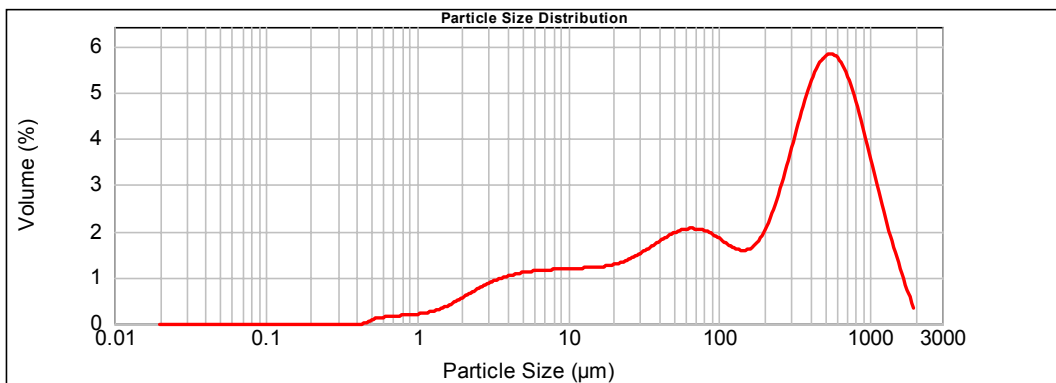
Figure D.4. Crystal size distribution of the solid taken from the reactor at 240 minutes (Experiment H2.5, Hisarcık 2 Colemanite, +250 µm, CaO/SO$_4^{2-}$ = 1.0, Stirring Rate = 500 rpm, T= 85°C)
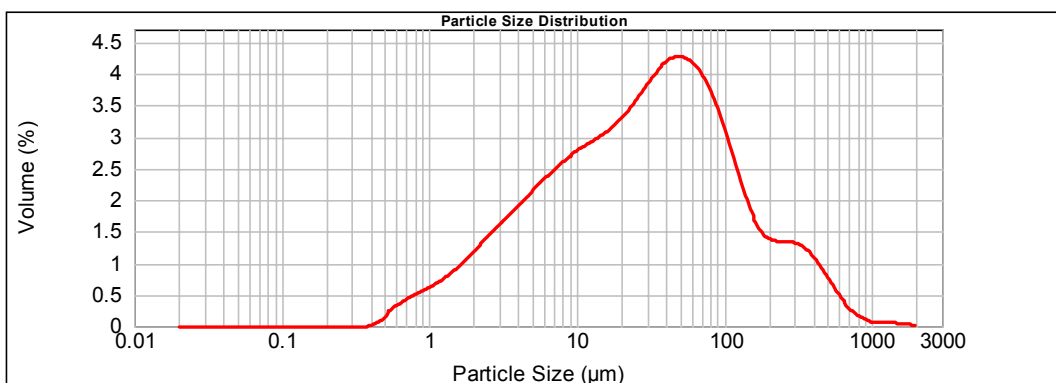
Figure D.5. Crystal size distribution of the solid taken from the reactor at 210 minutes (Experiment H2.8, Hisarcık 2 Colemanite, -250 µm, CaO/SO$_4^{2-}$ = 1.0, Stirring Rate = 500 rpm, T= 85°C)
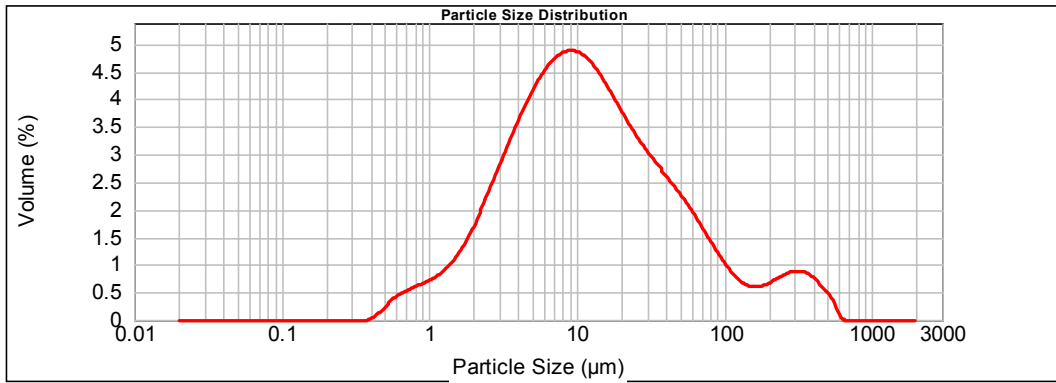
Figure D.6. Crystal size distribution of the solid taken from the reactor at 210 minutes (Experiment H3.1, Hisarcık 3 Colemanite, -150 µm, CaO/SO_4^{2-} = 1.0, Stirring Rate = 400 rpm, T= 80°C)
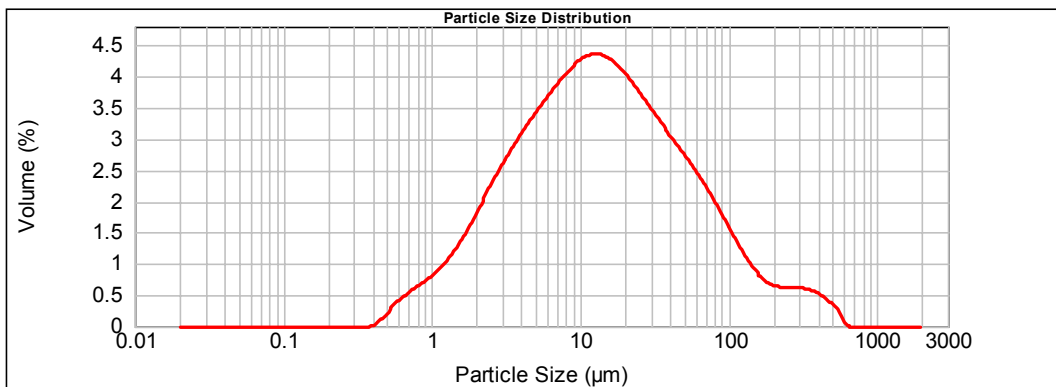
Figure D.7. Crystal size distribution of the solid taken from the reactor at 210 minutes (Experiment H3.2, Hisarcık 3 Colemanite, -150 µm, CaO/SO_4^{2-} = 1.0, Stirring Rate = 400 rpm, T= 85°C)
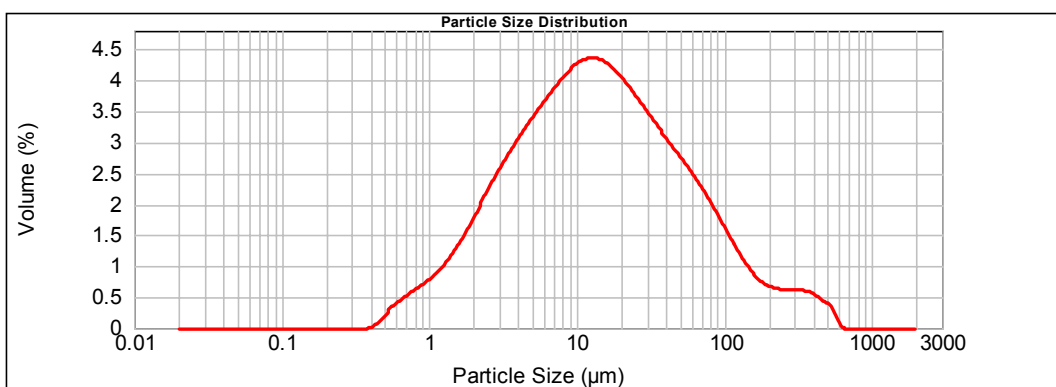
Figure D.8. Crystal size distribution of the solid taken from the reactor at 210 minutes (Experiment H3.3, Hisarcık 3 Colemanite, -150 µm, CaO/SO_4^{2-} = 1.0, Stirring Rate = 400 rpm, T= 85°C)
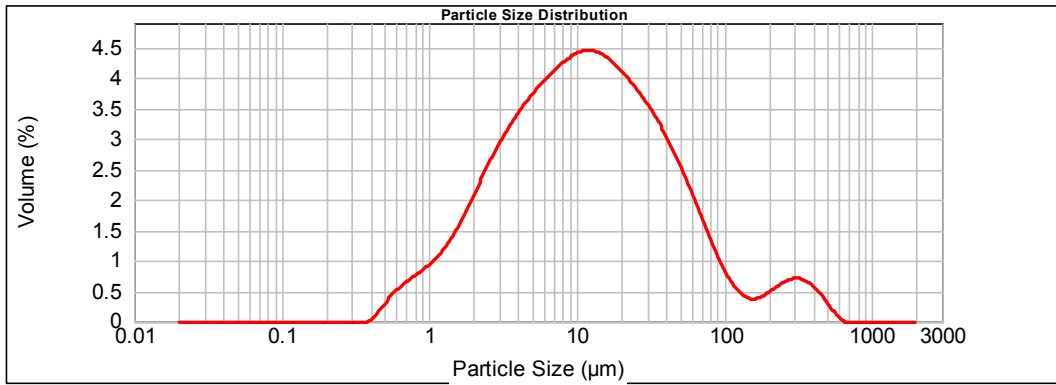
Figure D.9. Crystal size distribution of the solid taken from the reactor at 223 minutes (Experiment H3.4, Hisarcık 3 Colemanite, -150 µm, CaO/SO_4^{2-} = 1.0, Stirring Rate = 400 rpm, T= 85°C)

VARIATION OF DENSITY OF BORIC ACID SOLUTIONS WITH TEMPERATURE

Table E.1. Density of saturated boric acid solutions

Temperature	%Saturated Solution	Density (kg m^{-3})
0	2.61	1013
10	3.57	1015
20	4.77	1016
30	6.27	1017
40	8.10	1019
50	10.30	1023
60	12.89	1029
70	15.88	1035
80	19.30	1039
90	23.12	
100	27.33	

Table E.2. Variation of density of boric acid solutions (kg m^{-3}) with temperature

	1	2	3	4	5	6	7	8	9	10	11	12	13	14	15	16	17	18
100	963	966	970	973	977	980	983	985	988	990	993	995	997	999	1001	1003	1005	1007
95	966	970	973	976	980	983	986	989	992	995	997	1000	1003	1005	1008	1010	1012	1015
90	969	973	976	979	983	986	989	992	996	999	1002	1005	1008	1011	1014	1017	1019	1022
85	972	976	979	982	986	989	992	996	999	1002	1006	1009	1012	1016	1019	1022	1026	1029
80	975	979	982	985	989	992	996	999	1003	1006	1010	1013	1017	1020	1024	1028	1031	1035
75	978	981	985	988	992	995	999	1002	1006	1009	1013	1017	1021	1024	1028	1032	1036	
70	981	984	987	991	994	998	1001	1005	1009	1012	1016	1020	1024	1028	1032			
65	984	987	990	994	997	1001	1004	1008	1012	1015	1019	1023	1027	1031				
60	986	990	993	996	1000	1003	1007	1010	1014	1018	1022	1026						
55	989	992	995	999	1002	1006	1009	1013	1017	1020	1024							
50	991	995	998	1001	1005	1008	1012	1015	1019	1022								
45	994	997	1000	1004	1007	1010	1014	1017	1021									
40	996	999	1003	1006	1009	1013	1016	1019										
35	998	1001	1005	1008	1011	1014	1018											
30	1000	1003	1007	1010	1013	1016												
25	1001	1005	1009	1012	1015													
20	1003	1007	1010	1014														
15	1004	1008	1012	1015														
10	1005	1010	1013															